

In-situ generation of silica particles in solution styrene butadiene rubber – A possible material solution to improve the performance of rubber

Von der Fakultät Maschinenwesen

der

Technische Universität Dresden

Zur Erlangung des akademischen Grades

Doktoringenieur (Dr. Ing.)

angenommene Dissertation

Sankar Raman Vaikuntam

Geb. am 27. Juni 1982 in Tirunelveli, Tamilnadu, Indien

Tag der Einreichung	: 18.04.2017
Tag der Verteidigung	: 09.02.2018
Gutachter	: Prof. Dr. rer. nat. habil. Gert Heinrich : Prof. Dr. Anke Blume
Vorsitzender der Promotionskommission	: Prof. Dr.-Ing. habil. R. Lange

ACKNOWLEDGEMENT

First and foremost I would like to express my sincere gratitude to my supervisor **Prof. Gert Heinrich**, Head of Institute of Polymer Materials at Leibniz - Institute of Polymer Research Dresden (IPF Dresden) as well as former faculty of mechanical engineering at technical university of Dresden to carry out my doctorate in philosophy dissertation at Leibniz - Institute of Polymer Research Dresden in Germany. His understanding, encouraging, personal guidance and financial support have provided a good basis for the present thesis. I am greatly thankful for his detailed guidance, constructive comments and his important support throughout my work.

As well I wish to express my warm and sincere thanks to **Dr. Amit Das**, IPF Dresden, Germany, who supported me for his valuable advice, extensive discussions around my work and explorations in rubber research. I am also very thankful to **Jun. Prof. Dr. Sven Wießner**, Head of department of Elastomers, IPF Dresden as well as faculty of mechanical engineering at technical university of Dresden for his support, guidance and help throughout my dissertation. I wish to thank **Dr. Klaus Werner Stöckelhuber**, IPF Dresden for his support in technical discussions and co-operation throughout my dissertation. I am thankful to our technical staffs Mr. René Jurk, Mr. Thomas Götze for their introduction to our elastomer lab, helping with machines and other technical staffs in IPF Dresden for supporting me in performing various experiments.

I am very much thankful to Mrs. Anne Hofmann, Frau. Gudrun Schwarz for their kind helps in organizing conferences activities and official trips. I appreciate Mrs. Astrid Creutz and Miss. Nicole Kammer for being very helpful with administrative matters. I am thankful to members, co-workers of other departments and institute who have helped me in many respects during my work.

Finally I owe my loving thanks to my parent, my sister, my wife and my friends for their consistent support, affection and sacrifices during my doctorate dissertation.

Date: 09.02.2018

Sankar Raman Vaikuntam

Eidesstattliche Erklärung

Hiermit versichere ich, dass ich die vorliegende Arbeit ohne unzulässige Hilfe Dritter und ohne

Benutzung anderer als der angegebenen Hilfsmittel angefertigt habe; die aus fremden Quellen direkt oder indirekt übernommenen Gedanken sind als solche kenntlich gemacht.

I here certify that the submitted dissertation was solely done by me with the help of the specified sources and without any assistance from the third parties. I have acknowledged the referred sources properly.

Dresden, den 09.02.2018

Sankar Raman Vaikuntam

Abstract

In the field of tyre technology, silica filled tyres are generally considered as a lower energy consumption product due to their lower rolling resistance characteristics. Additionally, they can offer excellent grip on the wet and snowy conditions which are more essential from the safety perspective. However, the proper dispersion of the silica in rubber compounds is one of the challenging tasks to engineers, physicist and chemist. In this thesis, a very controlled *in-situ* silica based solution styrene butadiene rubber composites were developed and intensively investigated by the synthesis of sol-gel silica in presence of polymer solution. It means the silica particles were allowed to grow in the presence of rubber in the reaction mixture. It was observed that the sizes of the synthesized silica particles are rather larger than standard precipitated commercial silica particles. In depth morphological investigation revealed that the obtained sol-gel silica particles appear in strong cluster form with primary particle size of 10 - 15 nm and final aggregated size of 200 to 400 nm. Nevertheless, the final mechanical performance and other rubber related properties of *in-situ* derived silica composites are better in many important aspects for technical applications as compared with commercial silica at a given loading of fillers. Owing to the presence of more active hydroxyl group on the surface of sol-gel silica, the effective coupling between silica and rubber has been established. Furthermore, the permanent trapped rubber chains inside the large aggregates of sol-gel silica particles enable the compounds to offer good mechanical reinforcement, higher resilience, and dynamic mechanical properties. The present work is a humble approach to pave an alternative novel way for silica-rubber composite preparation in order to minimize the problem of silica mixing with the rubbers.

Kurzfassung

Auf dem Gebiet der Reifentechnologie zeichnen sich Kieselsäure-(Silika)-gefüllte Reifen aufgrund ihres charakteristisch geringeren Rollwiderstands allgemein als ein Produkt mit geringerem Energieverbrauch aus. Darüber hinaus bieten sie ein hervorragendes Nasshaftvermögen, welches eine essentielle physikalische Kenngröße für die Fahrsicherheit darstellt. Allerdings stellt eine optimale Dispergierung der Silikafüllstoffe in Kautschukmischungen eine anspruchsvolle Aufgabe für Ingenieure, Physiker und Chemiker dar. Im Rahmen der vorliegenden Arbeit wurden Silika / Styrol-Butadien-Kautschuk-Verbundwerkstoffe mittels eines *in-situ* Sol-Gel-lösungsmittelbasierten Reaktionsverfahrens entwickelt. Diese Technologie beruht auf der Nukleierung von Kieselsäure-Partikeln in Gegenwart des Elastomers in einer Syntheselösung. Dabei wurde beobachtet, dass die Partikel der so synthetisierten Silika-Teilchen größer sind, als die eines kommerziellen Standard-Silika-Füllstoffs. Eine umfassende morphologische Untersuchung zeigt, dass die *in-situ* synthetisierten Silikapartikel sphärisch sind und eine Primärteilchengröße von 10 bis 15 nm aufweisen. Diese nanoskaligen Teilchen agglomerieren sich zu größeren sphärischen Clustern mit einer Größe von 200 bis 400 nm und weisen somit eine andere Morphologie auf, als die kommerziell erhältlichen Silika-Füllstoffe. Die statisch- und dynamisch-mechanischen Eigenschaften, sowie weitere elastomerbezogene Eigenschaften der *in-situ* synthetisierten Silika/Styrol-Butadien-Kautschuk-Verbundwerkstoffe, wie z.B. Rückprallelastizität, mechanisch induzierte Wärmeentwicklung und Spannung-Dehnungshysterese, zeigen verbesserte Werte im Vergleich zu Elastomermaterialien gefüllt mit kommerzieller Kieselsäure. Eine erhöhte Anzahl von Hydroxylgruppen auf der Oberfläche der *in-situ* synthetisierten Silikapartikel, verbunden mit permanenter Adsorption der Polymerketten des Elastomers auf der Teilchenoberfläche ermöglicht die Ausbildung eines Elastomerverbundes mit verbesserter mechanischer Verstärkung mit oder ohne Einsatz eines haftvermittelnden Silans, wie z.B. TESPT (Bis [3-(triethoxysilyl)propyl]-tetrasulfid). Die Wechselwirkungen zwischen Elastomer und Füllstoff, zwischen den Füllstoffpartikeln, sowie der Verstärkungsmechanismus des *in-situ* synthetisierten Füllstoffes wurden mittels dynamisch-mechanischer Analyse (Amplitudentests), Festkörper-NMR und energiedispersiver Röntgenspektroskopie umfassend analysiert. Der vorliegende Ansatz verdeutlicht, dass die *in-situ* Generierung des Füllstoffes im Elastomer ein vielversprechendes und alternatives Verfahren zur Herstellung von Elastomermaterialien mit verbesserter Silika-Dispergierung, sowie erhöhter Elastomer-Füllstoff-Wechselwirkung bietet.

Contents

Chapter 1

1	General introduction	1
1.1	Aim and objective of work	4
1.2	Structure of thesis	5

Chapter 2

2	Literature review	9
2.1	History of rubber reinforcement by fillers	10
2.2	Carbon black reinforcement of rubbers	13
2.3	Silica reinforcement of rubbers	14
2.4	Needs and essentials in silica technology	16
2.5	State of the art: Sol-gel silica based rubber composites	19
2.6	Expectation in tyre compounds	23

Chapter 3

3	Experimental section	28
3.1	Materials	29
3.1.1	Rubber	29
3.1.2	Silica and silane coupling agents	29
3.1.3	Other rubber ingredients	30
3.2	Preparation sol-gel and precipitated silica based rubber compounds	31
3.2.1	Preparation of Rubber-silica masterbatches	31
3.2.2	Compounding with ingredients	31
3.2.3	Compounding formulations	33
3.2.4	Moulding	34
3.2.5	Sample abbreviation	34
3.3	Characterizations	35
3.3.1	Thermogravimetric analysis	35
3.3.2	Rheological study	35
3.3.2.1	Mooney viscosity	35
3.3.2.2	Dynamic filler flocculation	36
3.3.2.3	Vulcanization study	37

3.3.3	Fourier transform infrared analysis (FTIR)	37
3.3.4	Physio-Mechanical testing	38
3.3.5	Dynamic mechanical analysis (DMA)	39
	3.3.5.1 Temperature sweep	39
	3.3.5.2 Strain sweep	39
	3.3.5.3 Frequency sweep	40
3.3.6	Other rubber performances	40
	3.3.6.1 Heat build-up	40
	3.3.6.2 Rebound resilience	41
	3.3.6.3 Abrasion properties	41
3.3.7	Solid state NMR analysis	42
	3.3.7.1 Low field ^1H NMR-Double quantum experiments	42
	3.3.7.2 Solid state ^{29}S NMR experiments	45
3.3.8	Equilibrium swelling experiments	45
3.3.9	Liner friction tester	46
3.3.10	Tear-fatigue analyzer (TFA)	48
3.3.11	Morphology study	51
	3.3.11.1 Scanning electron microscopy (SEM)	51
	3.3.11.2 Energy dispersive X-ray spectroscopy (EDX)	52
	3.3.11.3 Transmission electron microscopy (TEM)	52
3.3.12	Dynamic light scattering analysis (DLS)	53
3.3.13	X-ray diffraction (XRD)	53
3.3.14	Estimation of silanol density	54
3.4	State of the art: In-situ silica-rubber reinforcement	54

Results and discussions

Chapter 4

4	Generation of in-situ silica in SSBR matrix	58
	4.1 Introduction	59
	4.2 Results and discussion	59
	4.2.1 Time dependent silica conversion study	59
	4.2.2 Characterization of the rubber compounds	62

4.2.3	Mechanical and dynamic mechanical properties	67
4.2.4	Other rubber performance	71
4.2.5	Morphology	74
4.3	Conclusions	75

Chapter 5

5	Properties and performance of in-situ silica filled SSBR composites with respect to precipitated silica filled SSBR composites	79
5.1	Introduction	80
5.2	Results and discussion	80
5.2.1	Estimation of amount of silica content	80
5.2.2	Investigation of silica flocculation and network analysis	81
5.2.3	Rheometric analysis	82
5.2.4	Mechanical properties	84
5.2.5	Dynamic mechanical properties	85
5.2.6	Other rubber performance properties	87
5.2.7	Hysteresis properties	90
5.2.8	Scanning electron microscopy	92
5.2.9	Friction co-efficient and friction master curves	93
5.2.10	Tear fatigue analyzer (TFA)-Crack propagation measurements	94
5.3	Conclusions	96

Chapter 6

6	Influence of silica-silane interaction and silica-rubber interfaces on the microscopic properties of rubber	99
6.1	Introduction	100
6.2	Results and discussions	101
6.2.1	Silica particle investigation	101
6.2.2	Estimation of crosslink density and rubber-silica interaction by Multiple Quantum NMR experiments	103
6.2.2.1	Unfilled SSBR vulcanizates	103
6.2.2.2	Silica filled composites	103
6.2.2.2.1	Commercial precipitated silica filled composites	105
6.2.2.2.2	<i>In-situ</i> sol-gel derived silica composites	106

6.2.3	Physical estimation of silanol groups situated on the surface of silica particle	110
6.2.4	²⁹ Si-Solid state NMR investigation of silica and silica composites	111
6.2.4.1	²⁹ Si-MAS NMR experiments	111
6.2.4.2	²⁹ Si- ¹ H Cross polarization experiments	112
6.2.5	Energy dispersive X-ray spectroscopy (EDX) analysis	113
6.3	Conclusions	116

Chapter 7

7	Effect of silica-silane interaction on the mechanical performance of silica filled solution styrene butadiene rubber	120
7.1	Introduction	121
7.2	Results and discussion	121
7.2.1	Mechanical properties	121
7.2.2	Dynamic mechanical properties	123
7.2.2.1	Strain sweep measurements	123
7.2.2.2	Temperature sweep measurements	124
7.2.3	Heat build-up properties	127
7.2.4	Rebound resilience	128
7.2.5	Abrasion properties	128
7.2.6	Molecular interpretation of silica-silica network and desorption of rubber chains from the silica surface by temperature dependent-strain sweep measurements	129
7.2.7	Effect of physical and chemical interfaces on crosslink density of rubber	136
7.3	Conclusions	138

Chapter 8

8	Conclusions and outlooks	142
---	--------------------------	-----

Abbreviations

i or i - silica	-	in-situ silica
x or ppt. silica	-	precipitated silica (commercial Ultrasil-VN3)
SSBR	-	solution styrene butadiene rubber
TEOS	-	Tetraethoxyorthosilicate
DMS	-	Diethoxy dimethyl silane
APTES	-	(3-Aminopropyl)triethoxysilane
ODTES	-	n-Octadecyltriethoxsilane
MPTES	-	(3-Mercaptopropyl)trimethoxysilane
TESPD	-	bis[3-(triethoxysilyl)propyl]disulfide
TESPT	-	bis[3-(triethoxysilyl)propyl]tetrasulfide
ZnO	-	Zinc oxide
CBS	-	N-Cyclohexyl 2-benzothioazole sulphinamide
DPG	-	Diphenyl guanidine
TGA	-	Thermogravimetric analysis
FTIR-ATR	-	Fourier transform infrared spectroscopy- Attenuated total reflection
SEM	-	Scanning electron microscopy
TEM	-	Transmission electron microscopy
MU	-	Mooney units
WLF equation	-	William-Landel-Ferry equation

DQ - NMR	-	Double Quantum Nuclear magnetic resonance
D_{res}	-	Residual dipolar coupling constant
$1/M_c$ and V_{FR}	-	Crosslink density measured by swelling method
MAS NMR	-	Magic angle spinning Nuclear magnetic resonance
EDX	-	Energy dispersive X-ray spectroscopy
DLS	-	Dynamic light scattering analysis
XRD	-	X-ray diffraction
CRI	-	Cure rate index
ARI	-	Abrasion resistance index

Chapter 1

General introduction

1 General introduction

The reinforcement of elastomer matrices and achieving a desired property to fit for a particular application is an art and science in the field of rubber science and technology¹. The rubber reinforcement mainly depends on three important parameters like type of polymer, type of filler and type of crosslink/degree of crosslink. The reinforcing capability of elastomers by fillers generally depends upon the nature of filler, particle size, surface area, structure, and surface reactivity of the fillers². According to the above mentioned criterion the rubber fillers are generally categorized into reinforcing, semi-reinforcing and non-reinforcing³. In this category, carbon black is one of the traditional fillers since it is occupying the rubber industry more than a century⁴. The reinforcing nature of carbon black is mainly accessed by its higher surface area, lower particle size and good affinity with polymer chains⁵. Other than carbon black nowadays, clay and clay minerals are modern reinforcing materials that are widely used for the preparation of polymer nanocomposites. However, the dispersion of such clay minerals in the polymer matrix is a big challenge due to the high surface energy of such clay minerals. They also form agglomerated structures when incorporated into the organic polymer matrix. The reinforcement phenomenon of elastomers in the presence of nanoclay is entirely differing from carbon black and other particulate fillers. The clays are multilayered silicates presented in nano or micron size particles⁶. The layered structure of clay is called as “gallery”. The reinforcement by layered silicates is occurred due to the opening of gallery platelets in polymer matrices⁷. When the polymer chains are not able to intercalate or exfoliate between the layered silicates platelets, phase separated morphology of composites are obtained. Those composite properties stay like a similar behaviour of traditional micro or macro composites⁸. However, the major purpose of intercalation is, to expand the interlayer spacing, to reduce layer-layer interaction between the silicate platelets and to improve the interaction between the clay platelet and the polymer matrix^{7,9}. In the case of intercalated nanocomposites, the polymer chain is intercalated between the silicate layers resulting well-ordered multilayer morphology which greatly improves the mechanical properties¹⁰.

Similarly, the most important particulate filler from the inorganic category is silica. Last two decades in the field of tyre technology, the silica reinforced tyres are gaining greater importance due to their versatile performance on lower rolling resistance, ice grip and high wet skid resistance¹¹. Due to the larger demands of energy (fuel) consumption and safety

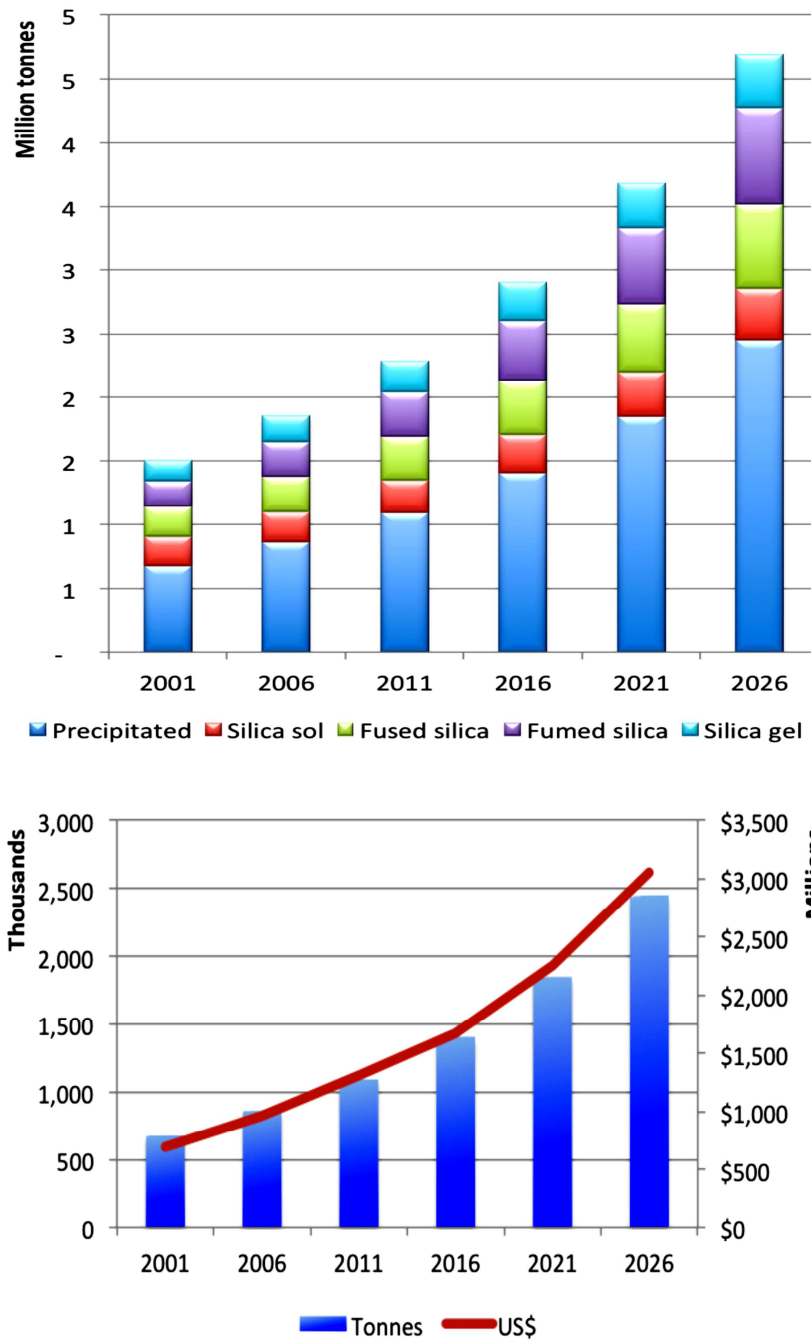


Figure 1.1 Global demand for all silica products in market and Global demand for precipitated silica in market trends and values from 2001 – 2026²⁷ (The last access date is 02.11.2016)

perspective the market of silica filled tyres are getting popular all over the world. Especially precipitated silica is one of the most common type's fillers for tyre industries. More, particularly, 'highly dispersible silica' (HDS)¹² is now more interesting for tyre industries as it offers superior tyre performance as compared with normal precipitated silica¹³. The global demands for specialty silica products are forecasted to increase around 3.0 million tons by

2026. The trend of precipitated silica consumption and their market values are given in figure 1.1²⁷.

On the other hand, some major issues have been encountered using silica in rubber product manufacturing. In contrast to the fugacious nature of free water, bound water, hydration water is held firmly in place as silanol groups of silica¹⁴. Silanol groups are mainly responsible for the hydrophilic nature of silica¹⁵. The network of hydrogen bonded silanol groups on the silica surface leads to higher viscosity, increase in hardness and stiffness of rubber compound during storage, poor dispersion, higher Payne effect, interrupting on vulcanization process (reduce the cure rate and increase the cure time) and lack in ease of processing¹⁶. Some of the above mentioned issues are rectified with the assistance of silane coupling agents, providing adequate mixing time and mixing cycles. Nevertheless, silica technology for tyres still needs some more improvements to solve the current environmental standards like lower CO₂ emission, lower fuel consumption and safety aspects. At the same time in case of silica filled rubber system, the major part of reinforcement and improvement in dynamic mechanical properties are mainly decided by the state of dispersion, addition of silane coupling agent and type of silica-rubber coupling either physical or chemical coupling. Considering above mentioned shortcoming of the existing technology, the need to deliver better performance and to better understand the complexity of such rubber system, the in-situ silica based rubber composites are considered and finally, the results are compared with standard precipitated silica.

1.1 Aim and objective of work

The incorporation and dispersion of silica in a rubber matrix is a complicated, highly time and energy consuming process for the production of rubber parts, like tyres¹⁷. The effective dispersion of silica in rubber is a great challenge to the chemist, physicist and engineers. The great difference in surface energies between silica and rubber leads to agglomerated and aggregated morphology of the silica particles¹⁸. A partial solution to this problem can be realized by the use of silane coupling agents in a special reactive mixing condition¹². In my present work, the silica particles are synthesized inside the polymer matrix using tetraethoxyorthosilicate (TEOS) as a silica precursor to get a good rubber-filler interaction and improved state of silica dispersion. To visualize the reinforcement effect, silica-rubber interaction and filler-filler interaction attributed by the sol-gel in-situ silica the developed composites are further compared with commercially available precipitated silica. The additional effects of silane coupling agents and the fundamental properties of in-situ

silica filled rubbers are also studied here. The prime motivation of the present work is to develop a novel method to disperse silica in styrene butadiene rubber matrix by adapting the sol-gel silica synthesis method. The choice of solution styrene butadiene rubber (SSBR) in this investigation is mainly considered due to their higher consumption in passenger car tyre manufacturing due to its excellent lower rolling resistance, improved wet & ice grip and abrasion properties^{11b}.

To understand the real performance of prepared silica composites, several state-of-the-art experimental methods are followed. In addition, the thesis also aims to gain fundamental understanding of silica formation in rubber with respect to higher loading of silica by sol-gel route and exploring the role of different ingredients used in the silica synthesis process. Finally, attention is paid on structure-property relationship, effect of silane modification of the sol-gel silica. The detailed study has been done to investigate the physio-chemical properties of silica in rubber which is finally influencing the reinforcement characteristics, network density of rubber and silica-silane-rubber interactions.

1.2 Structure of thesis

This thesis mainly addresses the preparation, properties and fundamental understanding of silica based rubber composites and its applications. The investigation started with a literature survey based on the history of rubber reinforcement by fillers, the factors involved on the reinforcement of fillers, rubber reinforcement by carbon black and precipitated silica and essentials in future silica technology. Simultaneously, the thesis is continued by the state of art of sol-gel silica technology used in polymer reinforcement and the major expectations in silica based tyre compound are given in chapter 2. The various materials used in the present study, their basic specifications, preparation of in-situ sol-gel derived silica and commercial silica composites; compounding formulations are given in detail in Chapter 3. Also the different experimental techniques used and their analytical background for the characterization of silica powders and silica filled composites are described briefly. The results and discussions of the work are given in Chapter 4 to 7:

Chapter 4: Generation of in-situ silica in SSBR matrix

In this part the basic scientific investigations are carried out to understand the silica particle growth inside the rubber, the time dependent sol-gel transition and silica particle formation. The prepared in-situ sol-gel silica compounds and composites were further studied by thermogravimetric analysis (TGA), Fourier infrared spectroscopy (FTIR-ATR), Mooney viscometer, silica flocculation characteristics, rheometric properties, mechanical and dynamic

mechanical properties, rebound resilience, heat build-up, abrasion properties, crosslink density measurements, morphology by SEM, TEM.

Chapter 5: Properties and performance of in-situ silica filled SSBR composites with respect to precipitated silica filled SSBR composites

To understand the reinforcing capability of in-situ derived silica based SSBR composites, the properties are further compared with commercial precipitated Ultrasil-VN3 silica composites. The conventional rubber experimental techniques like moving die rheometer, mechanical and dynamic mechanical properties, rebound resilience, heat build-up, abrasion properties, linear friction tester, tear fatigue analyser as well as some morphology investigations by SEM, TEM also have been utilized.

Chapter 6: Silica-silane interaction and silica-rubber interfaces on the microscopic properties of rubber

The reinforcement mechanism of silica in solution styrene butadiene rubber is investigated from the chemical point of view. The study has been elaborated into an effect of silica loading, the influence of silica-silane interaction, the influence of silane coupling agents and rubber-silica interfaces. This allows more systematically investigating the effect of filler system and the role of silane coupling agents on microscopic properties of the vulcanized rubber network.

Chapter 7: Effect of silica-silane interaction on the mechanical performance of silica filled solution styrene butadiene rubber

In this chapter the addition of different coupling agents like Diethoxy dimethyl silane (DMS), (3-Aminopropyl)triethoxysilane (APTES), n-Octodecyltriethoxysilane (ODTES), 3-Octanoylthio 1-propyl triethoxysilane (NXT), (3-Mercaptopropyl) trimethoxysilane (MPTES), bis[3-(triethoxysilyl)propyl]disulfide (TESPD) and bis[3-(triethoxysilyl)propyl]tetrasulfide (TESPT) in in-situ silica and commercial precipitated silica compounds are investigated. The used coupling agents are generally divided into two categories like mono-functional silane (physical) and bi-functional silane (chemical). The investigation turns in to how the physical and chemical interaction between silica and rubber contribute to the macro and micro properties of rubber.

Finally, the summary of the entire work, conclusions and outlooks are presented in Chapter 8.

References

1. (a) Hofmann, W., *Rubber technology handbook*. Hanser Publishers. Distributed in the USA by Oxford University Press: 1989; (b) Blow, C. M., *Rubber technology and manufacture*. 1971; (c) Mark, J. E.; Erman, B.; Roland, M., *The science and technology of rubber*. Academic press: 2013.
2. Evans, M. S., *Tyre compounding for improved performance*. iSmithers Rapra Publishing: 2002; Vol. 12, p112.
3. Donnet, J.-B.; Voet, A., *Carbon black: physics, chemistry, and elastomer reinforcement*. M. Dekker: 1976.
4. (a) Dannenberg, E., Bound rubber and carbon black reinforcement. *Rubber chemistry and technology* **1986**, 59 (3), 512-524; (b) Rigbi, Z., Reinforcement of rubber by carbon black. In *Properties of Polymers*, Springer: 1980; pp 21-68; (c) Studebaker, M. L., The chemistry of carbon black and reinforcement. *Rubber Chemistry and Technology* **1957**, 30 (5), 1400-1483.
5. Kraus, G., Reinforcement of Elastomers by Carbon Black. *Rubber Chemistry and Technology* **1978**, 51 (2), 297-321.
6. (a) Rooj, S.; Das, A.; Stöckelhuber, K. W.; Wang, D.-Y.; Galiatsatos, V.; Heinrich, G., Understanding the reinforcing behavior of expanded clay particles in natural rubber compounds. *Soft Matter* **2013**, 9 (14), 3798; (b) Das, A.; Mahaling, R.; Stöckelhuber, K.; Heinrich, G., Reinforcement and migration of nanoclay in polychloroprene/ethylene-propylene-diene-monomer rubber blends. *Composites Science and Technology* **2011**, 71 (3), 276-281.
7. Rooj, S.; Das, A.; Stöckelhuber, K. W.; Reuter, U.; Heinrich, G., Highly Exfoliated Natural Rubber/Clay Composites by “Propping-Open Procedure”: The Influence of Fatty-Acid Chain Length on Exfoliation. *Macromolecular Materials and Engineering* **2012**, 297 (4), 369-383.
8. Rajasekar, R.; Pal, K.; Heinrich, G.; Das, A.; Das, C., Development of nitrile butadiene rubber-nanoclay composites with epoxidized natural rubber as compatibilizer. *Materials & Design* **2009**, 30 (9), 3839-3845.
9. Das, A.; Costa, F. R.; Wagenknecht, U.; Heinrich, G., Nanocomposites based on chloroprene rubber: effect of chemical nature and organic modification of nanoclay on the vulcanizate properties. *European Polymer Journal* **2008**, 44 (11), 3456-3465.
10. (a) Das, A.; Wang, D.-Y.; Stöckelhuber, K. W.; Jurk, R.; Fritzsche, J.; Klüppel, M.; Heinrich, G., Rubber-Clay Nanocomposites: Some Recent Results. In *Advanced Rubber Composites*, Heinrich, G., Ed. Springer Berlin Heidelberg: Berlin, Heidelberg, 2011; pp 85-166; (b) Rooj, S.; Das, A.; Morozov, I. A.; Stöckelhuber, K. W.; Stoczek, R.; Heinrich, G., Influence of “expanded clay” on the microstructure and fatigue crack growth behavior of carbon black filled NR composites. *Composites Science and Technology* **2013**, 76, 61-68.
11. (a) Sarkawi, S. S.; Dierkes, W. K.; Noordermeer, J. W. M., MORPHOLOGY OF SILICA-REINFORCED NATURAL RUBBER: THE EFFECT OF SILANE COUPLING AGENT. *Rubber Chemistry and Technology* **2015**, 88 (3), 359-372; (b) Costa, F.; Saphiannikova, M.; Wagenknecht, U.; Heinrich, G., Layered Double Hydroxide Based Polymer Nanocomposites. In *Wax Crystal Control · Nanocomposites · Stimuli-Responsive Polymers*, Springer Berlin Heidelberg: 2008; Vol. 210, pp 101-168.
12. Blume, A.; Gatti, L.; Luginsland, H.-D.; Maschke, D.; Moser, R.; Nian, J.; Röben, C.; Wehmeier, A.; Rodgers, B., Silica and Silanes. *Rubber Compounding: Chemistry and Applications, Second Edition* **2015**, 251-332.
13. Stenzel, O.; Blume, A.; Luginsland, H.-D.; Uhrlandt, S.; Wehmeier, A., Highly dispersible silica for using in rubber. Google Patents: 2013.
14. Hair, M. L., Hydroxyl groups on silica surface. *Journal of Non-Crystalline Solids* **1975**, 19, 299-309.
15. Hewitt, N.; Ciullo, P., *Compounding precipitated silica in elastomers: theory and practice*. William Andrew: 2007.
16. (a) Bhowmick, A. K., *Current topics in elastomers research*. CRC press: 2008; p 801-810; (b) Basila, M. R., Hydrogen bonding interaction between adsorbate molecules and surface hydroxyl groups on silica. *The Journal of Chemical Physics* **1961**, 35 (4), 1151-1158.

17. Dierkes, W. K., *Economic mixing of silica-rubber compounds: interaction between the chemistry of the silica-silane reaction and the physics of mixing*. University of Twente: 2005.
18. Stöckelhuber, K. W.; Das, A.; Jurk, R.; Heinrich, G., Contribution of physico-chemical properties of interfaces on dispersibility, adhesion and flocculation of filler particles in rubber. *Polymer* **2010**, 51 (9), 1954-1963.

Chapter 2

Literature review

2 Literature review

2.1 History of rubber reinforcement by fillers

Rubbers are one of the important material category widely used in many range of applications, like general purpose floor mat to highly engineered aerospace tyre applications¹⁻³. From the perspective of strength, rubbers are considered as soft materials and it needs some of ingredients to achieve good mechanical performance, ozone and oxygen resistance etc. Reinforcement of rubbers by fillers is a common practice in the field of rubber science and technology. In the early years of 20th century, zinc oxide was the most widely used reinforcing filler in rubber and the abrasion resistance provided by that preferred filler in tyre treads⁴. It was also during this period that zinc oxide was discovered to be the activator for the newly emerging organic accelerators. In 1912 B. F. Goodrich purchased patent rights to tyre carcass cord and acquired carbon black compounding technology in tyres. By the end of World War I carbon black had replaced zinc oxide in pneumatic tyres tread compounds although it took more than five years thereafter for the tyre manufacturers to convince the general public that black tyres were superior performance than white⁴. In 1930s with the introduction of precipitated calcium carbonate and In 1940s with the development of calcium silicate and precipitated silica further eliminates zinc oxide from the tyres. Finally carbon black is considered as the premier reinforcing filler for rubbers⁴. The rubber fillers are generally classified into three main categories like reinforcing, semi-reinforcing and non-reinforcing fillers and some of the filler materials belong to these types are given in Fig. 2.1. The rubber fillers are technically classified according to their particle size, surface area, structure and surface activity which are the dominant characteristics which are mainly determining the rubber reinforcement⁵⁻⁶.

a) Particle size: The rubber fillers with particle size above 10000 nm (10 μm) are generally not used because such bigger particles can reduce the performance rather than the reinforcement⁵. The size of the filler particle exceeds the polymer interchain distance; the filler particle introduces an area of localized stress. This contributes to rupture of elastomer chains on continuous flexing or stretching. Likewise fillers with particle size between 1000 and 10000 nm (1 – 10 μm) are used as a diluents and usually do not contribute for significant effect on final rubber properties. Such fillers are considered as non-reinforcing or inert fillers. The main purpose of inert fillers is added to reduce the cost, to improve the processability and optimize the die-swell properties of the rubber compound. Semi-reinforcing fillers the particle sizes are ranges from 100-1000 nm and it improves strength and modulus to some extent.

These fillers are generally used to achieve moderate mechanical properties, improved set properties and higher damping properties. Reinforcing fillers are in the range of 1 to 100 nm, and are greatly improving the final mechanical properties like greater increase in modulus, strength, abrasion and tear resistance of rubber.

b) Surface area: Filler particle must have an intimate contact (adsorption) with the polymer chains to contribute to a good reinforcement of the composite. Fillers with larger surface area have a greater contact area with rubber chains and ultimately have higher potential to reinforce the rubber matrix⁶. The shape of the particle is also considered to be an important criterion for reinforcement. The particles with plane or layer shape have more specific surface available for contacting the rubber chains than spherical particles. Nano-clay and graphene have a planer shaped morphology that align with the rubber chains during mixing and processing thus contribute more reinforcement than a spherical shaped particle with similar average particle size⁵. Carbon black and silica are fillers exhibiting spherical shaped primary particles, but their aggregates and clusters are anisometric and considerably smaller than the particles of micro clay and others. They have more surface area per unit weight available to contact the rubber. The surface area for rubber grade carbon blacks are vary from 6 to 250 m²/g, precipitated silica range from 30 to 220 m²/g and micro clay ranges from 20 to 25 m²/g.⁵

c) Structure: According to the structure, the fillers are normally categorized into low structure and high structure⁵. The high structure filler has aggregates preferring high particle count, with those individual particles combined in chain-like clusters and random branching of additional particle. The higher structure in fillers turns the rubber into greater reinforcing potential. In case of silica and carbon black, a certain amount of structure existed by the manufacturers, but it can be lost after compounding. The high shear forces generated during rubber mixing will break down the weaker aggregates and agglomerates of aggregates. According to BS 2955:1993 standard, the agglomerate is considered as a group of particles loosely bound together by contact at their corners and edges, which can be broken by mechanical forces and dispersed readily. Aggregate is a group of particles, which are rigidly bound to each other as by growing together or by partial fusion and not dispersed readily⁵⁵. For rubber reinforcement, the primary particles are in the size of less than 30 nm and the secondary particles are in the range of 30 - 150 nm. The combination of multiple secondary particles around the range of 150 nm to 1 µm called as aggregates. The numerous aggregates are joined around the range 1 µm to 100 µm called as agglomerates. However the final

persistent filler structure that exists in the rubber compound significantly affects the processability and final properties of rubber products⁵.

d) Surface activity/functionality: A filler material with high surface area and high structure can still provide a relatively poor reinforcement, if it has a low specific surface activity⁵. The specific activity of the filler surface per square centimeter (cm^2) of filler-elastomer interface is determined by the chemical and physical nature of the filler surface in relation to that of the elastomer. The surface energy and polarity of filler and polymer matrix should be similar, to obtain best compatibility. Therefore, non-polar fillers are best suited to non-polar elastomers and polar fillers work efficiently in polar elastomers. Apart from this general physio-chemical compatibility rule, the potential reaction between the elastomer and active filler functional sites is playing an important role. The chemical nature of carbon black surface is variable. Some evidences exist in the literature for the presence of a small amount of carboxyl, phenol, lactone, quinone and other functional groups on the surface which promote a higher affinity to rubber^{7,56}. Along with this high surface area of carbon black, the close contact of rubber chains to chemically react and form a strong interfacial layer (gel or crosslink). The non-black fillers offer less affinity due to less surface activity towards elastomers. Most of the non-black fillers like silica, clays and silicates have a surface of silanols ($-\text{SiOH}$). These silanol groups behave as acids ($-\text{SiOH}^+$) and are chemically more active. These issues can be overcome by the addition of silane coupling agents⁵.

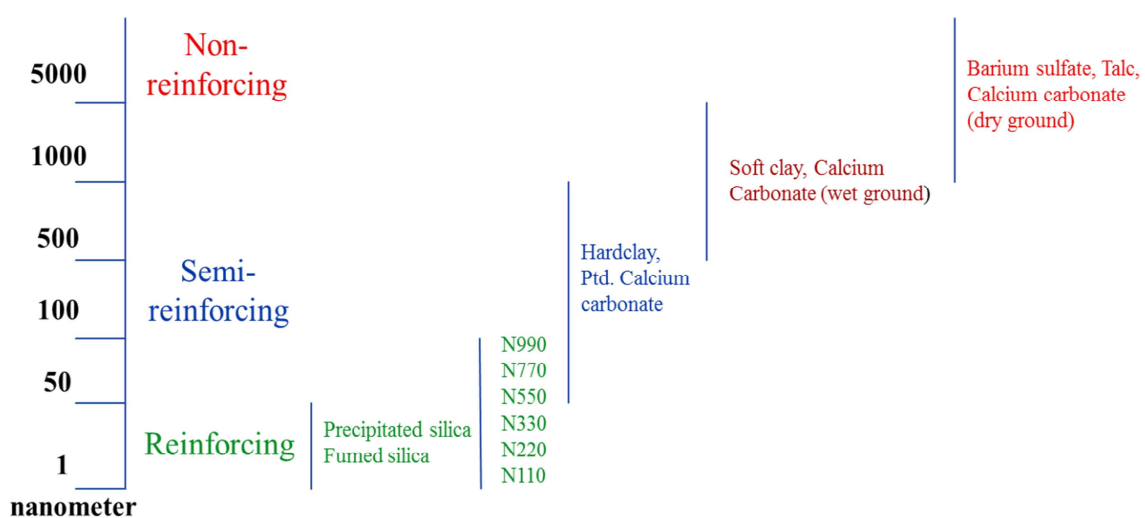


Figure 2.1 Classification of rubber fillers

2.2 Carbon black reinforcement of rubbers

Carbon black is an elemental carbon material presented in the form of fine amorphous particles. The particles are composed of randomly oriented microcrystalline layered arrays of condensed carbon rings^{5-6, 8}. Because of their random orientation, many arrays expose open layer edges with unsatisfied carbon bonds at the particle surface and provide the sites for chemical activity. Individual spherical carbon black primary particles do not exist and mostly it appears as aggregates, which may form clusters or chains of various sizes and configurations. The functional carbon black particles are actually highly aggregated in structure. The average particle size and aggregated structure are the major determinants of the utility of a given carbon black in a specific rubber compound. Prior to World War II, the channel black was the most predominant reinforcing material, prepared by the partial combustion of natural gas infringing on iron channels. According to particle size they classified in to hard processing channel black (HPC), medium processing channel black (MPC) and easy processing channel (EPC)^{6, 9}. The average particle size obtained from channel process is around 24 nm to 30 nm according to the type of channel grades; however, the channel blacks are not popular in rubber technology, because of its high cost.

Table 2.1 ASTM nomenclature of carbon blacks⁵⁷

ASTM Series	Classification	Average particle size (nm)
N100	SAF-Super Abrasion Furnace	11-19
N200	ISAF-Intermediate Super Abrasion Furnace	20-25
N300	HAF-High Abrasion Furnace	26-30
N400	FF-Fine Furnace	31-39
N500	FEF-Fast Extrusion Furnace	40-48
N600	GPF-General Purpose Furnace	49-60
N700	SRF-Semi Reinforcing Furnace	61-100
N800	FT-Fine Thermal	101-200
N900	MT-Medium Thermal	201-500

The thermal process is introduced in 1922, to make the largest particle size and lowest structure blacks. Thermal blacks are made by the thermal decomposition of natural gas in the absence of air in a cylindrical furnace. Thermal black grades are ranging from 100 to 500 nm of average particle size and used as a low cost functional extender fillers. Large particle size

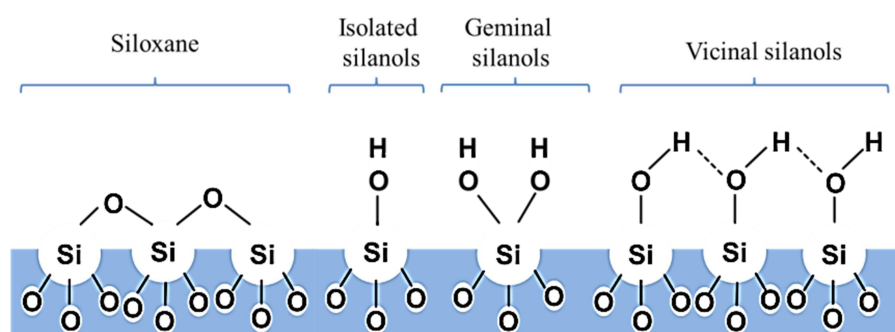
and lower structure enable higher loading, better resilience and lower hysteresis than highly reinforcing blacks.

In the early 1940s the channel blacks are replaced by the development of furnace blacks. The obtained furnace grades are relatively coarse particle structure and average size of particle is from 60 to 80 nm. After the invention of styrene butadiene rubber (SBR) the finer grade furnace blacks are developed. Furnace blacks are produced by the partial thermal decomposition of heavy oils or gases in a horizontal furnace. Furnace production offers the manipulation of reaction time and conditions, which result in some degree of tailored final products. Before 1968, carbon blacks nomenclature was informal and based on a variety of characteristics like level of abrasion, level of reinforcement, modulus of vulcanizates, processing properties, general applications, particle size and electrical conductivity⁵. In 1968, the ASTM committee established a new carbon black nomenclature system consisting of a prefix continued by a three digit number and given in Table 2.1. The prefix is either N for normal curing and S for slow curing characteristics of rubber. Channel blacks are usually yields slow curing and they have discontinued after all current rubber grade blacks are carry the N prefix. According to carbon black nomenclature, the first of the three digits indicates a range of average particle size in nanometer. The second and third digits are assigned by the ASTM committee to the developed new products¹⁰. In general low structure blacks are assigned lower numbers and higher structure blacks assigned as higher numbers.

2.3 Silica reinforcement of rubbers

In last few decades, precipitated silica has been used as reinforcing fillers in tyre tread compounds due to their versatile performance in terms of rolling resistance and wet skid resistance¹¹. The morphology and chemical structure of silica is an important criterion, playing major role on silica filled rubber composites¹²⁻¹³. The silica used in rubber is generally divided in to two main categories like precipitated and fumed silica. The precipitated silica is prepared by the reaction of sodium silicate (water glass) and sulphuric acid solutions or a mixture of carbon dioxide and hydrochloric acid are added simultaneously with agitation to water and precipitated under alkaline conditions⁴. The discrete silica particles initially form the primary particles, fuse into aggregates, which form loose agglomerates. The precipitate is filtered, washed of residual sodium sulfate or sodium chloride, dried and milled. The average primary particles are around 10-30 nm rather than the aggregates of 30-150 nm. The fumed silica is prepared by oxidation of silicon tetrachloride at very high temperatures. In this category fumed silica has a very low bulk density and the fumed silica reinforcement is well

popular for silicone rubber and other saturated rubbers. However, in the role of general purpose diene rubber reinforcement, fumed silica is not so popular because of its high price. Technically, precipitated silicas consist of high dense, low-structured aggregated particles. The size and structure of the precipitated silica aggregates/agglomerates are altered by the grinding or spray drying process. Silicas produced by pyrogenic process take the form of chain like branched aggregates which results in a low dense, highly fluffy powder¹⁴. Precipitated and fumed silica show significant differences in its loss on drying and loss on ignition. Precipitated silicas originate from an aqueous solution and therefore it contains a higher amount of water around 3 to 7%¹⁴. In this role, precipitated silica got more importance in tire applications because of its lower cost and easier capability to get modified in its chemical structure through silane reaction. In principle, fumed silica also can be modified by silane coupling agents. However, the degree of modification on fumed silica surface is limited due to the lower amount of silanol groups and lower coupling efficiency as compared to precipitated silica. Silica (silicon dioxide) is an amorphous material, consisting of silicon and oxygen atoms and connected in random network like three dimensional structure with appropriate amount of hydroxyl functionality (silanol, Si-OH). The generalized chemical name of silica is ‘silicon dioxide’. Due to the inherent chemical structure of silica, it is capable to absorb the atmospheric moisture and known as ‘‘hygroscopic material’’⁴. The chemical structure of the silica surface is given in scheme 2.1.



Scheme 2.1 Chemical structure of the silica surface

Generally, the silica surface contains three types of silanol groups: isolated, geminal and vicinal¹⁵. The silanol groups are directly responsible for the polarity and hygroscopic property of silica. The silanol groups have a strong tendency to form hydrogen bondings with neighboring particles which results the formation of aggregates. However, the reinforcing characteristic of silica is dependent on the specific surface area, particle size and distribution, porosity and silanol density^{4, 11}. Precipitated silica in rubber is usually considered as a

reinforcing and semi-reinforcing filler category. Due to the hydrophilic nature, it has poor compatibility and interaction with polymer chains when compared to carbon blacks. In further comparison to carbon black, the abrasion resistance, high viscosity during processing, slow cure rates is some of the drawbacks encountered by addition of silica in various rubbers. However, these issues have been further rectified by the use of silane coupling agents in silica filled rubber compounds. The nano/micro scale dispersion of silica is one of the key factors to determine the final performance of silica composites and further addition of silane coupling agent greatly improve the filler-polymer interactions. The essential role of silanes is to chemically modify the silica surface into a hydrophobic surface to reduce the filler-filler interaction as well as to enhance the rubber-filler interaction through the strong covalent bond with rubber chains in the case of sulphur containing silanes. There are plenty of silane coupling agents commercially available in the market. However, sulphur functionalized silane coupling agents are more common in tyre and other rubber product applications due to its dual coupling behavior between the polymer as well as silica. In this category (3-Mercaptopropyl)trimethoxysilane (MPTES), bis[3-(triethoxysilyl)propyl]disulfide (TESPD), bis[3-(triethoxysilyl)propyl]tetrasulfide (TESPT), 3-Octanoylthio 1-propyl triethoxysilane (NXT) are some of the sulphur based bi-functional silane coupling agents used in rubber industries. These silanes have the ability to modify the silica surface by silanization reaction as well as the sulphur atoms are capable to establish a covalent bond to the rubber chains. From the reinforcement point of view the precipitated silica combined with silane is offering superior performance compared to carbon black filled rubber systems in many aspects. Proper selection of silane coupling agent and effective silanization of silica are the major contributing parameters deciding the rolling resistance, wet grip properties and abrasion properties of tyres.¹⁶

2.4 Needs and essentials in silica technology

1. State of silica dispersion

Dispersion of silica in rubber is one of the major issues encountered in rubber industries. As mentioned previously, higher surface energy difference between silica and rubber and strong tendency to form hydrogen bonding with neighboring silica particles, which results in the formation of agglomerates. However, the incorporation of silane coupling agents enhances the silica dispersion in rubber. The development of highly dispersible silica (HDS)¹⁷

reinforces the rubber matrix efficiently and replaces carbon black partially or fully in the tyre tread compounds. Such HDS silica offers an improved rolling resistance, wet traction and without sacrificing the abrasion properties. Nevertheless, to improve the silica dispersion, rubber industries are consequently looking for improved mixing method, mixing cycles and alternative silane coupling agents.

2. Improved processability

Processability is the major issue in silica filled rubber compounds due to its hydrophilic nature which leads to poor compatibility rubber matrix. The strong hydrogen bonding between silica to polymer, interaction between silica to silica particles eventually leads to increase the viscosity and storage hardness of mixed stocks which affects the processability of rubber compounds⁴.

3. Low volatile content

To enhance the rubber-silica interaction most of the highly filled precipitated silica compounds are subjected to silane treatment which is generally called 'silanization'¹⁸. The active reaction between silica and silane lead to significant amount of ethanol formation, which is a volatile organic component and can cause some health problems and environmental issues¹⁹. Similarly, the formation of ethanol which reduces the rate of shear between the mixing chamber and rotor causes the reduction in mixing efficiency, longer mixing cycle and affecting the final quality of mix¹⁹.

4. Reduction in number of mixing cycles

Dispersion of silica in rubber is not a single parameter dependent process. The new developments in mixing equipment, mixing sequences and mixing cycles are also eventually needed to disperse the silica effectively in rubber matrix²⁰.

5. Low filler-filler interaction

The most of winter tyre tread compounds are containing large amount of silica (> 70 phr) to achieve improved wet skid properties and rolling resistance. The higher loading of silica in rubber leads to the percolated network of silica and these networks are more sensitive to dynamic mechanical strains²¹⁻²². This percolated network usually referred as interaction between filler to filler which is an adverse effect reduces the final performance of the

composites²³. It is necessary to make a rubber compound with lower filler-filler network and it can be only achieved through by the improved dispersion of silica in rubber compounds.

6. Improved abrasion resistance

The abrasion performance of silica filled rubber composites is lower than in carbon filled system. The new development in silica technology like highly dispersible silica, high surface area silica filled rubber composites mutually shows improved wet grip, rolling resistance properties without sacrificing the abrasion properties. However the achieved abrasion level is still inferior as compared with carbon filled system²⁴.

7. Hindering the vulcanization efficiency and reduce rate of vulcanization

Silanol groups are present on the surface of silica, which are able to react with oxygen or nitrogen containing compounds like glycols, water, alcohols, amines and divalent metal salts. Among these reactions that soluble zinc salts (ZnO and stearic acid mixture) forms during the vulcanization reaction is the major factor to be considered in silica compounding process. The reaction of the silica surface with soluble zinc salts is given in Figure 2.2 and the reaction takes place in two steps⁴. In the first step, the formation of soluble zinc ion by the reaction of zinc oxide with a fatty acid, secondly zinc becomes securely bound to one or two silanols. The insertion of zinc ion on the surface of silica transfers part of the free water and creates a heterogeneous surface in which the ratio of zinc-to-water is variable⁴. This ratio increases significantly, when the water is driven off by high mixing temperatures or when zinc oxide is added early in the mixing schedule. The ratio of zinc-to-water is reduced when the additions of silane, glycols or amine substances compete with soluble zinc for silanol attachment⁴. High ratios of zinc-to-water lead to a loss of soluble zinc from its cure activating function and lead to reductions in cure rate, mono and disulfide crosslinks and high strain modulus. These effects are accompanied by excessive elongation, set and heat build-up. At the same time, the presence of zinc on the silica surface reduces silica-polymer bond strength with a resulting loss in abrasion resistance⁴. Similarly silica containing compounds are accelerated with basic products such as diphenyl guanidine (DPG) or di-ortho-tolylquanidine (DOTG), a certain amount of accelerator is taken up by the silica and reduces the rate of vulcanization². A zinc-free curing system used with solution polymers or add the zinc salts after the silane modification has been effective in overcoming these characteristic silica compounding problems⁴.

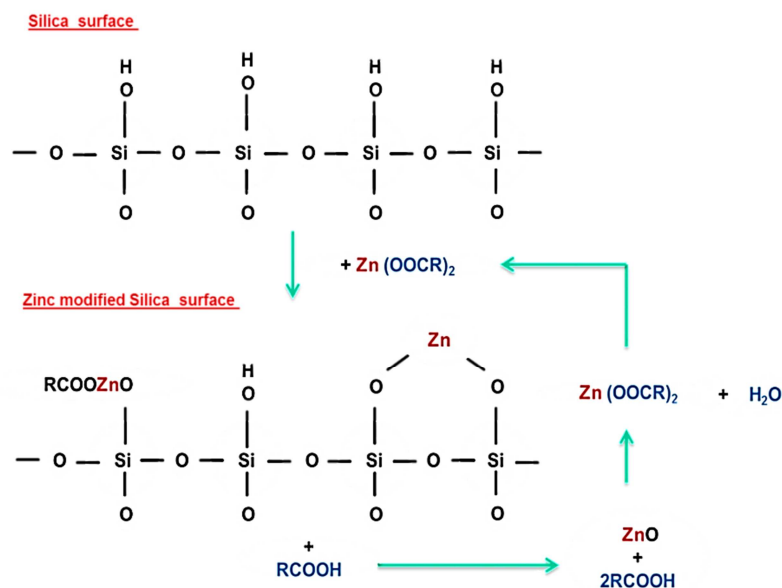


Figure 2.2 reaction between silica surface and soluble zinc salts

8. Narrow processing window leads to a compromise in limited rate of silanization at low temperature as well as scorch issues at higher temperature.

In silica-silane system the effective silanization is achieved between 140 °C to 160 °C mixing temperatures¹⁶. At the same time temperatures above 160 °C the silane molecules (sulphur contained) may undergo premature cure reactions¹⁶. The sulphur-sulphur bonds in silane coupling agents are weak and broken during the excess heat generated during the mixing process. This cleavage of silane sulphur molecules may donate free sulphur in to rubber compound mainly with high sulphur contained silane like TESPT. Above the 160 °C the available free sulphur can react with rubber causes the premature vulcanization²⁵.

2.5 State of the art: Sol-gel silica based rubber composites

The first in-situ sol-gel reaction in silicone rubber matrix was performed by J.E. Mark in 1981²⁶. Several techniques are developed to produce silica particles inside the rubbers such as latex method, solution method, in-situ polymerization method, swelling method and condensation of alkoxysilane.

a) Latex method

Latex method is one of the simplest methods to generate silica particles in rubber compared to other methods. The silica synthesis by latex technique is prepared by the addition of a silica precursor (TEOS) into concentrated natural rubber latex in presence of alkaline

catalyst (ammonia) with a controlled amount of water. Prasertsri et al.²⁷ prepared approximately 10-30 phr of silica in NR by this latex method. They have reported that without bis[3-(triethoxysilyl)propyl]tetrasulfide (TESPT), NR/in-situ silica composites exhibited higher reinforcement when compared to conventional silica filled NR composites. Tangpasuthadol et al.²⁸ also prepared NR/in-situ silica composites, Yoshikai et al.²⁹ prepared in-situ silica in SBR and NBR latex by sol-gel method and mentioned that the obtained silica particles are nearly 100-200 nm and the tensile strength of SBR and NBR was improved over of 30 MPa and 25 MPa respectively. The main advantages of latex technique is simple, cost effective, no need of additional catalyst (most of the latices are preserved under alkaline condition) to initiate the sol-gel reaction. There are few disadvantages like difficult to control the particle size by tuning the reaction conditions (temperature, pH etc.), avoiding premature coagulation of latex during the reaction and finally most of the rubbers are not often available in latex form.

b) Swelling method

Swelling method is also explored for the past few decades because of easy processing capability, controlled particle growth and low agglomeration tendencies. This method is involved in a two-step process; in the first step a thin sheet of rubber is swollen in a silica precursor (TEOS) for a certain period of time and in the second step the swollen rubber is immersed in the catalyst solution. The amount of silica in rubber is mainly controlled by the diffusion rate of TEOS into rubber and dwelling time of swollen rubber into the catalyst solution. Recently, Miloskovska et al.³⁰⁻³² studied the sol-gel silica formation by swelling method in natural rubber and EPDM rubber. They reported the diffusion mechanism of TEOS into rubber, silica formation and size particle size changing with respect to reaction conditions. Das et al.³³ reported the effect of sol-gel derived silica in TESPT silane grafted EPDM rubber and investigated the silica dispersion on the cure characteristics, dynamic mechanical performance of such composites. Last two decades there has been several works reported by Ikeda et al.³⁴⁻³⁷, Kohjiya et al.³⁸⁻³⁹, Murakami et al.⁴⁰⁻⁴¹, Tanahashi et al.⁴² about the in-situ silica filling in vulcanized as well as unvulcanized various rubber matrices. However, this process is relatively time consuming compare to other techniques because of the longer processing time. Nevertheless, swelling method is mainly suited for vulcanized rubbers, as most of the unvulcanized diene rubbers are soluble in silica precursor (TEOS) as well as it is difficult to achieve higher amount of silica in the rubber because of the near solubility parameter between the rubber and TEOS. Moreover, generating silica particles in

vulcanized rubber cannot be a good practice for rubber industries as it deforms the final shape of product and is also difficult to apply this technique for big rubber products like tyres.

c) in-situ polymerization method

In this method, the silica particles are prepared by the simultaneous synthesis of polymer as well sol-gel reaction together like as one pot method. Haraguchi et al⁴³ reported the hybrid composites based on phenolic resin and silica prepared by in-situ polymerization technique. They reported that the obtained composites are transparent and translucent properties in nature; the optical properties of such composites were altered by the size and aggregated behavior of silica in composites. Matějka et al⁴⁴ reported organic-inorganic hybrid composites based on rubbery crosslinked epoxy with in-situ sol-gel derived silica composites by simultaneous polymerization and sol-gel reaction. They mentioned that less than 10 vol% of silica in rubbery epoxy enhanced the two orders of magnitudes of tensile modulus as well as dynamic mechanical properties. Jang et al⁴⁵ reported the in-situ sol-gel process of polystyrene-silica hybrid material and the effect of silane coupling agents. Also they reported that the modification of silane enhances the thermal degradation properties of composites. Zhong Ma et al.⁴⁶ prepared polyacrylate-silica composites by sol-process via emulsion polymerization. The influence of synthesis conditions and effect of silica modification by APTES silane coupling agent were studied with respect to the composite properties. Also the dynamic light scattering study indicated that the size of the particles is around 177 nm. However the above mentioned methods are till now explored only on plastic based nanocomposites not in rubber based composites.

d) Condensation of alkoxysilanes

By this technique one can prepare the functionalized or organically modified silica particles by using different silane coupling agents. The silane coupling agents are highly reactive with water resulting into organo-inorganic nanoparticles. The silica nanoparticles prepared by this technique consist of modified alkyl or aliphatic chains, which improve the compatibility with polymer. Wahba et al⁴⁷ prepared silica-rubber nanocomposites by in situ sol-gel synthesis of trialkoxysilane as silica precursors with different functionalized silane coupling agents. The functional groups are included (a) alkyl and alkenyl groups like triethoxy(vinyl) (VTEOS), triethoxy(propyl)(PTEOS), triethoxy(octyl) (OCTEOS) (b) nitrogen containing alkyl groups like triethoxy(3-aminopropyl) (APTEOS), triethoxy(3-cyanopropyl) (CPTEOS), triethoxy(3-propylisocyanate) (ICTEOS) (c) sulphur containing

groups like trimethoxy(3-mercaptopropyl)(TMSPM), triethoxy(3-octanoylthio-1-propyl) (NXT), bis(3-triethoxysilylpropyl) disulphide (TESPD), bis(3-triethoxysilyl) tetrasulphide (TESPT). They reported that the functionality of silica precursors mainly contributes to the shape of the silica particles, filler-filler effect, filler-rubber interaction and dynamic performances of rubber composites. Pietrasik et al⁴⁸ reported silica-carboxylated nitrile butadiene rubber hybrids prepared by the N-(2 aminoethyl)-3-aminopropyltrimethoxy silane as a source of silica precursor as well as a crosslinker. They investigated such silica composites by using dielectric relaxation spectroscopy, differential scanning calorimetry and dynamic mechanical experiments. In this work, it is explained that the molecular chain dynamics of rubber in α and β relaxations are not significantly affected by amount of in-situ silica formed and interaction. However α' relaxation process is affected at higher temperature due to the presence nano-ionic domains comprised with silica and rubber chains. Siramanont et al⁴⁹ prepared the sol-gel silica particles from the three alkyltriethoxy silanes like vinyltriethoxy silane, ethyltriethoxy silane, i-butyltriethoxy silane together with tetraethoxysilane in natural rubber latex. They reported further that the obtained silica particles are less than 100 nm in size and well dispersed in rubber matrix, which improved the tensile and tearing properties of natural rubber as compared to the conventionally silica incorporated composites.

e) Solution method

In solution technique the rubber is initially dissolved in a suitable solvent, and then the simultaneous silica precursor, water and catalyst are added. By simply heating and continuous stirring on the system silica nanoparticles can be grown by sol-gel process. At the end of the reaction, the reaction mixture is solidified by the evaporation of solvent or pouring into non-solvents. This technique is relatively simple and more controllable technique to achieve better particle size and a higher amount of silica concentration in polymer. Bandyopadhyay et al⁵⁰ prepared in-situ silica in acrylic rubber by using this solution method in presence of acid catalyst and the developed composites contained 20-90 nm of silica, which was confirmed by TEM analysis. The formed silica is dispersed throughout the ACM matrix as explored by SEM analysis. The so prepared composites offer higher tensile strength, tensile modulus and higher thermal stability. Mokhothu et al⁵¹⁻⁵² prepared EPDM rubber based in-situ silica composites with TESPT silane coupling agent and reported the homogenous dispersion of silica.

2.6 Expectation in tyre compounds

Nowadays precipitated silica is one of the major rubber ingredients in passenger car tyre tread and in near future it may replace carbon black from different rubber products like tyres, belts, rollers, seals, gaskets, anti-vibration pads, fuel hoses etc. However, vehicle tyres are one of the important engineering products and are expected to serve different purposes like carrying the load of the vehicle, sufficient grip on the road, better steering forces to guide the vehicle, better damping between the road and vehicle, good durability at high speeds and low fuel consumption.

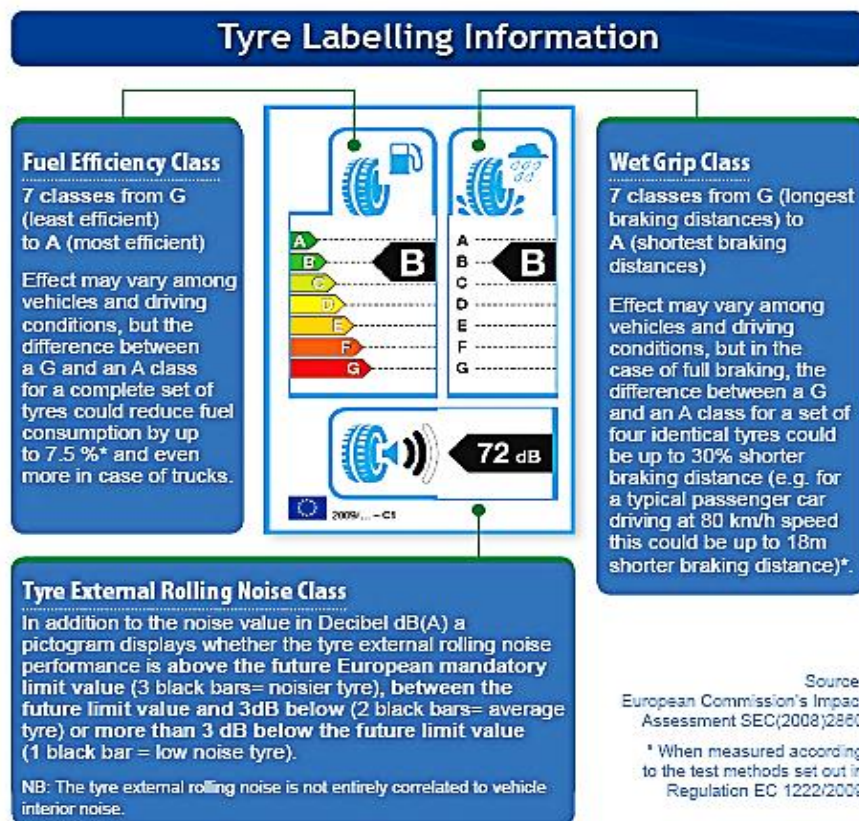


Figure 2.3 European Tyre labelling information⁵⁸

Simultaneously, in critical weather conditions like heavy rains and snow, the functional performance of tyres are further extended in the aspect of having better wet grip, ice grip properties as well as lower rolling noise. The tyre requirement and labelling information proposed by the European Tyre and Rubber Manufacturers Association⁵⁸ is given in Figure 2.3.

Considering the above critical issues the tyre manufacturers are trying to optimize the tyre performance in terms of wet grip, ice grip and rolling resistance including without scarifying

the abrasion behaviors when developing winter tyres. To achieve better tyre performance, the optimization of these parameters is usually considered as the balancing of ‘magic triangle’. The carbon black filled tyre compounds are initially a successful tyre material, because of its excellent abrasion resistance. After implementing the tyre labelling system, it is found that the carbon black filled tyres have higher loss factor ($\tan \delta$) at higher temperatures, which represents the higher rolling resistance of tyre tread compound and it is directly related to the higher fuel consumption of vehicles by tyres. These issues in tyres have been rectified by the partial (or major) replacement of carbon black by precipitated silica in tyre tread compounds (“Green tyres”). Especially precipitated silica filled solution styrene butadiene rubber compound in passenger car tyre application has become more popular due to their improved rolling resistance and wet skid resistance⁵³. The balance between the properties of the magic triangle is further extended to a ‘magic pentagon’ and precipitated highly dispersible silica filled solution styrene butadiene rubber system significantly improves this balances⁵⁴. The typical representation of tyre needs is given in Figure 2.4.

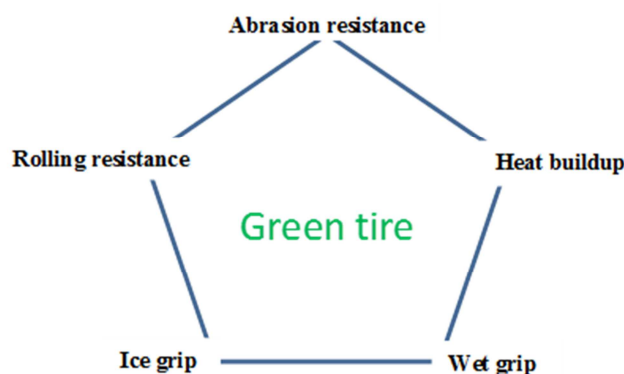


Figure 2.4 “Magic pentagon” in tyre technology

References

1. Rodgers, B., *Rubber compounding: chemistry and applications*. CRC Press: 2015, ISBN 9781482235494, 291-322.
2. Hofmann, W., *Rubber technology handbook*. Hanser Publishers. Distributed in the USA by Oxford University Press: 1989, ISBN 3446148957, 400-574.
3. Bhowmick, A. K., *Rubber products manufacturing technology*. CRC Press: 1994, ISBN 9780824791124, 1-932.
4. Hewitt, N.; Ciullo, P., *Compounding precipitated silica in elastomers: theory and practice*. William Andrew: 2007, ISBN 9780815515289, 1-525.
5. Ohm, R. F., *The vanderbilt rubber handbook*. RT Vanderbilt Company: 1990, 759.
6. Donnet, J.-B., *Carbon black: science and technology*. CRC Press: 1993, ISBN 9780824789756, 461.
7. Donnet, J.-B.; Voet, A., *Carbon black: physics, chemistry, and elastomer reinforcement*. M. Dekker: 1976, 0824763459, 351.

8. Morton, M., *Rubber technology*. Springer Science & Business Media: 2013, 62-63.
9. Blow, C. M., *Rubber technology and manufacture*. 1971, ISBN 0408005874, 561.
10. Morton, M., *Rubber technology*. Springer Science & Business Media: 2013, 69-72.
11. Blume, A.; Gatti, L.; Luginsland, H.-D.; Maschke, D.; Moser, R.; Nian, J.; Röben, C.; Wehmeier, A.; Rodgers, B., Silica and Silanes. *Rubber Compounding: Chemistry and Applications, Second Edition* 2015, 251-332.
12. Dierkes, W. K.; Cichomski, E.; Tolpekina, T.; Schultz, S.; Blume, A., *Influence of Silica Characteristics on Tire Performance Indicators*. In proceedings of 186th technical meeting, ACS Rubber division, Nashville, TN, USA: ACS Rubber Division 2014, 1-59.
13. Dierkes, W. K.; Blume, A., Silica Reinforcement. *Encyclopedia of Polymeric Nanomaterials* 2015, 2222-2228.
14. <https://www.aerosil.com/sites/lists/RE/DocumentsSI/Technical-Overview-AEROSIL-Fumed-Silica-EN>. last access date 22 July 2018.
15. Vilgis, T. A.; Heinrich, G.; Klüppel, M., *Reinforcement of polymer nano-composites: theory, experiments and applications*. Cambridge University Press: 2009, ISBN 9780511605314, 101-195.
16. Dierkes, W. K., *Economic mixing of silica-rubber compounds: interaction between the chemistry of the silica-silane reaction and the physics of mixing*. University of Twente: 2005, 233.
17. Stenzel, O.; Blume, A.; Luginsland, H.-D.; Uhrlandt, S.; Wehmeier, A., Highly dispersible silica for using in rubber 2015, US8597425B2.
18. Blume, A.; El-Roz, M.; Thibault-Starzyk, F., *Infrared study of the silica/silane reaction*, In proceedings 11th Fall rubber colloquium, Hannover, Germany 2014, 1-15.
19. Dierkes, W.; Noordermeer, J., Modeling and Practice of Ethanol-devolatilization of Silica-silane Rubber Compounds in an Internal Mixer. *International Polymer Processing* 2007, 22 (3), 259-265.
20. Leblanc, J.; Nijman, G., Engineering performance and material viscoelastic analyses along a compounding line for silica-based compounds, part 2: Nonlinear viscoelastic analysis. *Journal of applied polymer science* 2009, 112 (3), 1128-1141.
21. Ramier, J.; Gauthier, C.; Chazeau, L.; Stelandre, L.; Guy, L., Payne effect in silica-filled styrene-butadiene rubber: Influence of surface treatment. *Journal of Polymer Science Part B: Polymer Physics* 2007, 45 (3), 286-298.
22. Heinrich, G.; Klüppel, M., Recent advances in the theory of filler networking in elastomers. In Filled Elastomers Drug Delivery Systems, *Advances in Polymer science*, 2002, 106, 1-44.
23. Ten Brinke, J.; Debnath, S.; Reuvekamp, L.; Noordermeer, J., Mechanistic aspects of the role of coupling agents in silica-rubber composites. *Composites Science and Technology* 2003, 63 (8), 1165-1174.
24. Rattanasom, N.; Saowapark, T.; Deeprasertkul, C., Reinforcement of natural rubber with silica/carbon black hybrid filler. *Polymer Testing* 2007, 26 (3), 369-377.
25. Burhin, H., Quality control of "green tyre" compounds. *Kautschuk Gummi Kunststoffe* 2002, 55 (4), 175-182.
26. Mark, J.; Pan, S. J., Reinforcement of polydimethylsiloxane networks by in-situ precipitation of silica: A new method for preparation of filled elastomers. *Die Makromolekulare Chemie, Rapid Communications* 1982, 3 (10), 681-685.
27. Prasertsri, S.; Rattanasom, N., Mechanical and damping properties of silica/natural rubber composites prepared from latex system. *Polymer Testing* 2011, 30 (5), 515-526.
28. Tangpasuthadol, V.; Intasiri, A.; Nuntivanich, D.; Niyompanich, N.; Kiatkamjornwong, S., Silica-reinforced natural rubber prepared by the sol-gel process of ethoxysilanes in rubber latex. *Journal of applied polymer science* 2008, 109 (1), 424-433.

29. Yoshikai, K.; Ohsaki, T.; Furukawa, M., Silica reinforcement of synthetic diene rubbers by sol–gel process in the latex. *Journal of applied polymer science* 2002, 85 (10), 2053-2063.
30. Miloskovska, E.; Friedrichs, C.; Hristova-Bogaerds, D.; Persenair, O.; van Duin, M.; Hansen, M. R.; de With, G., Chemical Mapping of Silica Prepared via Sol–Gel Reaction in Rubber Nanocomposites. *Macromolecules* 2015, 48 (4), 1093-1103.
31. Miloskovska, E.; Hansen, M. R.; Friedrich, C.; Hristova-Bogaerds, D.; van Duin, M.; de With, G., In Situ Silica Nanoparticle Formation in a Rubber Matrix Monitored via Real-Time SAXS and Solid-State NMR Spectroscopy. *Macromolecules* 2014, 47 (15), 5174-5185.
32. Miloskovska, E.; Nies, E.; Hristova-Bogaerds, D.; van Duin, M.; de With, G., Influence of reaction parameters on the structure of in situ rubber/silica compounds synthesized via sol-gel reaction. *Journal of Polymer Science Part B: Polymer Physics* 2014, 52 (14), 967-978.
33. Das, A.; Jurk, R.; Werner Stöckelhuber, K.; Heinrich, G., Silica-Ethylene Propylene Diene Monomer Rubber Networking by In Situ Sol-Gel Method. *Journal of Macromolecular Science, Part A: Pure and Applied Chemistry* 2007, 45 (1), 101-106.
34. Ikeda, Y.; Tanaka, A.; Kohjiya, S., Effect of catalyst on in situ silica reinforcement of styrene–butadiene rubber vulcanizate by the sol–gel reaction of tetraethoxysilane. *J. Mater. Chem.* 1997, 7 (3), 455-458.
35. Ikeda, Y.; Kohjiya, S., In situ formed silica particles in rubber vulcanizate by the sol-gel method. *Polymer* 1997, 38 (17), 4417-4423.
36. Ikeda, Y.; Katoh, A.; Shimanuki, J.; Kohjiya, S., Nano-Structural Observation of in situ Silica in Natural Rubber Matrix by Three Dimensional Transmission Electron Microscopy. *Macromolecular Rapid Communications* 2004, 25 (12), 1186-1190.
37. Ikeda, Y.; Tanaka, A.; Kohjiya, S., Reinforcement of styrene-butadiene rubber vulcanizate by in situ silica prepared by the sol-gel reaction of tetraethoxysilane. *Journal of Materials Chemistry* 1997, 7 (8), 1497-1503.
38. Kohjiya, S.; Ikeda, Y., Reinforcement of general-purpose grade rubbers by silica generated in situ. *Rubber chemistry and technology* 2000, 73 (3), 534-550.
39. Kohjiya, S.; Katoh, A.; Shimanuki, J.; Hasegawa, T.; Ikeda, Y., Three-dimensional nano-structure of in situ silica in natural rubber as revealed by 3D-TEM/electron tomography. *Polymer* 2005, 46 (12), 4440-4446.
40. Murakami, K.; Iio, S.; Ikeda, Y.; Ito, H.; Tosaka, M.; Kohjiya, S., Effect of silane-coupling agent on natural rubber filled with silica generated in situ. *Journal of materials science* 2003, 38 (7), 1447-1455.
41. Murakami, K.; Osanai, S.; Shigekuni, M.; Iio, S.; Tanahashi, H.; Kohjiya, S.; Ikeda, Y., Silica and Silane Coupling Agent for in Situ Reinforcement of Acrylonitrile-Butadiene Rubber. *Rubber Chemistry and Technology* 1999, 72 (1), 119-129.
42. Tanahashi, H.; Osanai, S.; Shigekuni, M.; Murakami, K.; Ikeda, Y.; Kohjiya, S., Reinforcement of Acrylonitrile–Butadiene Rubber by Silica Generated in situ. *Rubber Chemistry and Technology* 1998, 71 (1), 38-52.
43. Haraguchi, K.; Usami, Y.; Yamamura, K.; Matsumoto, S., Morphological investigation of hybrid materials composed of phenolic resin and silica prepared by in situ polymerization. *Polymer* 1998, 39 (25), 6243-6250.
44. Matějka, L.; Dukh, O.; Kolařík, J., Reinforcement of crosslinked rubbery epoxies by in-situ formed silica. *Polymer* 2000, 41 (4), 1449-1459.
45. Jang, J.; Park, H., In situ sol-gel process of polystyrene/silica hybrid materials: Effect of silane-coupling agents. *Journal of applied polymer science* 2002, 85 (10), 2074-2083.
46. Ma, J.-Z.; Hu, J.; Zhang, Z.-J., Polyacrylate/silica nanocomposite materials prepared by sol–gel process. *European Polymer Journal* 2007, 43 (10), 4169-4177.

47. Wahba, L.; D'Arienzo, M.; Donetti, R.; Hanel, T.; Scotti, R.; Tadiello, L.; Morazzoni, F., In situ sol–gel obtained silica–rubber nanocomposites: influence of the filler precursors on the improvement of the mechanical properties. *RSC Advances* 2013, 3 (17), 5832.
48. Pietrasik, J.; Gaca, M.; Zaborski, M.; Okrasa, L.; Boiteux, G.; Gain, O., Studies of molecular dynamics of carboxylated acrylonitrile-butadiene rubber composites containing in situ synthesized silica particles. *European Polymer Journal* 2009, 45 (12), 3317-3325.
49. Siramanont, J.; Tangpasuthadol, V.; Intasiri, A.; Na-Ranong, N.; Kiatkamjornwong, S., Sol-gel process of alkyltriethoxysilane in latex for alkylated silica formation in natural rubber. *Polymer Engineering & Science* 2009, 49 (6), 1099-1106.
50. Bandyopadhyay, A.; Bhowmick, A. K.; De Sarkar, M., Synthesis and characterization of acrylic rubber/silica hybrid composites prepared by sol-gel technique. *Journal of Applied Polymer Science* 2004, 93 (6), 2579-2589.
51. Mokhothu, T. H.; Luyt, A. S.; Messori, M., Reinforcement of EPDM rubber with in situ generated silica particles in the presence of a coupling agent via a sol–gel route. *Polymer Testing* 2014, 33, 97-106.
52. Mokhothu, T. H.; Luyt, A. S.; Morselli, D.; Bondioli, F.; Messori, M., Influence of in situ-generated silica nanoparticles on EPDM morphology, thermal, thermomechanical, and mechanical properties. *Polymer Composites* 2015, 36 (5), 825-833.
53. Heinrich, G.; Vilgis, T., Why Silica Technology Needs S-SBR in High Performance Tires?: The Physics of Confined Polymers in Filled Rubbers. *KGK. Kautschuk, Gummi, Kunststoffe* 2008, 61 (7-8).
54. Heinrich, G., *Advanced rubber composites*. Springer Science & Business Media: 2011, 239.
55. Nichols, G.; Byard, S.; Bloxham, M.J.; Botterill, J.; Dawson, N.; Dennis, Andrew.; Diart, D.; North, C.N.; Sherwood, J.D.; A review of the terms of agglomerate and aggregate with a recommendation for nomenclature used in powder and particle characterization. *Journal of Pharmaceutical sciences* 2002, 91(10), 2103-2109.
56. Maurice Morton, *Rubber technology*. third edition, Chapman and hall publication, ISBN 0412539500, 1995, 69.
57. John S. Dick., *Rubber technology-compounding and testing for performance*, 2nd edition, Hanser publications, ISBN 978-3-446-42155-4, 2009, 301-303.
58. www.etrma.org/tyres/tyre-labelling, last access date: 22 July 2018.

Chapter 3

Experimental section

3 Experimental section

3.1 Materials

3.1.1 Rubber

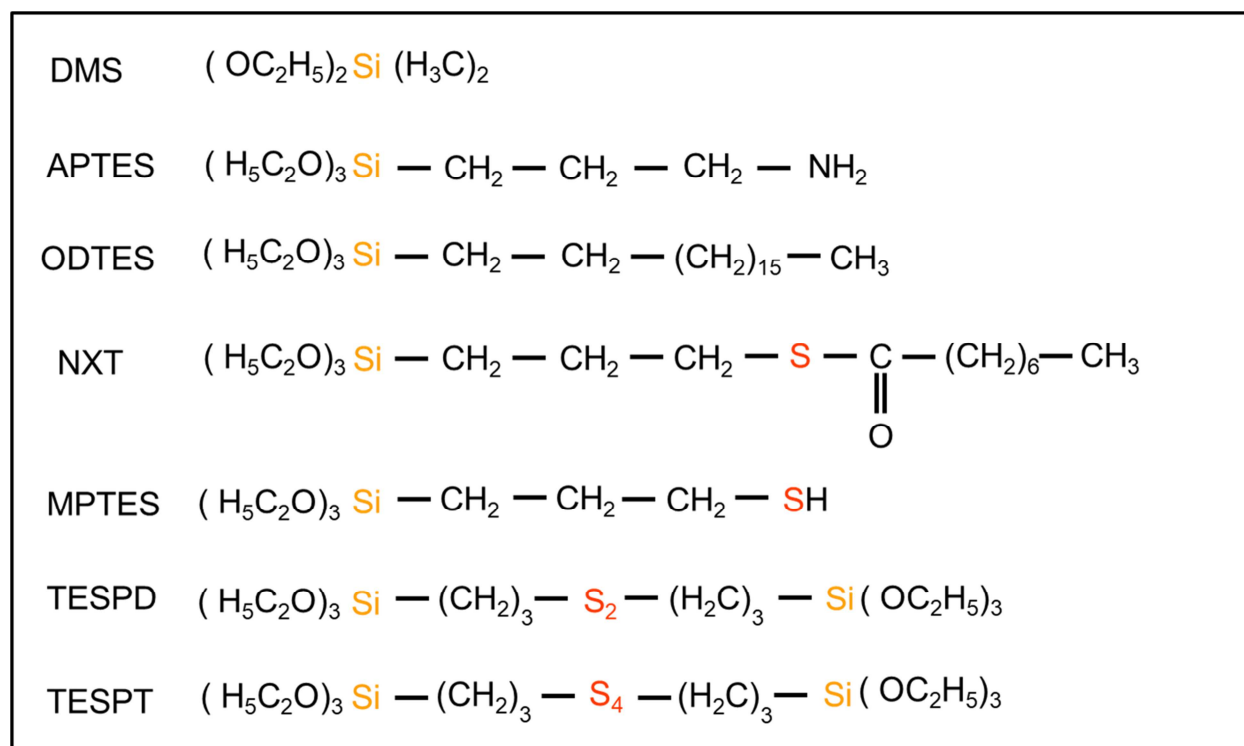
Solution styrene butadiene rubber (SSBR) BUNA 2525-0 VSL HM was supplied by Lanxess AG, Germany. The rubber containing 25 % of vinyl content, 25% of styrene content with the Mooney viscosity (ML (1+4) 100 °C) of 56 was used for this study.

3.1.2 Silica and silane coupling agent

The precipitated silica (ULTRASIL VN3 GR) was kindly supplied by Evonik Industries (Essen, Germany), having a purity of 99 %. The specific surface area (N_2) of precipitated silica 175 m²/g, heating loss percent of around 5.5 at 2h, 105 °C (ISO 787-2) electrical conductivity of < 1300 μ S/cm with pH of 6.2. The chemical structures and details of used different silane coupling agents were given in scheme 3.0 and table 3.1.

Table 3.1 Technical details of different silane coupling agents

Chemical name	Supplier	Molecular weight (g/mol)	Purity (%)
Tetraethoxyorthosilicate (TEOS)	Sigma-Aldrich	208.32	96
Diethoxydimethyl silane (DMS)	Sigma-Aldrich	148.28	97
(3-Aminopropyl) triethoxysilane (APTES)	Sigma-Aldrich	221.37	99
n-Octodecyltriethoxysilane (ODTES)	Sigma-Aldrich	374.68	98
3-Octanoylthio 1-propyl triethoxysilane (NXT)	Momentive	364.61	99
(3-Mercaptopropyl)trimethoxysilane (MPTES)	Evonik	196.33	99
bis[3-(triethoxysilyl)propyl]disulfide (TESPD)	Evonik	474.82	99
Bis(3-triethoxysilylpropyl)tetrathiolane (TESPT)	Evonik	538.94	99



Scheme 3.0 Chemical structure of different silane coupling agents

3.1.3 Other rubber ingredients

The details about the other rubber ingredients and chemicals used in this work are given in Table 3.2.

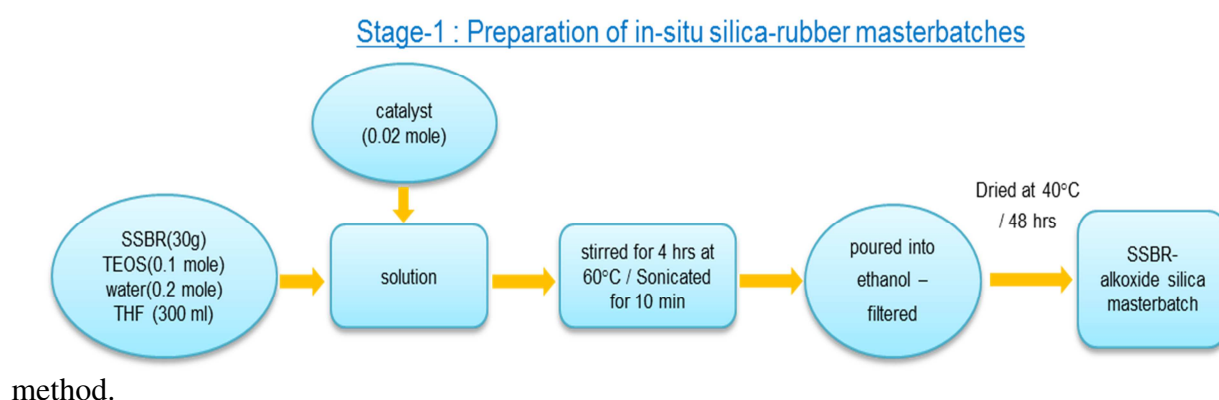
Table 3.2 Technical details of different chemicals

Chemical name	Supplier	Molecular weight	Purity (%)
N-butylamine	Acros organics	73.13	99
Zinc oxide	Acros organics	81.38	99.5
Stearic acid	Acros organics	284.47	97
N-Cyclohexyl 2-benzothioazole sulphinamide (CBS)	BAYER-Vulkacite CZ	264.405	99.5
Diphenyl Guanidine (DPG)	Lanxess chemicals	211.26	99.5
Sulphur	Acros organics	32.05	99.5

3.2 Preparation of sol-gel in-situ silica and precipitated silica based rubber compounds

3.2.1 Preparation of rubber-silica masterbatches

The preparation of SSBR-silica composites was carried out in two stages. In the first stage, silica-rubber masterbatches were prepared. To a rubber solution with 30 g of SSBR in 300 ml of THF (tetrahydrofuran), 0.1 mole of TEOS and 0.2 moles of water were added in a round bottom flask. Then 0.02 moles of n-butylamine were added as a catalyst and the whole homogenous mixture was stirred and refluxed for 4 hours at 60 °C. The obtained white viscous solution mixture was ultrasonicated for 10 min to avoid the pre-agglomeration of silica particles. The sonicated solution was then slowly poured into 900 ml of ethanol to solidify and precipitate the silica-rubber phase immediately. The precipitated mass was collected by simple filtering process, washed with ethanol and dried for 48 hours at 40°C in hot air oven to evaporate the trace solvents. The dried mass contained only the SSBR matrix with sol-gel silica particles. By varying the quantity of TEOS and water (with the same mole ratio of 1:2) different volume fractions of silica in rubber were prepared and quantified by TGA. The detailed synthesis procedure in flow chart is given in scheme 3.1. For the investigation of in-situ silica particles, the particles were removed from the immediate synthesis of in-situ silica in rubber solution by directly pouring into THF solvent instead of ethanol. The removed particles were washed multiple times using THF by centrifugal



Scheme 3.1 Flow chart of in-situ silica-SSBR masterbatches preparation

3.2.2 Compounding with ingredients

In the second stage, the rubber-silica masterbatches were compounded with pure SSBR, silane and the vulcanizing ingredients. Hereby, in a first step, the SSBR/in-situ silica

masterbatch with an appropriate amount of raw SSBR was given into a Haake Rheomix 600P internal mixer (Fig. 3.1a).

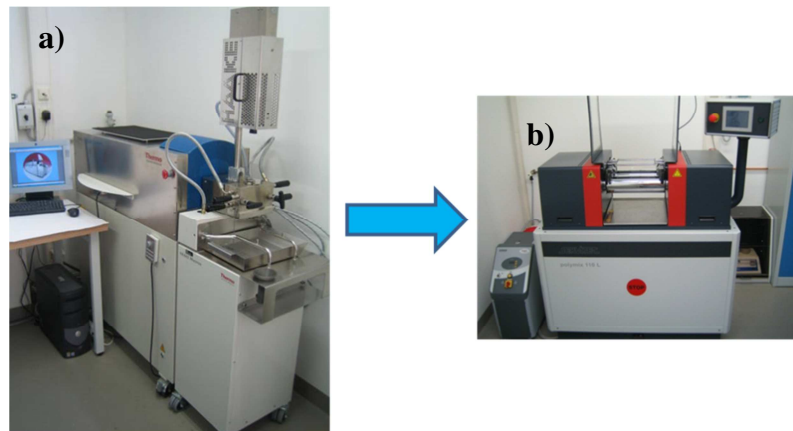
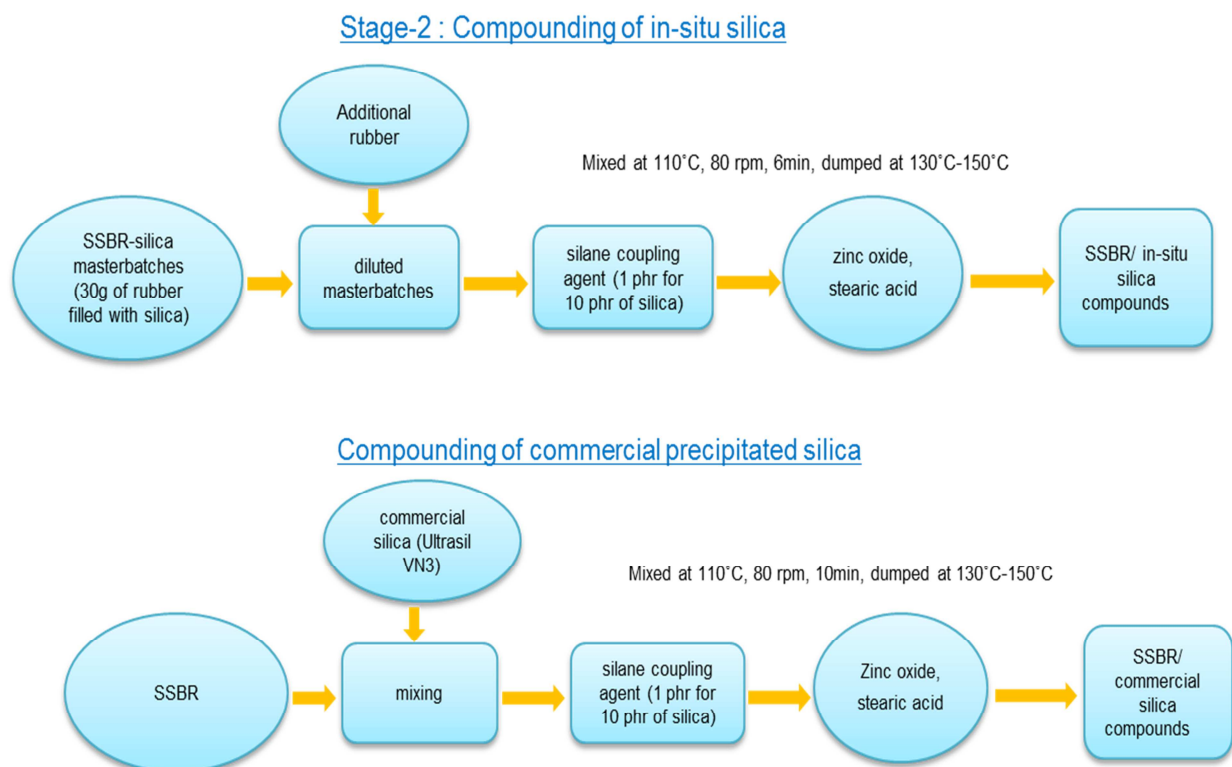


Figure 3.1a) Haake internal mixer b) Two roll mixing mill



Scheme 3.2 Flow chart of in-situ silica and commercial silica compounding

Additional raw SSBR served to fine-tune the rubber-silica concentration. After sufficient mixing, other rubber ingredients: zinc oxide (2 phr), stearic acid (3 phr) and TESPT coupling agent (1 phr for 10 phr of silica) were added sequentially. The compounding process was performed at 110 °C and 80 rpm for 6 min and the compounds were dumped at a temperature

of ~130 to 150 °C. The flow chart of in-situ and commercial precipitated silica compounding was given in scheme 3.2.

3.2.3 Compounding Formulations

Table 3.3 Formulation of precipitated ULTRASIL VN3 silica based SSBR compounds

Ingredients	Gum	x-silica	x-silica with silane
SSBR	100	100	100
ZnO	3	3	3
Stearic acid	2	2	2
silica	-	10, 20, 30, 40 and 50	10, 20, 30, 40 and 50
TESPT	-	-	1, 2, 3, 4 and 5
CBS	1.4	1.4	1.4
DPG	1.7	1.7	1.7
Sulphur	1.4	1.4	1.4

Table 3.4 Formulation of in-situ silica based SSBR compounds

Ingredients		i-silica	i-silica with silane
SSBR/in-situ	silica	110, 120, 130, 140 and 150	110, 120, 130, 140 and 150
master batches*			
ZnO		3	3
Stearic acid		2	2
TESPT		-	1, 2, 3, 4 and 5
CBS		1.4	1.4
DPG		1.7	1.7
Sulphur		1.4	1.4

*The amount of silica in rubber compounds are estimated from the thermogravimetric analysis. The final weight loss above 700°C is obtained from thermogravimetric analysis is considered as an amount of silica presented in the compounds.

In a second step, the vulcanizing chemicals CBS (1.4 phr), DPG (1.7 phr) and sulphur (1.4 phr) were added to the compound in a two-roll mixing mill (Polymix-110L, Servitec Maschinen Service GmbH, Wustermark, Germany, Fig. 3.1b) at 50 °C for 10 min with a constant friction ratio of 1:1.2. Likewise commercial silica based rubber composites were

prepared by sequential addition of rubber, zinc oxide, stearic acid, silica (commercial precipitated silica, ULTRASIL-VN3 GR) and TESPT coupling agent into the Haake internal mixer. The mixing process was performed at 110°C and 80 rpm for 10 min; a similar procedure is followed as mentioned for in-situ silica for the incorporation of vulcanization chemicals.

3.2.4 Moulding

The final compounded SSBR/in-situ and commercial silica samples were then allowed to mature for approximately 24 hours at room temperature. The matured samples were further subjected to rheometric study using rubber process analyzer (Scarabaeus SIS-V50, Scarabaeus GmbH, Wetzlar, Germany) to find the optimum cure time. After that the compounds were vulcanized into sheets of 2 mm thickness at 160 °C by the use of a compression molding press (Fig 3.2).



Figure 3.2 Compression moulding machine

3.2.5 Sample abbreviation

The samples are abbreviated based on the type of silica, amount of silica, and followed by the type of silane. e.g.: i-30_DMS, x-30_TESPT, etc. ‘i’ and ‘x’ denote in-situ silica or commercial silica (Ultrasil-VN3) respectively, the numbers denote the amount of silica loading in ‘*phr*’, (30 means 30 phr silica filled compound), the abbreviated text for different silane coupling agents are mentioned at the end. Diethyl dimethoxy silane (DMS), 3(aminopropyl) triethoxysilane (APTES), n-octodecyltriethoxysilane (ODTES), 3-octanoylthio 1-propyl triethoxysilane (NXT), (3-mercaptopropyl)trimethoxysilane (MPTES), bis[3-(triethoxysilyl) propyl]disulfide (TESPD) and bis[3-(triethoxysilyl)propyl] tetrasulfide (TESPT).

3.3 Characterizations

3.3.1 Thermogravimetric analysis

The amount of silica in the rubber compounds was investigated by thermogravimetry (TGA Q 5000 from TA Instruments, New Castle, USA) at a heating rate of 20 K/min under nitrogen atmosphere up to 600 °C and then under oxygen atmosphere from 600-800 °C (Fig 3.3). From the samples containing only silica and rubber, the quantitative content of silica and the conversion of silica from the precursor can be calculated by the following simple expressions.

$$\text{Silica content (\%)} = \frac{\text{weight of residue}}{\text{weight of composite}} \times 100 \quad (3.1)$$

$$\text{Conversion (\%)} = \frac{\text{experimental amount of SiO}_2}{\text{theoretical amount of SiO}_2} \times 100 \quad (3.2)$$



Figure 3.3 Thermogravimetric analyzer

3.3.2 Rheological study

3.3.2.1 Mooney viscosity

Measurement of the viscosity of unfilled and filled rubber compounds were carried out in a Mooney viscometer (Montech Rheotechnologies, Buchen, Germany, Fig 3.4). The conventional large rotor was used and the measurement conditions were ML (1+4) at 100°C (One minute of preheating time and four minutes of measurement time). The Mooney viscosity of the rubber compounds were noted at fourth minute of the measurement. The gradient of shear induced viscosity drop (thixotropic behaviour) of *in-situ* silica included rubber compounds were calculated as the difference between the Mooney units at 0 and 4 minutes.



Figure 3.4 Mooney viscometer

3.3.2.2 Dynamic filler flocculation

Filler flocculation characteristics and vulcanization kinetics of the rubber compounds were studied using a Scarabaeus SIS-V50 rubber process analyser, Wetzlar, Germany (Fig 3.5). A three stage flocculation study was carried out at 120°C and 1.67 Hz. In the first step a high dynamic strain of ~25 % was applied to destroy all the filler agglomerates in the sample. In second stage, a low dynamic shear strain (1.4 %) was applied for 2 hours to study the reformation of the filler-filler networks. In the third stage dynamic strain from 0 to 70 % was applied to study the Payne effect¹. The flocculation tendency of silica particles and their strain dependency (Payne effect) were calculated by the following equations,

$$\text{Flocculation (\%)} = \frac{G'_{120min} - G'_{0min}}{G'_{0min}} \times 100 \quad (3.3)$$

$$\text{Amplitude of payne effect} = G'_{0\%} - G'_{70\%} \quad (3.4)$$

Where, G'_{120min} is the shear modulus at 120 minutes and G'_{0min} is the shear modulus during the beginning of the experiment, $G'_{70\%}$ is the modulus at 70% dynamic shear strain and $G'_{0\%}$ is the modulus at ~ 0% dynamic strain.

3.3.2.3 Vulcanization study

Vulcanization studies of the rubber-silica composites were conducted in the same instrument in isothermal time sweep mode at 160 °C for 60 minutes.



Figure 3.5 Rubber process analyser for the determination of processing characteristics

3.3.3 Fourier transform infrared analysis (FTIR)

To study the silica formation in rubber, solution samples were taken at different periods of time and poured immediately into ethanol. The solidified mass was dried at 30 °C for 2 hours and used for further Fourier transform infrared (FTIR) analysis.



Figure 3.6 Bruker Vertex 80v - FTIR spectrometer

To separate the *in-situ* prepared silica powder the final reaction mixture was poured into THF and washed by means of centrifugation process for 5 cycles. Attenuated total reflection (ATR) FTIR spectra were taken using a Bruker - Vertex 80v spectrometer, Ettlingen, Germany (Fig 3.6) equipped with both HgCdTe-detector and Golden Gate ATR-unit (Specac). The spectral region was 4000 - 600 cm^{-1} and 4 cm^{-1} spectral resolution was applied. 100 scans were co-added to every spectrum. To compare the spectra properly the data were

normalized using band of CH₂-stretching vibration at 2915 cm⁻¹ as a reference (internal thickness band)².

3.3.4 Physio-mechanical testing

The tensile tests were performed at DIN S2 dumbbell specimens as per the DIN 53504, using Zwick/Roell-Z010 material testing machine, Ulm-Einsingen, Germany (Fig 3.7) with an optical elongation sensor at a cross head speed rate of 200 mm/min at room temperature. Hysteresis experiments were carried out with uniaxial tensile cyclic experiments using dumbbell shape tensile samples. The samples were stretched for 3 cycles with different strains of 50%, 100% and 150%. The hysteresis loss (H: the quantity of energy dissipated during cyclic loading and unloading) was calculated from the area of hysteresis loop which is obtained by the work done during extension (W_1) and retraction (W_2)³. $H = W_1 - W_2$. Hysteresis loss of the vulcanizates mainly depends on the input energy (W_1). The energy dissipation is relative to the applied energy on loading cycle which is calculated by area under the extension curves W_1 ⁴. The hardness of rubber composites was measured by Bareiss Shore-A hardness tester (Bareiss Prüfgerätebau GmbH, Oberdischingen, Germany).



Figure 3.7 Mechanical material testing machine

3.3.5 Dynamic mechanical analysis (DMA)

3.3.5.1 Temperature sweep

The dynamic mechanical analysis of different silica filled composite was performed on a dynamic mechanical thermal spectrometer (Gabo Qualimeter, Ahlden, Germany, model Eplexor-150N) in tension mode (Fig 3.8). The temperature sweep experiments were performed at frequency of 10 Hz between -60 °C and 80 °C with a heating rate of 2 K/min, 0.5 % dynamic strain and 1 % static strain.



Figure 3.8 Dynamic mechanical analyzer

3.3.5.2 Strain sweep

The amplitude sweep measurements were performed on Eplexor-2000 N in tension mode at room temperature, at a constant frequency of 10 Hz, 60 % pre-strain and dynamic strain from 0.01-30 %. Hydrodynamic reinforcement values for the samples were calculated using the Chen-Acrivos model⁵⁻⁶ (Eq. 3.5). It is assumed that at high values of dynamic strain there would be no filler-filler interaction and the dynamic modulus of composite will be only influenced by hydrodynamic reinforcement⁷(Fig 3.9). The experimentally obtained strain sweep values and extrapolated higher strain values are further fitted with Kraus model (Eq. 3.6) to understand the quantitative information about filler dispersion and filler-filler networks from the strain sweep measurements.

$$E_c = E_m(1 + 2.5\varphi + 5\varphi^2) \quad (3.5)$$

$$E'(\gamma_c) = E'_\infty + (E'_i - E'_\infty)/(1 + (\gamma/\gamma_c)^{2m}) \quad (3.6)$$

E_c and E_m are the low strain dynamic elastic moduli of the composite and pure matrix obtained from dynamic strain sweep measurements, φ is the volume fraction of silica presented in a vulcanizates, γ_c is a critical strain amplitude defining the maximum breakdown

of filler-filler network (or strain at which the maximum modulus reduction occurs), γ is the tensile strain amplitude, E'_i and E'_∞ are the initial and final modulus of rubber composites respectively (here E'_∞ is the modulus extrapolated by Chen-Acrivos function and which is equal to E_c), m is a strain amplitude (strain sensitivity) constant.

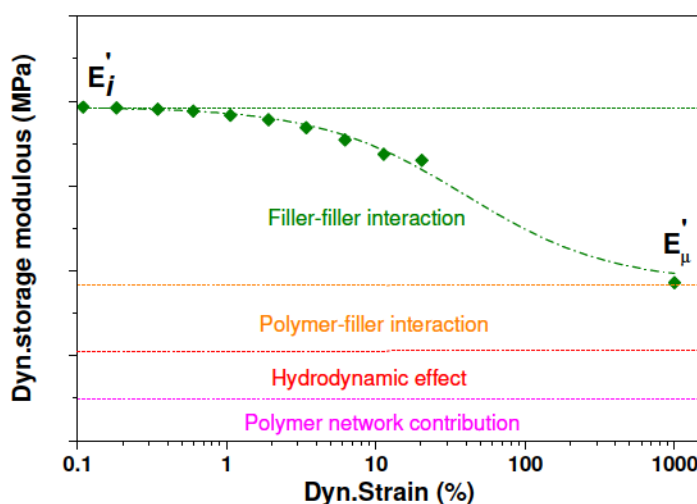


Figure 3.9 Different material properties on the contribution of storage modulus in filled rubber system

3.3.5.3 Frequency sweep

To generate master curves, frequency sweep experiment was carried on Eplexor-150N instrument from 0.5 to 50 Hz, with every 5 °C increase from 0 °C to 80 °C. The machine software utilizes the time temperature super position principles (WLF equation) to generate master curves.

3.3.6 Other rubber performances

3.3.6.1 Heat build-up

The heat build-up experiment was conducted in the Eplexor 2000 N, according to DIN 53533 standards. The samples were preconditioned at 50°C for 30 min and the measurement was performed with 1 MPa preload and 4.45 MPa of dynamic compression load. Solid cylindrical sample with dimensions $\varnothing 17\text{mm} \times 25\text{ mm}$ was used for analysis. The heat developed inside the sample was measured by a sharp tip thermocouple at the end of the measurement. The dynamic compression set due to dynamic strain was measured after 1 hour of heat build-up measurement. The heat build-up and compression set was calculated by Eq. 3.7 and Eq. 3.8 respectively.

$$\text{Heat build up } (^{\circ}\text{C}) = T_2 - T_1 \quad (3.7)$$

$$\text{Compression set } (\%) = \frac{H_i - H_f}{H_i} \times 100 \quad (3.8)$$

Where, T_1 is the initial temperature of the specimen and T_2 is the core (inside) final temperature of the specimen, H_i and H_f are the initial and final height of sample.

3.3.6.2 Rebound resilience

Rebound resilience of the composites was determined by resilience tester (Bareiss Prüfgerätebau GmbH, Oberdischingen, Germany) according to DIN 53512, ISO 4662 free fall pendulum method (Fig 3.10) at 20°C and 60°C. Circular specimen of 60 mm diameter and 5 mm thickness was utilized.



Figure 3.10 Free fall pendulum based rebound resilience tester

3.3.6.3 Abrasion properties

The abrasion experiments were conducted in a DIN rotating drum abrader (Fig 3.11) according to DIN 53516 / DIN ISO 4649 standard test procedure. The circular sample with dimensions $\varnothing 16.1$ mm x 4.2 mm was used. The abrasion resistance index (ARI) and relative volume loss (ΔV_{rel}) were calculated by the standard given formulas in Eq. 3.9 and Eq. 3.10.

$$ARI = \frac{\Delta m_r \times \rho_t}{\Delta m_t \times \rho_r} \times 100 \quad (3.9)$$

where, Δm_r is the mass loss of the standard rubber test piece #1 in mg, ρ_r is the density of standard rubber #1 in g/cm^3 , Δm_t is the mass loss of the test rubber piece in mg, and ρ_t is the density of the test rubber in g/cm^3 .

$$\Delta V_{rel} = \frac{\Delta m_t \times \Delta m_{const}}{\rho_t \times \Delta m_r} \quad (3.10)$$

where, Δm_{const} is the measured mass loss in standard reference rubber in mg, Δm_r is the mass loss of the standard rubber #1 test piece in 'mg', Δm_t is the mass loss of test rubber piece in mg, and ρ_t is the density of the test rubber in g/cm^3 .



Figure 3.11 DIN rotating drum abrasion tester

3.3.7 Solid state NMR analysis

3.3.7.1 Low field ^1H NMR-Double quantum experiments



Figure 3.12 Bruker minispec mq20-low field ^1H NMR spectrometer

Double quantum (DQ) NMR experiments were carried out to understand the effect of crosslink density on rubber by the incorporation of filler and silane coupling agent. The DQ measurement was performed on Bruker minispec mq20 (Bruker Biospin GmbH, Rheinstetten, Germany) low-field time-domain ^1H NMR spectrometer (Fig 3.12) with the operating of 20MHz (0.5Tesla) at 110 °C. The 90° and 180° pulse lengths were 3.1 and 5.8 μs respectively with dead time of 15 μs . This is a novel and powerful method to measure the crosslink density of crosslinked rubbers and rubber composites by detecting the weak residual dipolar coupling⁸ existing in polymer networks. The presence of crosslinks in rubber increases the non-isotropic fast segmental motions of rubber chains. Due to the non-isotropic behaviour of crosslinked rubber, the dipole-dipole couplings between the protons in

monomeric units are not averaged out (like low molecular weight liquids) but a residual dipolar coupling persists⁹.

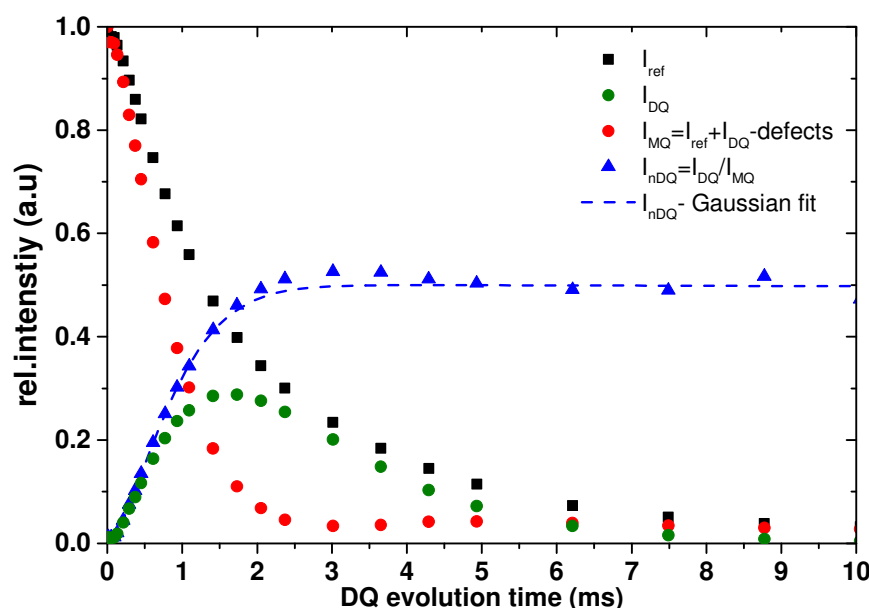


Fig 3.13 Reference intensity (I_{ref}), Double Quantum build intensity (I_{DQ}), defect-corrected overall relaxation function ($I_{\Sigma MQ}$) and the normalized Double Quantum buildup curve (I_{nDQ}) for vulcanized SSBR gum sample (unfilled and vulcanized with 2 phr of Sulphur) as a function of DQ evolution time (τ_{DQ}). The dotted lines represents Gaussian fit of dipolar couplings based on Eq.12a

The residual dipolar coupling is proportional to the crosslink density of the vulcanized network. DQ-NMR measurements generate two main signal components (see Fig 3.13). A reference intensity decay curve (I_{ref}) and Double quantum buildup curves (I_{DQ}). The sum of both components ($I_{ref} + I_{DQ}$) consists of the whole magnetization of entire sample, which means the contributions of dipolar coupled networks and uncoupled network defects (like sol-gel fraction, dangling chain ends and loops). Dipolar coupled networks exhibit faster non-exponential relaxation as compared to uncoupled network, which has slower exponential decay¹⁰. To correct the raw I_{DQ} build up data arise from the dipolar coupled network for the long time relaxation effect, the data is treated with suitable relaxation function ($I_{\Sigma MQ}$) divided by point to point. This function (Eq. 3.11) is utilized to extract the non-elastic or uncoupled network fraction from the entire sample.

$$I_{\Sigma MQ} = I_{ref} + I_{DQ} - B \exp(-2\tau_{DQ}/T_2) \quad (3.11)$$

The defect fraction B can be calculated easily by an exponential fit to the data range, where I_{DQ} reached to zero (i.e a DQ evolution time beyond 9 ms) and T_2 is transverse relaxation decay (non-exponential). In permanently crosslinked networks $I_{\Sigma MQ}$ is used to normalize the DQ filtered intensity by removing the relaxation effect on the experimental data. Thereby, DQ buildup data can be normalized, obtaining $I_{nDQ} = I_{DQ}/I_{\Sigma MQ}$. The obtained normalized DQ intensity (I_{nDQ}) is further fitted with the mentioned Gaussian distribution function (Eq. 3.12a) of dipolar coupling according to

$$I_{nDQ}(D_{res}, \sigma_G) = \frac{1}{2} \left(1 - \frac{\exp\left\{\frac{\frac{2}{5}D_{res}^2\tau_{DQ}^2}{1+\frac{4}{5}\sigma_G^2\tau_{DQ}^2}\right\}}{\sqrt{1+\frac{4}{5}\sigma_G^2\tau_{DQ}^2}} \right) \quad (3.12a)$$

The residual dipolar coupling D_{res} values are directly proportional to the crosslink density of the polymer network, σ_G represent the distribution of crosslinks throughout the sample. I_{nDQ} is independent of the time scale of chain segmental motion and related to the network structure therefore to the residual dipolar coupling constant D_{res} in rad/s was given as $D_{res}/2\pi$ in the unit of frequency (Hz) for simplicity¹¹. It is well established D_{res} is directly related to the dynamic chain order parameter (S) and given in Eq. 3.12b.

$$D_{res} \propto S = \frac{1}{2} [(3\langle \cos^2(\theta) \rangle) - 1] = \frac{3R}{5N} \quad (3.12b)$$

Where $\langle \cos^2(\theta) \rangle$ denotes the time average overall conformations of network chains and $[(3\langle \cos^2(\theta) \rangle) - 1]$ denotes the structural average over all segments in rubber sample. The θ indicates to the instantaneous segmental orientation with respect to the end-to-end vector of the particular chain. N is the number of statistical segments between constrains and $R=1$. Therefore D_{res} is a direct measurement of the real crosslink density and the detected crosslink density is a combined quantity of chemical crosslinks (sulphur bridges) as well as physical crosslinks (entanglements)¹². D_{res} values are obtained from the slope of the normalized DQ intensity curves. The obtained D_{res} values from the Gaussian fit represents the amount of crosslinks existed⁹. σ_G is sensitive to the spatial distribution of crosslinks and was successfully evaluated to homopolymer networks, like natural rubber, butadiene rubber and silicone rubber¹³. Due to the huge heterogeneity in the chemical structure of styrene butadiene rubber and copolymers, the broad D_{res} distribution was observed in samples and it minimizing the effect of network structure¹⁴. For that reason σ_G is not discussed in this work. The experimental $D_{res}/2\pi$ values are used in this work to investigate the influence of filler

content, chemical properties of filler, effect of silane coupling agent on the crosslink density of rubber.

3.3.7.2 Solid state ^{29}Si NMR experiments

The solid state ^{29}Si -NMR experiments were performed on the in-situ and commercial silica powders as well their respective SSBR composites. The NMR experiments were performed on a Bruker Avance 300 NMR spectrometer (Bruker Biospin GmbH, Rheinstetten, Germany) operating at Larmor frequencies of 60 MHz and 300 MHz for ^{29}Si and ^1H respectively. A Bruker BL 4 HX double resonance probe accepting 4 mm o.d. rotors with a magic angle sample spinning (MAS) rate of 5 kHz was used. Direct excited ^{29}Si spectra with a repetition time of 10 s had been recorded of the pure silica samples. Because of the extensive longitudinal relaxation time of ^{29}Si these spectra was semi quantitative, however they are time consuming. Therefore, ^{29}Si - ^1H CPMAS spectra of the filled polymer samples have been recorded using a contact time of 2 ms.

3.3.8 Equilibrium swelling experiments

For crosslink density measurements by equilibrium swelling method, three different geometrical samples like circular, square and triangular with 2 mm thickness were weighed and submerged in toluene (molar volume (V_s) = 106.2 mL/mol, density (ρ_s) = 0.87 g/cm³) bath for 72 hours at room temperature (25 °C) in sealed glass vials and kept it in to a dark place to prevent the samples from the photo degradation effect. After that, the taken samples were wiped with tissue paper to remove the excess solvent adsorbed on the sample surface and weighed on a high precision balance. Finally the samples were dried at 60 °C until to achieve the constant weight. The initial weight, swollen weight and final dried weight of samples were to be used to calculate the crosslink density of gum and silica filled composites. The crosslink density of gum and *in-situ* silica filled SSBR composites were investigated by equilibrium swelling method. The volume fraction of rubber (v_r) is determined¹⁴ by Eq. 3.13.

$$v_r = \frac{\frac{w_d - f_{ins} w_i}{\rho_r}}{\frac{w_d - f_{ins} w_i}{\rho_r} + \frac{w_o}{\rho_s}} \quad (3.13)$$

Where, w_i , w_s and w_d are the initial weight of samples before swelling, swollen and dried samples after swelling, respectively. w_o is the equilibrium weight of solvent absorbed by the

samples. $w_0 = w_s - w_d$, f_{ins} is the weight fraction of the insoluble substances like silica and zinc oxide. The classical Flory-Rehner equation is utilized with regard to the volume fraction to calculate the crosslinking density ($\nu_{\text{FR}} = 1/M_c$). Two types of network models¹⁵ have been proposed to analyze the network structures of cross-linked polymers which are the Affine (Eq. 3.14) and the Phantom network (Eq. 3.15) model; the equations are as follows.

$$\ln(1 - v_r) + v_r + \chi v_r^2 = -\frac{\rho_r}{M_c} V_s \left(v_r^{\frac{1}{3}} - \frac{2v_r}{f} \right) \quad (3.14)$$

$$\ln(1 - v_r) + v_r + \chi v_r^2 = -\frac{\rho_r}{M_c} V_s \left(1 - \frac{2}{f} \right) v_r^{\frac{1}{3}} \quad (3.15)$$

Hereby, ρ_r is the density of rubber, V_s is the molar volume of toluene, χ is the Flory-Huggins interaction parameter (0.413) for SBR-toluene and f is the crosslink functionality.

3.3.9 Linear friction tester

The friction experiments were performed on a tribometer-linear friction tester at the Deutsche Institut für Kautschuktechnologie (DIK), Hannover, Germany and the schematic diagram of friction tester is shown in Figure 3.14a. The test samples are prepared by the size of 20 mm × 20 mm × 10 mm prepared by the compression molding machine. The edges of the samples are chamfered to avoid the buckling effect of rubber sample when contacting the asphalt surface and shown in figure 3.14b. The friction tester can be operated at the temperature of 2 °C to 100 °C with the velocity of 0.1 mm/s to 300 mm/s by varying the load from 1 bar to 7 bar. The current experiments were performed at 15 °C, 2 bar load with the velocity of 0.1 mm/s to 300 mm/s.

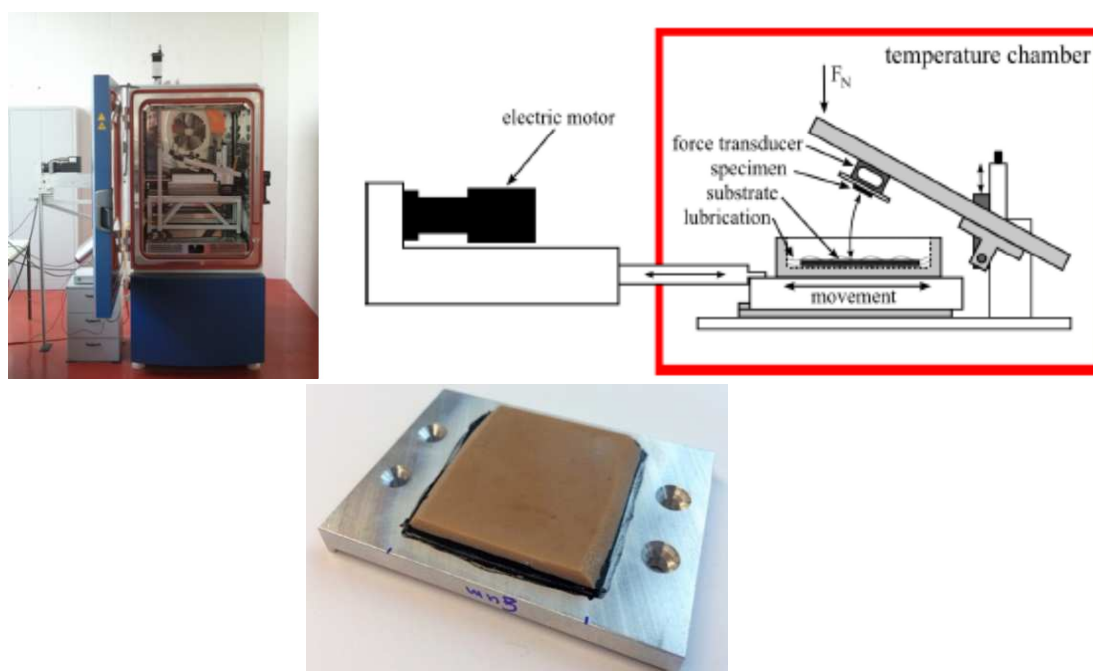


Figure 3.14 a) Linear friction tester instrument b) Sample probe

Table 3.5 The glass transition temperature of rubber samples used and estimated friction measurement temperature by WLF principle

Sample	T_g (°C)	T_{calc} (Calculated temperature) (°C)	Hardness Shore A	Crosslink density ($\times 10^{-4}$ g/cc)
Gum	-27.8	14.96	42	1.463
i-30	-27.8	14.96	56	2.128
i-30s	-26.0	15.63	59	2.718
x-30	-28.2	14.81	56	1.571
x-30s	-26.8	15.33	57	2.202

The experiments were carried out at fine asphalt surface filled with water to understand the friction properties of rubber composites in the wet condition. It is generally considered that ABS wet braking temperature for tyre tread compound is approximately 40 °C and the slipping velocity is around 1m/s. The used linear friction tester is not able to reach such a mentioned velocity; due to that reason the time-temperature superposition principle was utilized to calculate the right temperature for 10 mm/s (the measureable velocity by machine). The universal WLF constants ($C1 = 17.44$ and $C2 = 51.6$ K) were used to calculate the test temperature with the help of glass transition temperature of composites¹⁶. The glass transition

temperature (T_g) of gum and silica filled composites were estimated by the dynamic mechanical temperature sweep measurements¹⁷. Based on the T_g of rubber composites and using WLF superposition principle the estimated friction measurement temperature was approximately 15 °C and represented in Table 3.5. That means the friction behaviour of the SSBR-silica compound measured at 10 mm/s and 15°C which corresponds to 1 m/s at 40°C¹⁸⁻¹⁹.

3.3.10 Tear-fatigue analyzer (TFA)

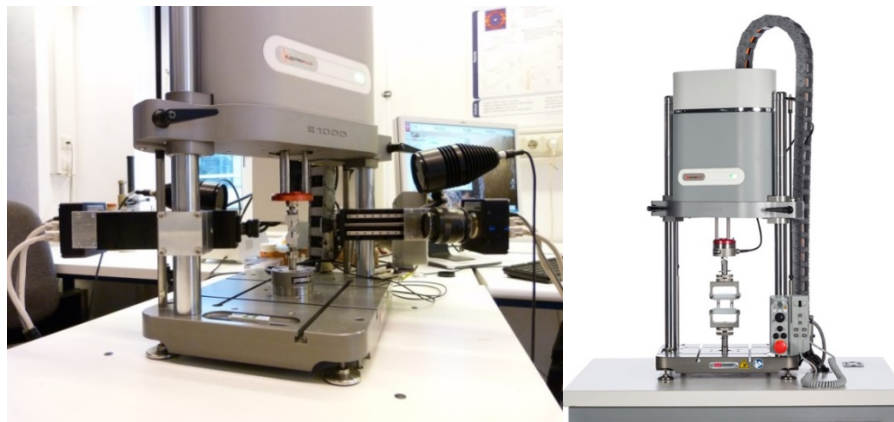


Figure 3.15 - Instron Electroplus E1000 used for Tear-Fatigue analysis

The crack propagation behaviour of composite was investigated by Instron Electroplus E1000 from Norwood, Massachusetts, USA (Fig 3.15). Pure shear specimens (Fig 3.16) were used for crack propagation experiments with span length $L_0 = 10$ mm, thickness $B = 1$ mm, width $W = 80$ mm. The initial cut was generated manually with the length a_0 of 25 mm on one side edge of the specimen which develops into the crack length a , is sufficiently long compared to the length of L_0 . The experiments were carried out at 23 °C with 1 N of pre-force and the further details about the experiments can be found in the following references²⁰⁻²³. In early stages Rivlin and Thomas²⁴ reported the tearing energy as the characteristic parameter of fatigue crack growth behaviour of elastomeric materials and it is defined as $T = -(\delta W / \delta A)$, where W is the elastic strain energy, A is the interfacial area of grown crack.

Based on the assumption of Rivlin and Thomas²⁴, the pure shear specimen can be divided into four regions. The material in region A_1 is unstrained, in region D is the complicated deformation due to the crack tip, C is the pure shear deformation region and an edge effect

region is denoted as A , when the crack length increases by da . The deformation state in region D does not change but shift parallel in the crack growth direction. In this case, the volume of region C is $L_0 \times B \times da$ smaller and the elastic stored energy in this volume is released. For a pure shear test specimen geometry the tearing energy T_P is independent of the crack length.

$$T_P = w \cdot L_0 \quad (3.16)$$

Where w is the elastic pure shear strain-energy density measured from the unloading stress-strain curve of un-notched specimen. Two uncracked samples with different width (80 mm and 60 mm) are used to calculate the pure shear elastic strain energy density w in order to remove the energy contribution of edge effect region.

$$w = \frac{\text{Elastic strain energy of 80 mm sample} - \text{Elastic strain energy of 60 mm sample}}{(80\text{mm} - 60\text{mm}) \times 10\text{mm} \times 1\text{mm}} \quad (3.17)$$

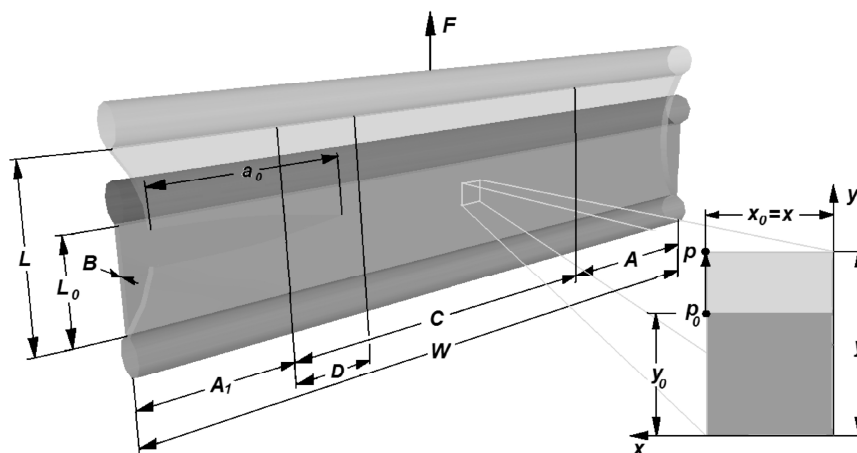


Figure 3.16 Schematic diagram of pure shear test specimen with visualization of regions under different stress conditions

Gent, Lindley and Thomas²⁵ determined experimentally the rate of crack growth da/dn in dependence on the tearing energy T for rubber materials and the typical relationship is given in Fig 3.17. Lake and Lindley²⁶ divided the double logarithmic plot into four regions which mainly characterize different tear behaviour of viscoelastic material. The value of T is lower

than T_0 , crack growth proceeds at a constant rate (r) and the crack growth is independent of dynamical loading but affected by environmental attack.

$$\frac{da}{dn} = r \text{ when } T \leq T_0 \quad (3.18)$$

In the region-II between T_0 and T_I denotes a transition between a nucleation and propagation of crack growth.

$$\frac{da}{dn} = A(T_I - T_0) + r \text{ when } T_0 \leq T \leq T_I \quad (3.19)$$

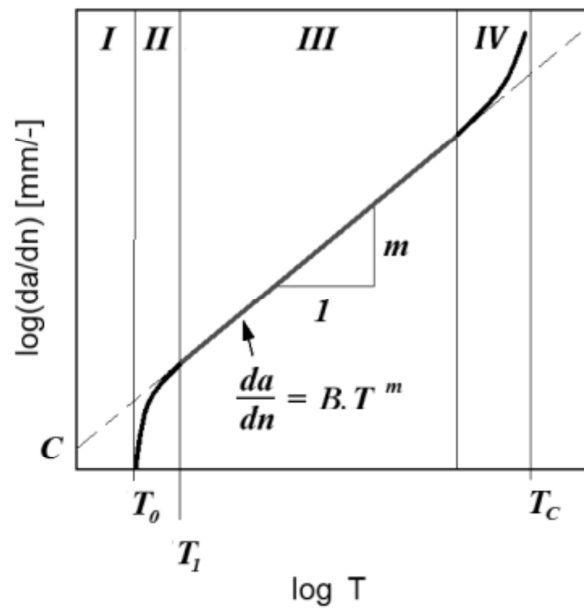


Figure 3.17 Double logarithmic plot of crack growth rate (da/dn) versus tearing energy (T)

After this transient region, the crack propagates in a region between T_I and T_c of stable crack growth which is represented in the region-III. The relationship between a stable fatigue crack growth rate da/dn and tearing energy is described by Paris-Erdogan²⁷ with the power law equation given in the following equation.

$$\frac{da}{dn} = B.T^m \text{ when } T_I \leq T \leq T_c \quad (3.20)$$

Where, B and m are material constants. T_I denotes the onset of the stable crack propagation regime and T_c is the critical tearing energy which marks the transition to the instable regime.

In the final region-IV the tearing energy T_c proceeds to the instable state of crack growth and the crack growth rate will become essentially infinite.

$$\frac{da}{dn} = \infty \text{ when } T \leq T_c \quad (3.21)$$

The region-III was considered as the region that corresponds to crack growth rates found in the engineering fatigue range.

3.3.11 Morphology study

3.3.11.1 Scanning electron microscopy (SEM)

Scanning electron micrographs of composites were taken by Ultra plus electron microscope (Fig 3.18) from Carl Zeiss NTS GmbH, Oberkochen, Germany, 3 kV, 30 μm aperture size and SE2 detector. A strip of sample was subjected to brittle fracture after exposure to liquid nitrogen. The fractured surface was further sputter coated with 3nm platinum using BAL-TEC SCD 500 sputter coater and examined under the SEM at zero tilt angle.



Figure 3.18 Ultra plus-scanning electron microscope

3.3.11.2 Energy dispersive X-ray spectroscopy (EDX)

The specimens were attached with adhesive tape onto a specimen holder and coated with approximately 10 nm thin amorphous carbon film (SCD 500 coater, Leica Microsystems GmbH, Wetzlar, Germany) to prevent charging and investigated in scanning electron microscope (SEM) Ultra 55 (Carl Zeiss Microscopy GmbH, Oberkochen, Germany) equipped with Quantax XFlash 5060 energy dispersive X-ray (EDX) spectrometer (Bruker Nano GmbH, Berlin, Germany). The acquired spectra were quantified with ESPRIT Software (by Bruker) by PB-ZAF method. The both in-situ and commercial silica were modified by silane coupling agents inside the rubber during the mixing process and did not contain any other rubber ingredients. Approximately 2 g of silane modified silica rubber masterbatch was swollen in THF for 7 days, then stirred for few hours and then rinsed with THF by centrifugation process. The rinsing process was carried out with THF for several times to remove any unreacted silane molecules and the rubber chains which are loosely adsorbed on the silica surface. Finally the removed filler particles are dried at room temperature for 48 hrs and investigated by EDX spectroscopy.

3.3.11.3 Transmission electron microscopy (TEM)

The dispersion of silica in rubber matrix was investigated by using TEM model LIBRA 120 PLUS (Fig 3.19) by Carl Zeiss SMT with 120 kV acceleration voltage and bright field illumination. The ultra-thin sections of silica composites were prepared by ultramicrotomy (Leica Ultracut UCT, Leica microsystems GmbH, Wetzlar Germany) at -120 °C.



Figure 3.19 TEM-Libra 120 plus

3.3.12 Dynamic light scattering analysis (DLS)

The silica particle size and distribution was measured by the help of dynamic light scattering analyser, Dyna Pro-nanostar (Wyatt instruments, California, USA) with a measurement size range from 0.2 to 2500 nm by using 785nm laser wave length (Fig 3.20). The experiment was carried out at 25°C with a dispersion of silica powders in ethanol. The light scattering measurements was performed for 3 samples with minimum of 25 scans for each samples. The best and consistent data can be utilized for the analyses.



Figure 3.20 Dynamic light scattering instrument

3.3.13 X-ray diffraction (XRD)



Figure 3.21 XRD 3003 T/T diffractometer

X-Ray diffraction analysis was performed using 2 circle diffractometer XRD 3003 T/T (Fig 3.21, GE inspection technologies/Seifert-FPM, Freiberg, Germany) with Cu-K α radiation generated at 30 mA and 40 kV in the range of $2\theta = 1^\circ$ to 16° using 0.05° as the step length. The in-situ silica powder sample was prepared by the immediate pouring of synthesized final reaction mixture (after completing the sol-gel reaction and contains in-situ silica in rubber

solution) into THF and washed by centrifugation process for several cycles. The separated in-situ silica powder was dried at 40 °C for 48 hours. The precipitated silica powder was used as it is procured.

3.3.14 Estimation of silanol density

The silica surface is characterised by a great number of superficial hydroxyl (silanol) groups. The silanol groups situated on the silica surface are categorized into three chemical structures like isolated, vicinal and geminal hydroxyl groups. The inherent reinforcement characteristics of silica mainly depend on the surface area and functionality. The estimation of the specific number of silanol groups situated on the silica surface was calculated by Eq. 3.22,²⁸

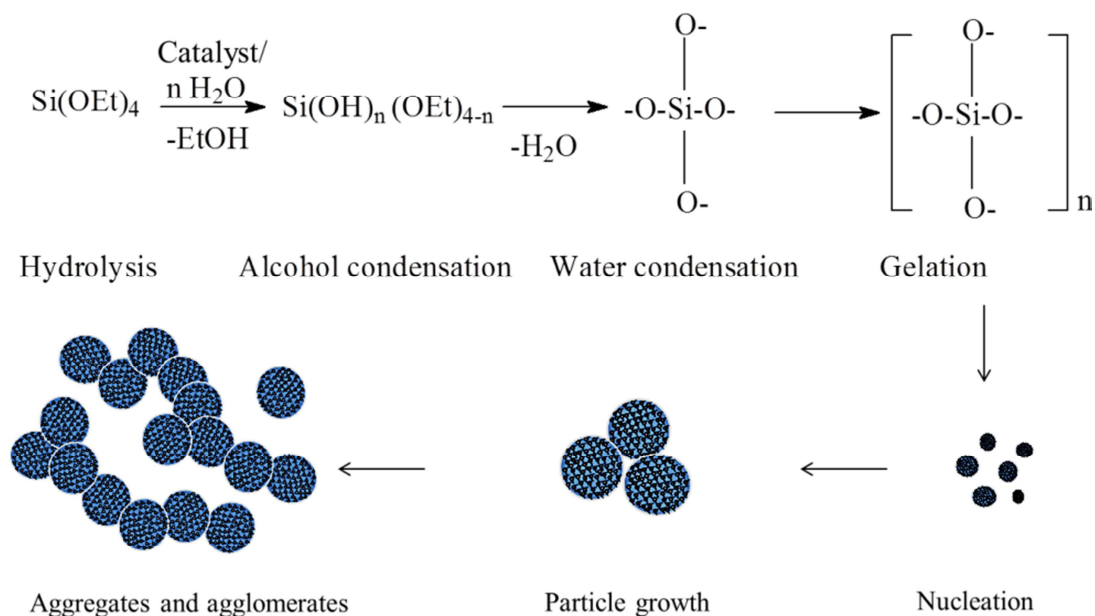
$$n_{SiOH} / nm^2 = \frac{\frac{(Final\ Weight\ loss - moisture)}{100} \times \left(\frac{2}{18}\right) \times 6.0210 \times 10^{23}}{Specific\ surface\ area\ N_a \times 10^{18}} \quad (3.22)$$

Where, final weight loss in % at 800 °C (obtained from thermogravimetric analysis), moisture content in % (estimated by drying of silica powder at 110 °C for 2 hrs by ISO 787-2 standards), N_a is the Avogadro number (6.0210×10^{23}), the specific surface area of silica (estimated by BET nitrogen adsorption measurements). The BET nitrogen adsorption for specific surface area of in-situ silica nanoparticles and commercial silica powder was measured at 77.4 K by Autosorb-1, Quantachrome, USA. The silica powders were preconditioned at 80 °C for 2hrs in a vacuum oven before BET measurements.

3.4 State of the art: In-situ silica-rubber reinforcement

In our approach we have adapted solution method to prepare silica particles in rubber. The solution method possesses good control throughout the sol-gel reaction. As well it is easy to control the processing parameter by the way one can control the silica particle growth. The generation of silica particles inside the rubber can offer a possibility of good silica-polymer interaction although enhanced silica dispersion. Also the generation of silica in rubber exhibit excellent processability in terms of lower Mooney viscosity, low flocculation behavior, reduces the average mixing cycle time with improved dispersion and silanization by silane. Also this method is offering the generation of higher quantities of silica in rubber compared to other sol-gel method. In the present study, we have followed the sol-gel route to generate silica nanoparticles in presence of a solution of raw SSBR. The silica concentration as well as the size of the particle is controlled by tuning of reaction conditions like TEOS-

water ratio, type of catalyst (acid or alkaline), reaction pH and temperature, type of solvent and viscosity of reaction medium. The generalized synthesis route of sol-gel silica via TEOS is given in Scheme 3.3.



Scheme 3.3 Schematic representation of silica particle formation through sol-gel reaction

References

1. Stöckelhuber, K. W.; Svistkov, A. S.; Pelevin, A. G.; Heinrich, G., Impact of Filler Surface Modification on Large Scale Mechanics of Styrene Butadiene/Silica Rubber Composites. *Macromolecules* 2011, *44* (11), 4366-4381.
2. Koenig, J. L., *Spectroscopy of polymers*. Elsevier: 1999, ISBN 9780444100313, 491.
3. Kar, K. K.; Bhowmick, A. K., High Strain Hysteresis Loss of Rubber Vulcanizates under Pure Shear and Constrained Extension and Influence of Filler. *Rubber Chemistry and Technology* 2000, *73* (1), 56-73.
4. Harwood, J. A. C.; Payne, A. R.; Whittaker, R. E., Stress-Softening and reinforcement of rubber. *Journal of Macromolecular Science, Part B* 1971, *5* (2), 473-486.
5. Hsiao-Sheng, C.; Acrivos, A., The effective elastic moduli of composite materials containing spherical inclusions at non-dilute concentrations. *International Journal of Solids and Structures* 1978, *14* (5), 349-364.
6. Domurath, J.; Saphiannikova, M.; Ausias, G.; Heinrich, G., Modelling of stress and strain amplification effects in filled polymer melts. *Journal of Non-Newtonian Fluid Mechanics* 2012, *171-172*, 8-16.
7. Heinrich, G.; Klüppel, M.; Vilgis, T. A., Reinforcement of elastomers. *Current opinion in solid state and materials science* 2002, *6* (3), 195-203.

8. Saalwächter, K.; Heuer, A., Chain Dynamics in Elastomers As Investigated by Proton Multiple-Quantum NMR. *Macromolecules* 2006, *39* (9), 3291-3303.
9. Mujtaba, A.; Keller, M.; Ilisch, S.; Radusch, H. J.; Thurn-Albrecht, T.; Saalwächter, K.; Beiner, M., Mechanical Properties and Cross-Link Density of Styrene–Butadiene Model Composites Containing Fillers with Bimodal Particle Size Distribution. *Macromolecules* 2012, *45* (16), 6504-6515.
10. Saalwächter, K., Proton multiple-quantum NMR for the study of chain dynamics and structural constraints in polymeric soft materials. *Progress in Nuclear Magnetic Resonance Spectroscopy* 2007, *51* (1), 1-35.
11. Saleesung, T.; Reichert, D.; Saalwächter, K.; Sirisinha, C., Correlation of crosslink densities using solid state NMR and conventional techniques in peroxide-crosslinked EPDM rubber. *Polymer* 2015, *56*, 309-317.
12. Mora-Barrantes, I.; Rodríguez, A.; Ibarra, L.; González, L.; Valentín, J. L., Overcoming the disadvantages of fumed silica as filler in elastomer composites. *Journal of Materials Chemistry* 2011, *21* (20), 7381.
13. Valentín, J. L.; Posadas, P.; Marcos Fernández, A.; Ibarra, L.; Rodríguez, A., Effect of a fatty amine on processing and physical properties of SBR compounds filled with silane–silica particles. *Journal of applied polymer science* 2006, *99* (6), 3222-3229.
14. Valentín, J. L.; Mora-Barrantes, I.; Carretero-González, J.; López-Manchado, M. A.; Sotta, P.; Long, D. R.; Saalwächter, K., Novel Experimental Approach To Evaluate Filler–Elastomer Interactions. *Macromolecules* 2010, *43* (1), 334-346.
15. Vieyres, A.; Pérez-Aparicio, R.; Albouy, P.-A.; Sanseau, O.; Saalwächter, K.; Long, D. R.; Sotta, P., Sulfur-Cured Natural Rubber Elastomer Networks: Correlating Cross-Link Density, Chain Orientation, and Mechanical Response by Combined Techniques. *Macromolecules* 2013, *46* (3), 889-899.
16. Ferry, J. D., *Viscoelastic properties of polymers*. John Wiley & Sons: 1980, ISBN 9780471048947, 672.
17. Raman, V. S.; Das, A.; Stockelhuber, K. W.; Eshwaran, S. B.; Chanda, J.; Malanin, M.; Reuter, U.; Leuteritz, A.; Boldt, R.; Wie; Heinrich, G., Improvement of mechanical performance of solution styrene butadiene rubber by controlling the concentration and the size of in situ derived sol-gel silica particles. *RSC Advances* 2016, *6* (40), 33643-33655.
18. Le Gal, A.; Yang, X.; Klüppel, M., Evaluation of sliding friction and contact mechanics of elastomers based on dynamic-mechanical analysis. *The Journal of chemical physics* 2005, *123* (1), 014704.
19. Lang, A.; Klüppel, M. In *Temperature and Pressure dependence of the friction properties of tire tread compounds on rough granite*, KHK 11th Fall Rubber Colloquium, 2014.
20. Stoczek, R.; Heinrich, G.; Gehde, M., The influence of the test properties on dynamic crack propagation in filled rubbers by simultaneous tensile and pure shear test mode testing. *Const Models Rubber VI* 2009, 345-349.
21. Stoczek, R.; Heinrich, G.; Reincke, K.; Grellmann, W.; Gehde, M., Einfluss der Kerbeinbringung auf die Rissausbreitung in elastomeren Werkstoffen. *KGK. Kautschuk, Gummi, Kunststoffe* 2010, *63* (9), 364-370.
22. Stoczek, R.; Heinrich, G.; Reincke, K.; Grellmann, W.; Gehde, M., Rissausbreitung in Elastomeren Werkstoffen unter dynamischer Beanspruchung: Einfluss der Kerbeinbringung. *KGK. Kautschuk, Gummi, Kunststoffe* 2011, *64* (3), 22-26.
23. Ghosh, P.; Stoczek, R.; Gehde, M.; Mukhopadhyay, R.; Krishnakumar, R., Investigation of fatigue crack growth characteristics of NR/BR blend based tyre tread compounds. *International Journal of Fracture* 2014, *188* (1), 9-21.

24. Rivlin, R.; Thomas, A. G., Rupture of rubber. I. Characteristic energy for tearing. *Journal of polymer Science* 1953, 10 (3), 291-318.
25. Gent, A.; Lindley, P.; Thomas, A., Cut growth and fatigue of rubbers. I. The relationship between cut growth and fatigue. *Journal of Applied Polymer Science* 1964, 8 (1), 455-466.
26. Lake, G. J.; Lindley, P. B., Cut growth and fatigue of rubbers. II. Experiments on a noncrystallizing rubber. *Journal of Applied Polymer Science* 1964, 8 (2), 707-721.
27. Paris, P. C.; Erdogan, F. In *A critical analysis of crack propagation laws*, ASME: 1963.
28. Meier, J. G.; Fritzsche, J.; Guy, L.; Bomal, Y.; Klüppel, M., Relaxation Dynamics of Hydration Water at Activated Silica Interfaces in High-Performance Elastomer Composites. *Macromolecules* 2009, 42 (6), 2127-2134.

Chapter 4

Generation of *in-situ* silica in SSBR matrix

The results of this chapter have been published in RSC Advances 6 (2016) 33643-33655.

4.1 Introduction

Effective dispersion of silica in rubber and achieving the improved filler-polymer interaction are major challenges in the field of tyre and rubber technology¹⁻². New developments in precipitated silica technology, rubber mixing technology and new compounding methods are still not enough to achieve good dispersion of silica in rubbers. In the last few decades, there have been reports suggesting that *in-situ* generation of silica particles inside the rubber matrix is one of the easiest methods to achieve improved dispersion of silica in the rubber matrix. It is also reported that such technique would offer improved silica-polymer interaction. By the way, there are many silica synthesis methods like swelling, latex, solution, condensation of silanes to generate silica particles inside a rubber³⁻²¹. In this chapter, the solution based sol-gel method is adapted to generate silica particles inside an uncrosslinked SSBR matrix. Efforts are given to understand the fundamentals about silica formation in the rubber, like, (i) the amount of silica formed inside the rubber, (ii) the time based conversion of TEOS into silica, (iii) the sol-gel silica reaction kinetics and finally (iv) the total amount of silica formed at the end of sol-gel reaction. Further studies are carried out with the unvulcanized and vulcanized *in-situ* sol-gel derived silica compounds and composites. The Mooney viscosity measurement is carried out to understand the processability of *in-situ* silica filled rubber compounds. The silica flocculation in unvulcanized rubber is studied in detail with respect to increase in silica volume fraction. Finally, mechanical, dynamic mechanical, resilience, heat build-up and abrasion properties of *in-situ* silica filled composites are investigated for the vulcanized rubber composites. Throughout the investigations, experimental studies are conducted with and without the presence of TESPT silane coupling agent to understand the filler-polymer interaction between *in-situ* sol-gel silica and rubber. The reinforcing effect of *in-situ* silica in rubber and the effective role of TESPT silane in *in-situ* silica composites are elaborately studied by different laboratory tests²².

4.2 Results and discussion

4.2.1 Time dependent silica conversion study

The time dependent silica particle growth inside SSBR matrix (approximately 30 phr silica in rubber solution and the prepared composite is designated as i-30) investigated by thermogravimetric analysis is depicted in Fig. 4.1a. The final weight obtained above 700 °C is considered as the amount of silica presented in rubber⁷. Fig. 4.1a shows the increase in

amount of residue with time (every 30 min) indicating the conversion of TEOS into silica. Fig. 4.1b represents the amount of silica in the masterbatch with time calculated as per Eq. 3.1 and the conversion of silica obtained from Eq. 3.2 (in chapter 3). The amount of residue obtained in the first 30 min is ~25 % and the conversion is ~60 %. An overall conversion rate of ~98 % is observed within 240 min. For the samples with the highest conversion, almost 2-4 % weight loss is observed between 100 °C and 350 °C and this may be due to the evaporation of trace catalyst, solvent and TEOS⁹.

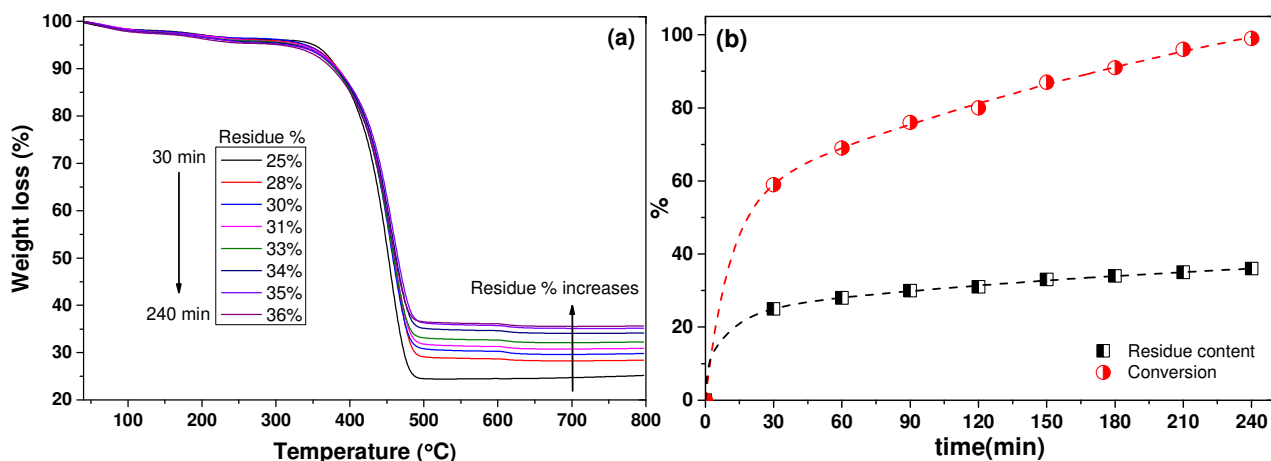


Figure 4.1.(a) Time dependent silica conversion from TEOS inside the SSBR matrix analysed by thermogravimetric analysis (b) a percentage of silica conversion and residue with respect to reaction time

Fig 4.2a depicts ATR-FTIR spectra of raw SSBR and TEOS used for the *in-situ* silica synthesis. For raw SSBR bands are observed at 909 cm^{-1} and 967 cm^{-1} due to wagging vibrations of cis 1,2 and trans 1,4 -CH butadiene groups²³ respectively. In the case of TEOS, a strong band observed at 1070 cm^{-1} represents the stretching vibration of Si-O-C groups. At the same time, multiple bands are observed in the $3000\text{-}2800\text{ cm}^{-1}$ region for all pure substances, which pertains to the -CH₂- and -CH₃ stretching vibrations²⁴. The qualitative kinetics of silica particle growth inside the rubber matrix analysed by ATR-FTIR technique is depicted in Fig 4.2b. The novel growing band at 1044 cm^{-1} as a function of reaction time can be clearly seen and represents the Si-O-Si stretching vibration of silica oxide that is converted from the TEOS²⁵. The silica band at 1044 cm^{-1} is getting more intensive gradually what confirms the silica concentration increase in the SSBR²⁶. The second broad band appears in the silica-rubber system around 3310 cm^{-1} , which is not observed for pure TEOS as well as for raw rubber. These broad band corresponds to the stretching vibrations of hydroxyl groups (-OH) from the silica surface or could also be due to the water adsorbed on the surface of the

generated silica particles²⁷. Fig 4.2c demonstrates the comparison of ATR spectra of pure *in-situ* silica powder and final reaction mixture (at 240 min) with ATR-FTIR spectrum of a commercial silica powder. The spectra's coincidence of self-synthesized and commercial silicas (bands appeared around 1044 cm^{-1}) confirms the expected synthesis in rubber system.

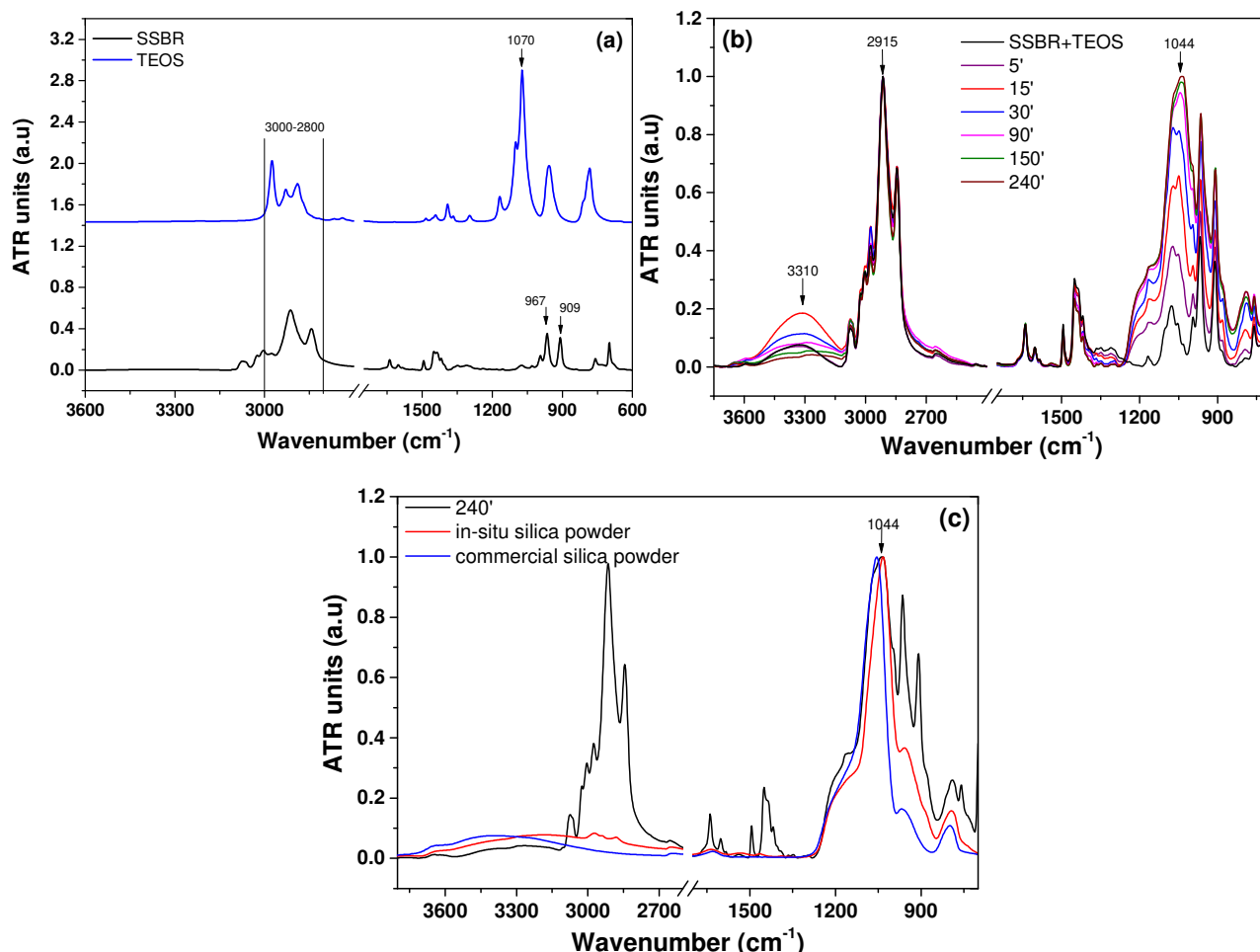


Figure 4.2a) ATR-FTIR spectra of pure chemical substances used for *in-situ* silica synthesis **b)** Normalized ATR spectra of the solidified reacting mixture as kinetic data of sol-gel reaction **c)** ATR spectra of pure *in-situ* silica, commercial silica powder and final reaction mixture at 240 min

The quantitative determination of *in-situ* silica present in silica-rubber masterbatches estimated by thermogravimetric analysis is presented in Fig. 4.3. Higher amounts of silica could be produced with the use of higher amount of TEOS and water. As shown in Fig. 4.3, the amount of residue increases with the increase in amount of TEOS and water. The final weight loss obtained at 800°C is considered as the amount of silica present in the rubber masterbatch. Therefore, from the final weight the amount of *in-situ* silica present in the system is calculated by Eq. 3.1 (in chapter 3) and converted into phr¹⁴.

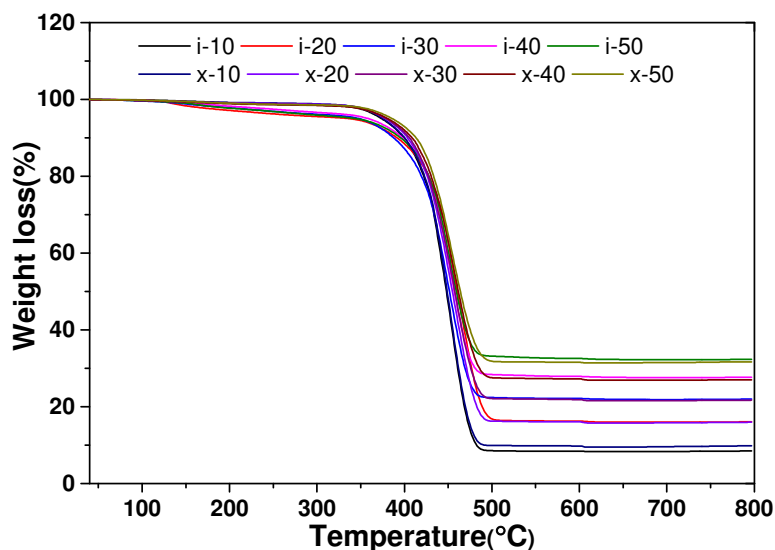


Figure 4.3 Thermogravimetric analyses of *in-situ* and commercial silica-rubber masterbatches

To cross check the amount of *in-situ* silica in the masterbatches, commercial precipitated silica compounds are prepared with similar volume fraction and subjected to thermal analysis (samples designated as 'x' in fig 4.3). The experimental result reveals a similar temperature loss profile for both the samples with approximately the same final weight loss. This further confirms the estimated amount of *in-situ* silica in the masterbatches to be around 10-50 phr. Fig 4.3 demonstrates no weight loss for commercial silica compounds at 100 °C - 350 °C affirming the presence of small amount of catalyst, solvent and TEOS in the *in-situ* silica compounds⁹.

4.2.2 Characterization of the rubber compounds

Fig. 4.4 compares the Mooney viscosities of commercial and *in-situ* silica compounds and extracted data are summarized in Table 4.1. Gum SSBR shows a lowest value of 59 MU and increases significantly with increase in silica content. *In-situ* silica based SSBR compounds exhibits lower Mooney viscosity compared to commercial silica compounds²⁸. A lower Mooney viscosity is always preferred as the compounds display good rheological properties and ease of processing.

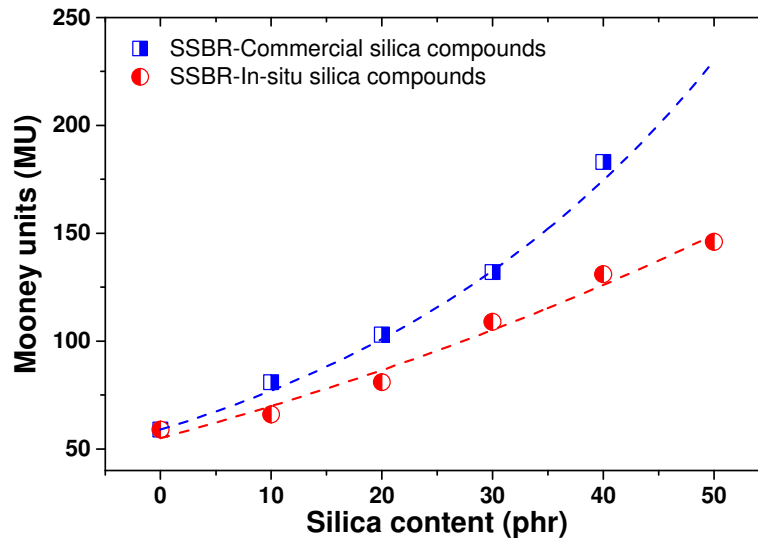


Figure 4.4 Effect of Mooney viscosity with different silica fraction in SSBR at 100 °C

The Mooney viscosity of a 50 phr commercial silica (without plasticizers or oil) compound is too high and could not be evaluated as it exceeds the measuring capability of the instrument. The commercial silica form a filler-filler network structure resulting in an increase in Mooney viscosity. In contrast, *in-situ* silica particles forms less networks or weak networks and are freely mobile when subjected to shear. Such characteristics could be the reason for the lower viscosity of the *in-situ* compounds. Interestingly, the gradient of viscosity drop under shear stress of *in-situ* and commercial silica compounds are almost similar for the same volume fraction²⁹.

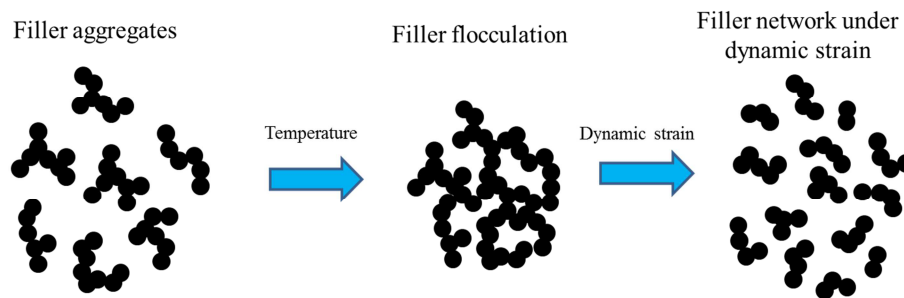
Table 4.1 Mooney viscosity of varies silica filled SSBR compounds

Samples	Commercial silica			<i>In-situ</i> silica		
	*MU ₁	*MU ₄	*MU ₁₋₄	MU ₁	MU ₄	MU ₁₋₄
Gum	80	59	21	80	59	21
10	126	81	45	100	66	34
20	147	103	44	123	82	41
30	177	131	46	156	110	46
40	229	183	46	177	131	46
50	NA	NA	NA	224	147	77

*MU₁ and *MU₄ are Mooney units (MU) at 1 and 4 min. *MU₁₋₄ is difference in MU at 1 and 4 min.

The filler flocculation and filler-filler networks in silica-rubber masterbatches are investigated to understand the agglomeration and aggregation tendency of the *in-situ* silica particles during processing. Due to the difference in surface energies between rubber and silica, the silica

particles tend to aggregate and agglomerates. Such a tendency of fillers to form agglomerates in the rubber is technically called as filler flocculation³⁰. This affects the processability and final properties of the compounds to a large extent. Formation of filler networks can substantially influence the elastic modulus of highly filled rubber compounds. To understand such effects, dynamic strain sweep measurements are conducted. The dynamic filler flocculation and strain dependent filler-filler network characteristics are depicted in Scheme 4.1.



Scheme 4.1 Schematic representation of filler flocculation and filler-filler network break-down under dynamic strain sweep measurements

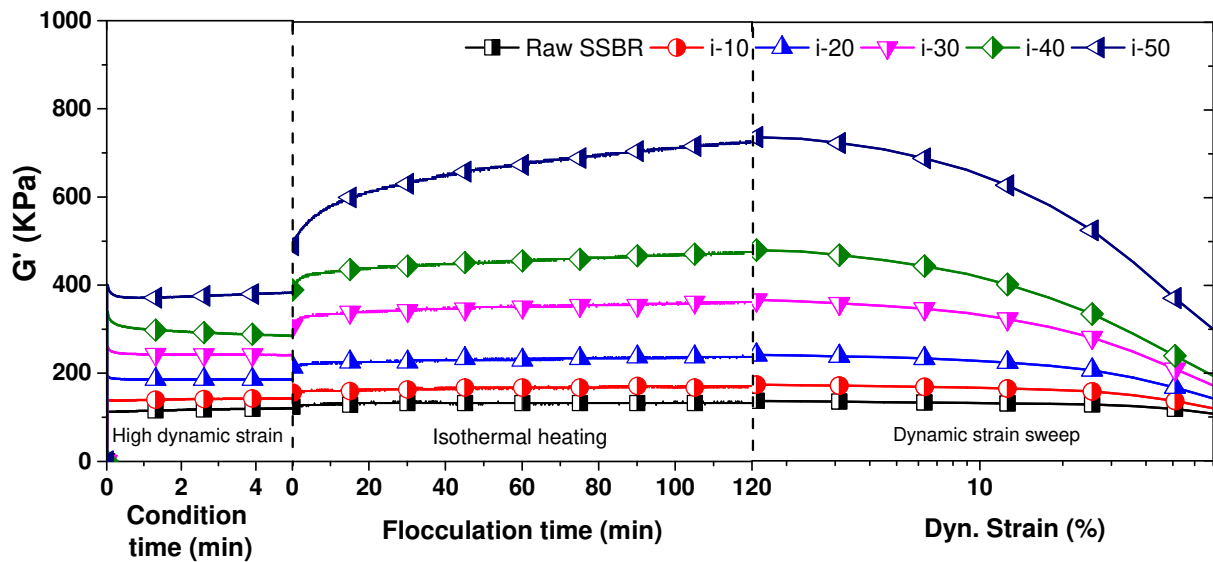


Figure 4.5 Dynamic filler flocculation and strain sweep measurements

Fig. 4.5 shows the three different stages involved in the filler flocculation study. In a first stage, a constant 25 % dynamic strain is applied for 5 min assuming a complete destruction of the filler networks. The dynamic shear modulus is higher for higher volume fractions of silica due to hydrodynamic effect. The experiment is then continued to the second stage with low strain amplitude of 1.4% for 120 min to facilitate filler network reformation. With time, a

slow increase in the shear moduli (G') of the filled compounds is observed and shown in Fig. 4.5. The increase in G' is dependent on the volume fraction of the filler and the filler-filler aggregation characteristics. Therefore, high silica content would result a higher aggregation tendency. Finally in the third stage, the compounds are subjected to strain sweep measurements (Payne effect up to 70% dynamic strain) and the experimental results show that highly filled silica rubber compounds exhibit faster reduction of the G' values. The rate of flocculation and the amplitude of Payne effect are calculated quantitatively as per Eq. 3.3 and Eq. 3.4 (in chapter 3) respectively and depicted in Fig. 4.6.

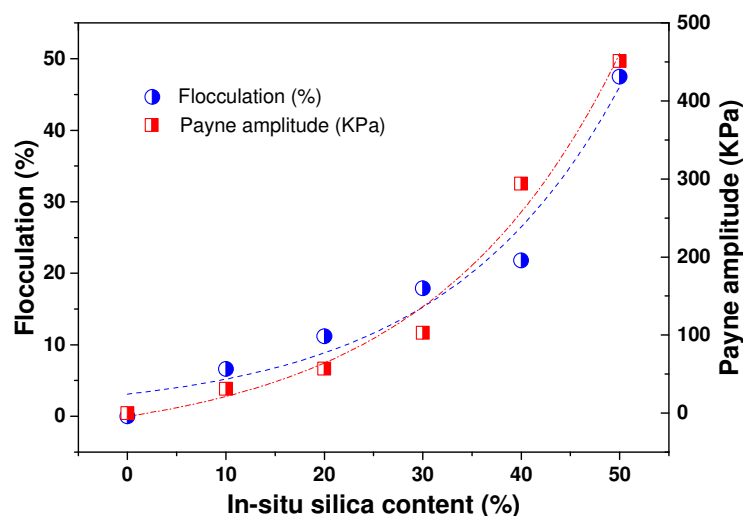


Figure 4.6 Flocculation and dependent Payne effect of *in-situ* silica-SSBR compounds

Vulcanization characteristics of *in-situ* silica SSBR composites are summarized in Table 4.2 and their respective cure curves are given in Fig. 4.7. The unfilled SSBR gum compound exhibits higher scorch time (t_2) and optimum cure time (t_{90}), compared to *in-situ* silica filled compounds. Interestingly, the scorch times and optimum cure times of the *in-situ* silica filled composites without silane coupling agent are almost similar for all filler content. The result clearly shows the vulcanization behaviour of SSBR not being affected by the increasing amounts of *in-situ* silica. Such results are unique as compared to commercial silica filled compounds which retard the vulcanization reaction at higher filler concentrations leading to higher scorch times and optimum cure times due to its acidic nature³¹. Since *in-situ* silica particles are generated through alkaline catalysis sol-gel reaction, it does not affect the vulcanization kinetics even at higher concentrations. Meanwhile, in presence of silane coupling agent the scorch times are similar, whereas the composites show higher optimum cure times with increasing silane concentration.

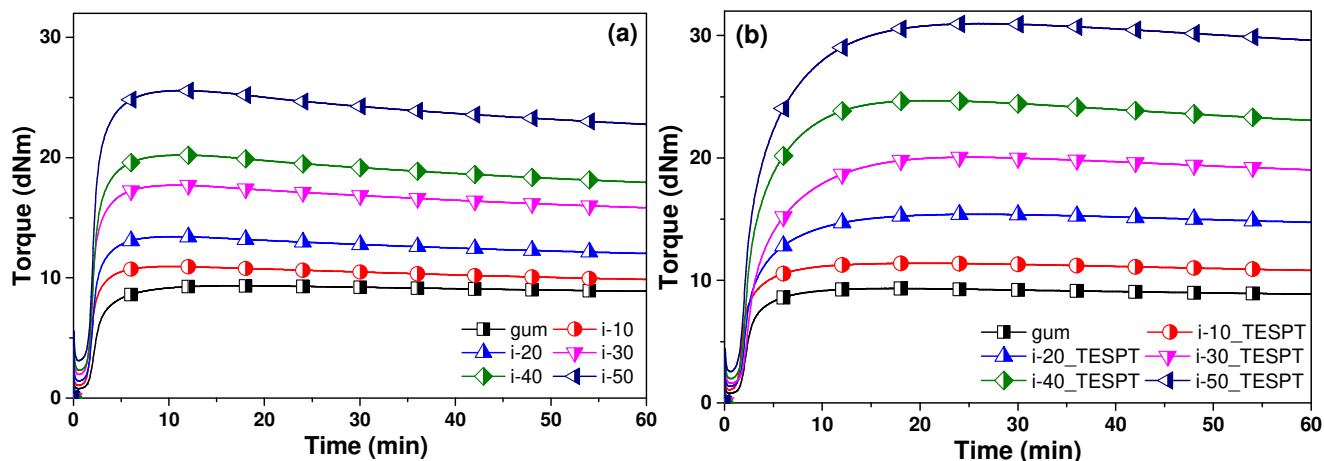


Figure 4.7 Vulcanization curves of SSBR/*in-situ* silica composites (a) absence and (b) presence of silane coupling agent

Table 4.2 Vulcanization characteristics of SSBR/*in-situ* silica composites

Compounds	t_2 (min)	t_{90} (min)	S'_{min} (dNm)	S'_{max} (dNm)	CRI (min^{-1})
Gum	2.35	5.56	0.78	9.34	31.15
i-10	2.05	4.11	1.06	10.95	48.54
i-20	2.11	4.00	1.42	13.43	52.91
i-30	1.59	4.19	1.96	17.7	38.46
i-40	2.05	4.11	2.31	20.21	48.54
i-50	1.59	4.10	3.11	25.58	39.84
i-10_TESPT	1.56	5.33	0.99	11.6	26.52
i-20_TESPT	2.23	9.23	1.32	15.38	14.28
i-30_TESPT	2.01	11.12	1.58	20.03	10.76
i-40_TESPT	2.17	12.10	2.01	24.69	10.07
i-50_TESPT	1.59	13.45	2.89	30.98	8.43

The cure rate index [CRI = $100 / (\text{Optimum cure time } (t_{90}) - \text{scorch time } (t_2))$] of the rubber compounds decrease with higher dosage of the silane coupling agent. It is evident that the rate of cure is affected by the incorporation of silane, as higher CRI values are observed in the absence of the silane coupling agent. Therefore, *in-situ* silica compounds show faster cure characteristics in the absence of silane³². The maximum torque (S'_{max}) increases with the amount of *in-situ* silica in both pristine as well as silane assisted composites, nevertheless, a higher maximum torque is observed for silane assisted *in-situ* silica composites. Additionally, pristine *in-situ* silica compounds exhibit reversion signifying higher proportion of polysulfidic crosslink bridges³³⁻³⁴. The comparison of cure characteristics of *in-situ* silica filled system with precipitated silica system is explained in Chapter 5. The silanol density, specific surface

area, pH of silica particles are some of the important properties strictly influence on the vulcanization characteristics of rubber. The physical, chemical properties of synthesized *in-situ* silica, precipitated silica powders, their rubber composites are discussed in detail at Chapter 6.

4.2.3 Mechanical and dynamic mechanical properties

The stress-strain characteristics of *in-situ* silica in presence and absence of silane coupling agent are analysed are tabulated in Table 4.3 and depicted in Fig. 4.8. The tensile strength and tensile modulus of SSBR composites are improved significantly by the *in-situ* silica. The stress-strain behaviour of the filled composites in absence of silane coupling agent shows gradual increase in moduli and tensile strength compared to the unfilled vulcanizate.

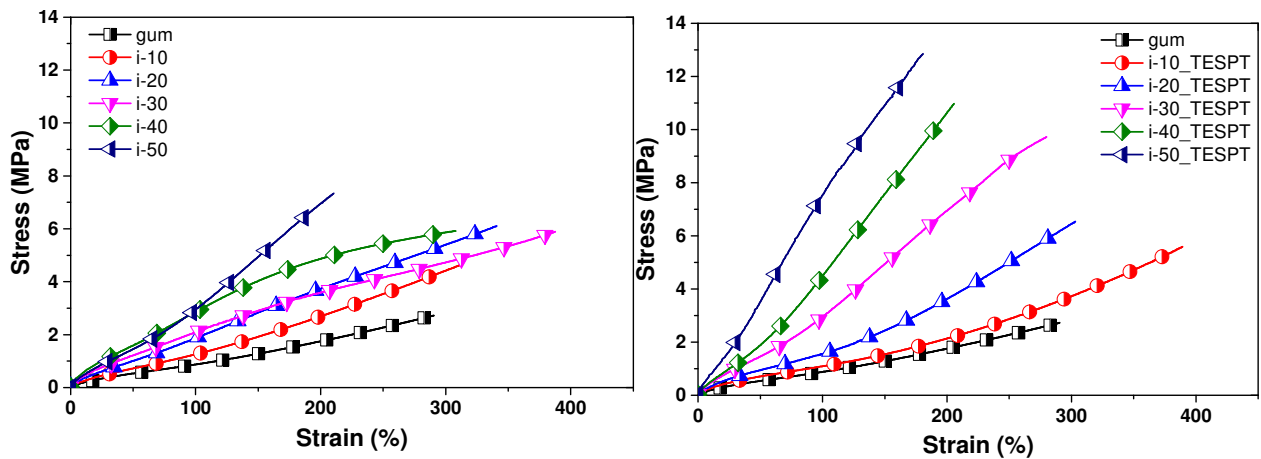


Figure 4.8 Tensile properties of SSBR/*in-situ* silica composites in (a) absence and (b) presence of silane coupling agent

Nevertheless, the composites with silane coupling agent offer better filler-polymer interactions, exhibiting a substantial improvements in moduli and tensile strength. Unfortunately, as a consequence of better filler-polymer interaction by silane, the stiffness of matrix increases compromising the elongation at break. Moreover, the stress-strain plots of *in-situ* silica composites with silane display higher modulus in the low strain region. To quantify the amount of reinforcement enhanced by the silica particles, the reinforcing efficiency³⁵ is

$$RE = \frac{M_{100\% \text{ filled}} - M_{100\% \text{ gum}}}{wt\% \text{ of silica}}$$

Table 4.3 Stress-strain properties of SSBR/*in-situ* silica composites

Samples	100% (MPa)	200% (MPa)	300% (MPa)	Tensile strength (MPa)	Reinforcing efficiency (%)	Elongation at break (%)	Hardness (Shore A)
Gum	0.87	1.76	-	2.72	-	290	42
i-10	1.27	2.69	4.42	4.65	4.59	310	48
i-20	1.87	3.73	5.40	6.10	6.25	340	53
i-30	2.10	3.59	4.73	5.88	5.53	390	56
i-40	2.87	4.87	5.87	5.92	7.24	308	60
i-50	2.93	6.98	-	7.53	6.38	449	63
i-10_TESPT	1.08	2.13	3.72	5.58	2.43	390	48
i-20_TESPT	1.56	3.62	6.45	6.53	4.38	305	54
i-30_TESPT	2.95	6.95	-	9.72	9.57	280	59
i-40_TESPT	4.25	-	-	10.98	12.58	205	61
i-50_TESPT	7.53	-	-	12.5	21.31	180	68

The dynamic mechanical properties of unfilled SSBR and its *in-situ* silica composites studied over a temperature range of -60 °C to 80 °C are depicted in Fig. 4.9 and various important parameters are summarized in Table 4.4. Fig. 4.9(a, c) illustrates the gradually increasing storage moduli of the *in-situ* silica composites according to the silica fraction. From Table 4.4, improvements in the dynamic mechanical properties of *in-situ* silica composites due to enhanced filler-polymer interaction by the silane coupling agent could be visualized. Fig. 4.9b and Fig. 4.9d shows the $\tan \delta$ plot for the *in-situ* silica SSBR composites. It is well known that addition of silica in rubber reduces $\tan \delta$ max values and further reduction would be observed upon incorporation of silanes³⁶. In Fig. 4.9b the glass transition temperature (T_g) is slightly shifted to higher temperatures for all the composites. But in Fig. 4.9d, i.e. with the presence of silane coupling agents, the T_g shifts are significant³⁵. This result indicates an effective silanization which might be associated with the formation of strong nano layer of immobilized rubber chains around the silica surface³⁰. Thus restricted mobility of rubber chains by silane modified silica surface causes the shift in T_g ³⁷. From the temperature sweep studies, *in-situ* silica reinforces the SSBR matrix very well and dynamic behaviour of the composites are further improved with the presence of coupling agents¹⁵.

The dynamic mechanical strain sweep measurements are performed to understand the filler-filler interaction and strain induced softening of the composites. The obtained experimental results are fitted with Kraus equation (Eq. 3.6) by extrapolating to 1000 % strain; where only hydrodynamic reinforcement exists (see Eq. 3.5 in chapter 3). The results

are plotted in Fig. 4.10 and the quantitative information about the Payne effect is tabulated in Table 4.5.

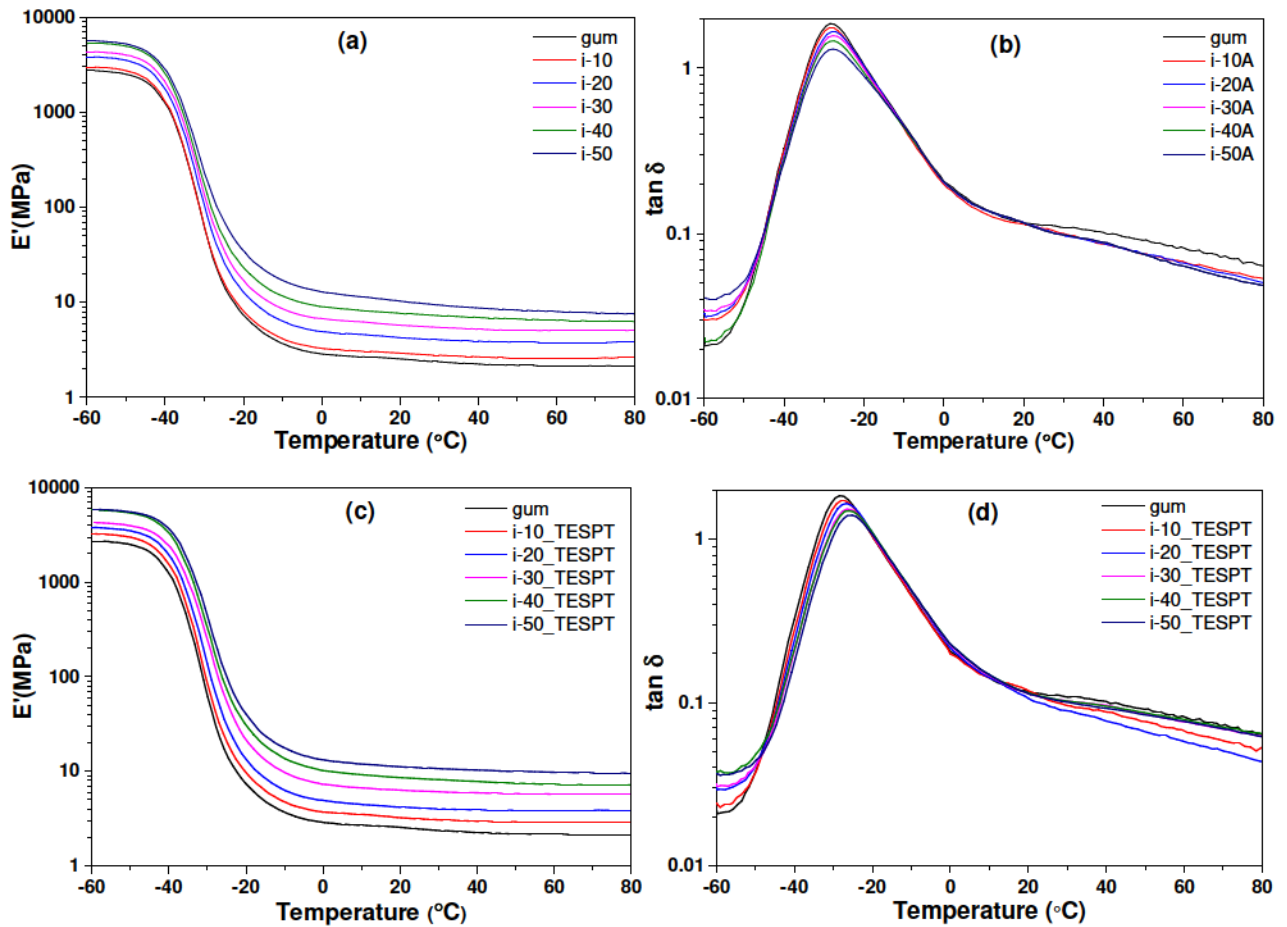


Figure 4.9 Dynamic mechanical temperature sweep analysis of *in-situ* silica-SSBR nanocomposites. (a) & (c) storage modulus and (b) & (d) tan delta graph for SSBR/*in-situ* silica composites in absence and presence of coupling agent

In Fig. 4.10, the solid lines represent samples without silane and dotted lines represent the presence of silane coupling agents in the Kraus fitting function³⁸. As the volume fraction of silica is increased in the rubber matrix, well percolated filler-filler networks are formed. With the incorporation of silane coupling agent, the *in-situ* silica rubber compounds display an increase in the dynamic storage modulus. This effect is contrary to commercial precipitated silica filled composites; as silane incorporation reduces the storage modulus¹⁵.

Table 4.4 Dynamic mechanical properties of SSBR/*in-situ* silica composites

Samples	E' @ 0°C (MPa)	E' @ 25°C (MPa)	E' @ 60°C (MPa)	tan δ _{max}	T _g (°C)
Gum	2.85	2.44	2.14	1.78	-27.8
i-10	3.29	2.90	2.59	1.74	-27.5
i-20	4.88	4.13	3.79	1.65	-27.0
i-30	6.58	5.58	5.05	1.56	-26.7
i-40	9.05	7.41	6.48	1.51	-27.1
i-50	12.78	9.81	7.97	1.49	-27.5
i-10_TESPT	3.68	3.12	2.89	1.72	-27.0
i-20_TESPT	6.06	5.33	5.06	1.61	-26.8
i-30_TESPT	7.20	6.12	5.74	1.53	-26.5
i-40_TESPT	10.2	8.32	7.26	1.51	-26.0
i-50_TESPT	13.2	10.85	9.75	1.41	-25.2

Similar effects (increase in dynamic modulus) are usually observed for carbon nanotubes filled system³⁹⁻⁴⁰. However, Payne effect is observed for the *in-situ* silica compounds both in the presence and absence of silane coupling agent. At the same time, the critical strain value (γ_c) of the composites reduces with increase in silica fraction. Such behaviour indicates a higher dependency of the filler networks towards dynamic strain as the filler fraction increases. The silane incorporated composites show higher critical strain values, meaning the filler networks are less susceptible to the dynamic strain. Accordingly, silane incorporation significantly improves the dynamic performance of the composites by improving the filler-polymer interaction. The amplitude constant (m) constantly decreases with increase in filler content and lies in-between 0.43 to 0.54³⁸.

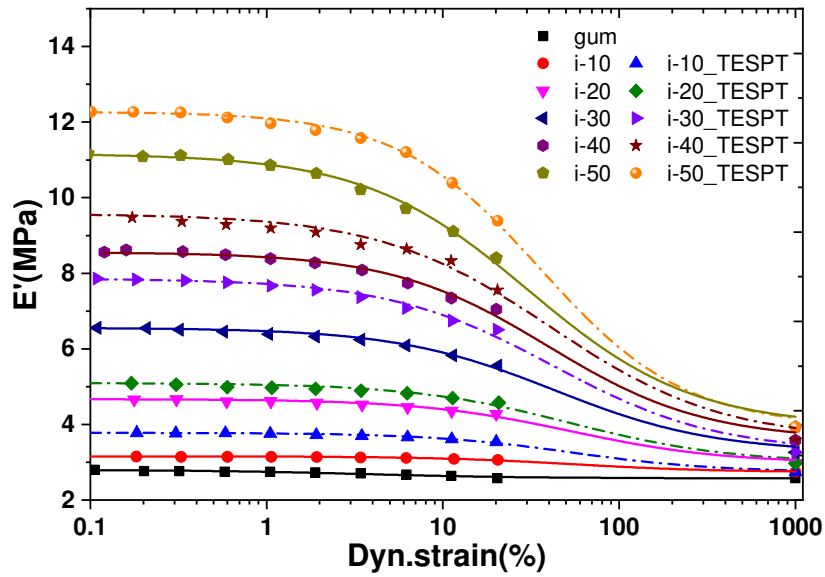


Figure 4.10 Strain dependency of dynamic elastic modulus for the SSBR/*in-situ* silica composites (symbols represent experimental data and lines represent the fitted Kraus equation)

Table 4.5 Calculated strain dependent dynamic properties of composites by Kraus function

Sample	$E'_i - E'_\infty$ (MPa)		Critical strain (γ_c) %		Amplitude constant (m)	
	<i>In-situ</i> w/o silane	<i>In-situ</i> with silane	<i>In-situ</i> w/o silane	<i>In-situ</i> with silane	<i>In-situ</i> w/o silane	<i>In-situ</i> with silane
	Gum	0.22	-	-	-	-
10	0.42	1.04	55.06	53.53	0.54	0.53
20	1.70	2.12	53.24	53.38	0.50	0.48
30	3.30	4.60	42.97	41.93	0.48	0.46
40	4.98	5.99	39.48	40.85	0.49	0.45
50	7.23	8.34	30.59	35.92	0.47	0.43

*w/o defines with out

4.2.4 Other rubber performance

Some important rubber performance parameters like rebound resilience, heat build-up, abrasion, swelling in solvent was also evaluated and obtained results were depicted in Fig. 4.11 and Fig. 4.12. At room temperature, the resilience values are found to be reducing with increase in the amount of fillers (Fig. 4.11a). At the same time, resilience properties are

greatly improved with the addition of silane in the *in-situ* silica composites⁹; even the high temperature (60°C) resilience properties are improved.

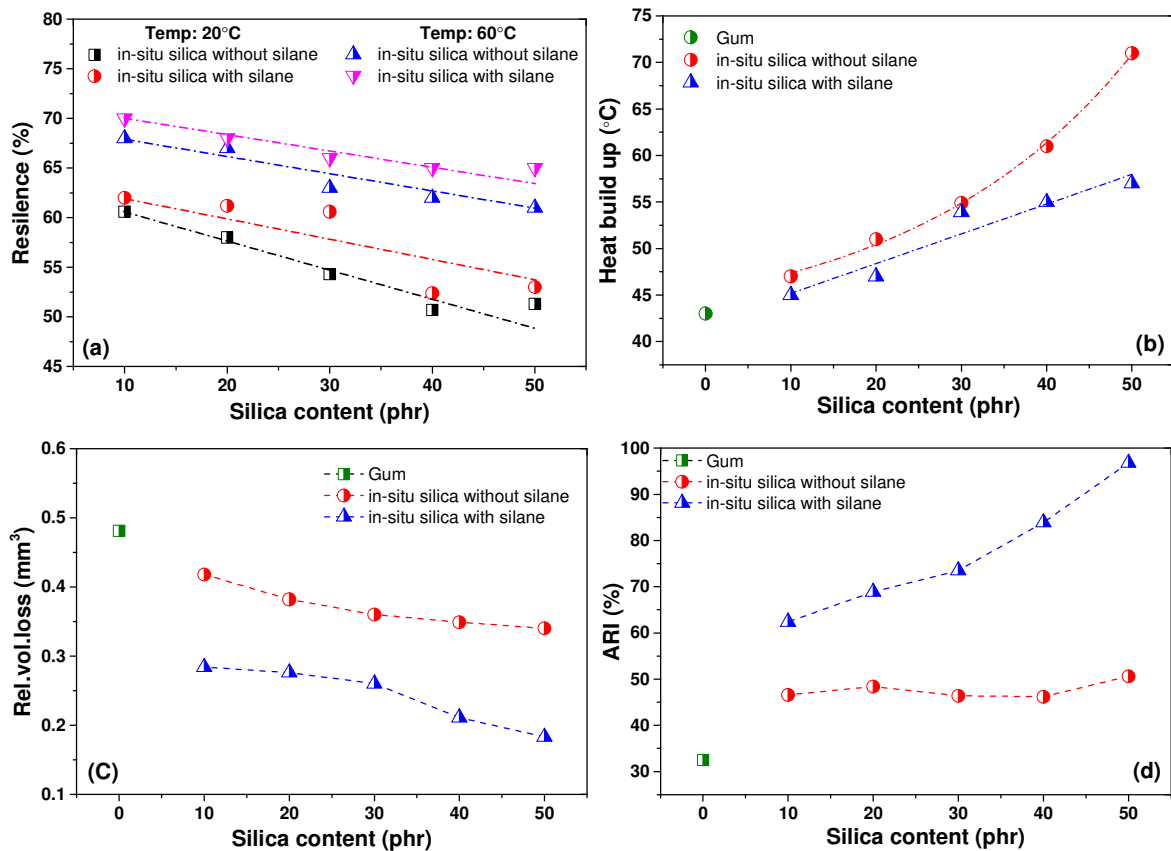


Figure 4.11.a) Rebound resilience characteristics, b) Heat build-up properties, c) Relative volume loss, and d) Abrasion resistance index (ARI) % of *in-situ* silica filled SSBR composites

The heat build-up properties of *in-situ* silica filled SSBR composites in presence and absence of silane coupling agent are investigated as per Eq. 3.7 (in chapter 3) and plotted in Fig. 4.11b. The unfilled gum vulcanizate shows the least heat build-up inside the core of the sample. At the same time, as the amount of silica fraction increases in the SSBR, the degree of heat generation and build-up inside the composites is increases significantly. Inclusion of rigid particles in a viscoelastic material would exhibit excessive heat generation by increasing the internal friction due to poor filler polymer interaction and a lower heat loss⁴¹. Eventually, incorporation of silane coupling agent in the silica filled system reduces heat generation and increases the heat loss of the material by improving the filler-polymer interaction due to silanization³⁵.

The abrasion properties of *in-situ* silica filled SSBR compounds are plotted in Fig. 4.11c and Fig. 4.11d. The abrasion resistance index (calculated by Eq. 3.8 in chapter 3)

clearly depicts the improved resistance of the composites towards friction with the addition of *in-situ* silica. At the same time, addition of silane coupling agent results in better resistance towards abrasion. The silane improves the abrasion characteristics through better filler-polymer interaction. The relative volume loss (calculated by Eq. 3.9 in chapter 3) is also significantly reduced by increasing the silica fraction and silane coupling agent.

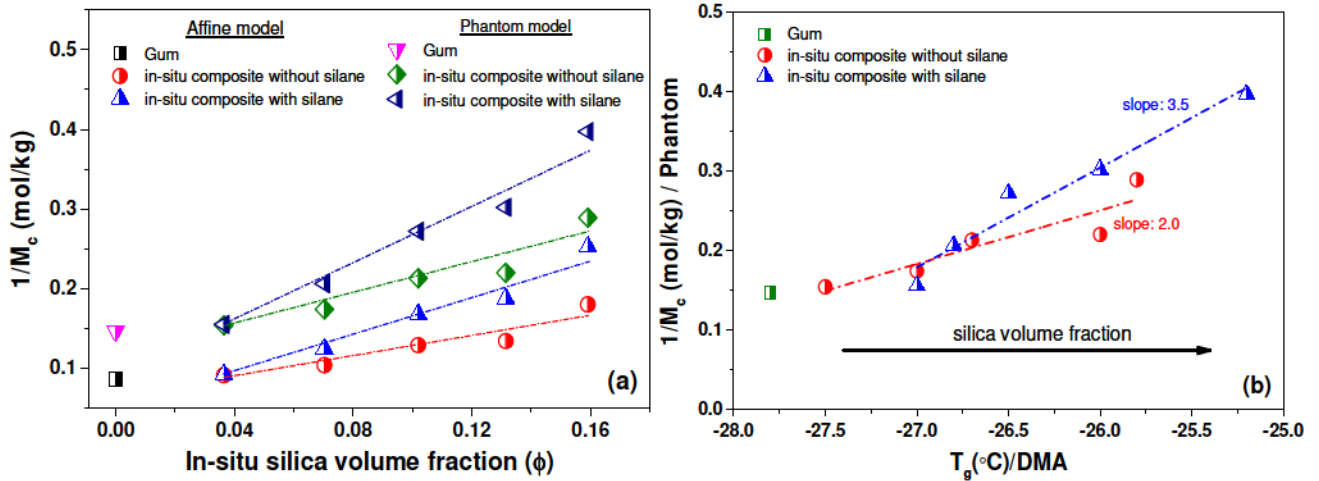


Figure 4.12.a) Effect on crosslink density of SSBR with respect to silica fraction and silane b) the correlation between T_g and crosslink density

The crosslink densities of gum and *in-situ* silica filled SSBR composites are calculated by equilibrium swelling based Flory-Rehner equations Eq. 3.11 and Eq. 3.12 (in chapter 3). The estimated crosslink densities based on affine and phantom network model are depicted in Fig. 4.12a. The crosslink density of SSBR gradually increases with the volume fraction of silica. Also, the silane coupled *in-situ* silica composites exhibit higher crosslink densities, compared to the unsilanized composites³⁵. The enhanced crosslink density of silane incorporated SSBR composites is due to the chemically bonded silane coupling agent on the surface of the filler and improved filler-rubber interaction⁴². Fig.4.12b shows the plot of crosslink density obtained from phantom network model against the glass transition temperature (T_g) measured by the dynamic mechanical analyzer (DMA). Linearity is observed between crosslink density and T_g with increasing volume fraction of filler. In the absence of silane the obtained slope is 2.0, however with the incorporation of silane a higher slope of 3.5 is observed. This confirms that crosslink density and T_g of composites are majorly dependent on the silanization reaction as well as filler volume fraction. This correlation further evidences the enhanced silica-rubber interaction by the silane.

4.2.5 Morphology

To understand the *in-situ* silica-rubber interaction and interfacial adhesion in presence and absence of silane coupling agent, fracture surface of the composites are analyzed by SEM. In Fig. 4.13a, the 30 phr *in-situ* silica composite without silane shows aggregated particles with average particle size of around 200-300 nm. The fracture surface shows some kind of holes, which represent the poorly adhered particles being pulled out from the matrix during cryo-fracture. In Fig. 4.13b, by presence of coupling agent, the *in-situ* silica particles are fully covered by rubber layers. The micrograph signifies the superior adhesion of the *in-situ* silica fillers with the rubber matrix as a benefit of the silane coupling agent.

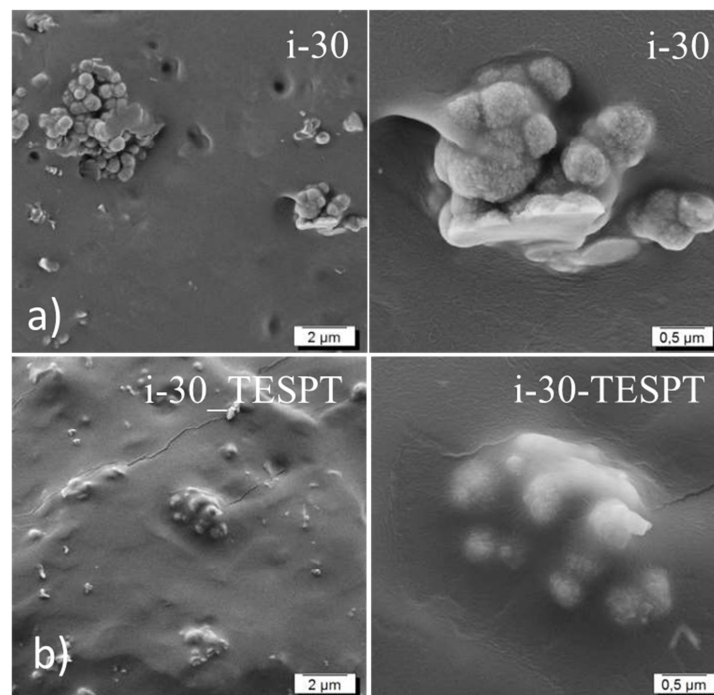


Figure 4.13 SEM micrographs of cryo-fracture failure surface investigation of *in-situ* silica composites (a) absence and (b) presence of TESPT silane coupling agent at low and high magnifications

The particle size and dispersion of silica nanoparticles in rubber matrix is one of the most critical parameters, which determine the overall performance of the nanocomposite. Aggregates and agglomerates of filler particles in a rubber matrix act as stress concentration points resulting in early failure. Fig. 4.14 displays the TEM images of silane coupled SSBR/*in-situ* silica composites. The silica particles are moreover individual and bigger in size with average particle size of around 200 to 300 nm. Silane coupling agents improve the dispersion of silica particles and some particles that exist interconnected during synthesis.

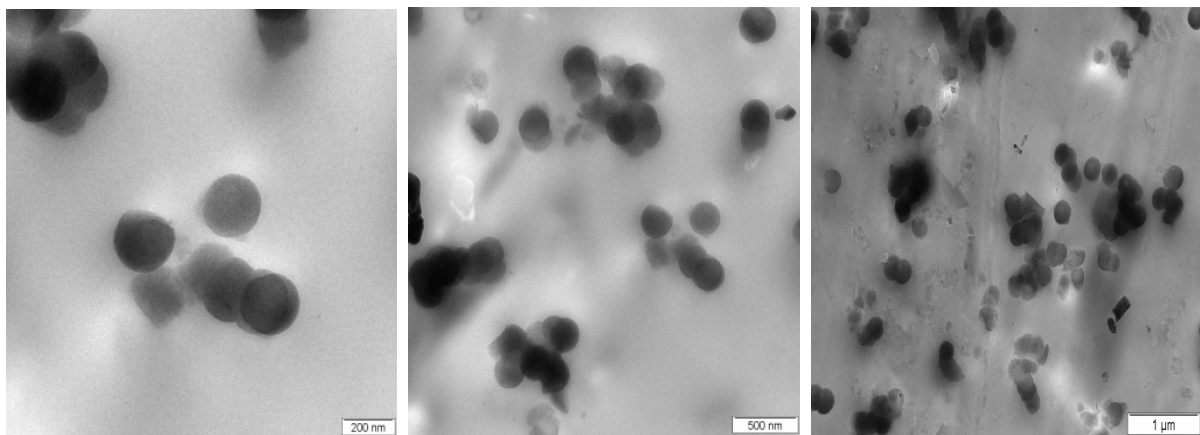


Figure 4.14 TEM images of silane modified SSBR/*in-situ* silica composites

4.3 Conclusions

The amount of *in-situ* silica formation in rubber was controlled by the exact addition of silica precursor and water and by increasing the TEOS:Water ratio in the rubber solution. The total amount of silica converted from TEOS was around 98% with an overall reaction time of 240 min and of which 50% of silica was converted within the first 30min. From the ATR-FTIR investigations, the intensity of Si-O-Si stretching vibration of silica oxide at 1044 cm^{-1} increased as a function of reaction time, representing successful conversion of silica from TEOS. The flocculation and Payne effect measurements of *in-situ* silica filled rubber compounds showed increased flocculation and filler-filler interaction with respect to the amount of silica in rubber. The silica formed inside the rubber improved the mechanical and dynamic mechanical properties significantly compared to gum vulcanizates. From Payne effect measurements, the critical strain was estimated by Kraus model and was found to gradually reduce with increasing amount of silica in rubber. This study evidenced the silica-silica network in rubber to be mainly dependent on the volume fraction of filler, which reduces further with the addition of TESPT coupling agent. The rebound resilience is significantly reduced with the increase in volume fraction of silica. The heat build-up and abrasion properties of the filled rubber were significantly improved by the *in-situ* silica. Addition of TESPT silane in the *in-situ* silica composites further improved the mechanical reinforcement and few other performances as well. The SEM and TEM investigations stated that the *in-situ* derived silica particles were mostly individual and bigger in size, with average particle size of around 200 to 500 nm. The detailed study on *in-situ* silica powder separated from the rubber matrix is described in chapter 6. In briefly the primary particle size of synthesised *in-situ* silica is around 10 nm and a group of primary particles are fused together

to form a 200 to 500 nm of spherical aggregates or spherical clusters. The spherical aggregates are sometime exhibited as individual aggregates as well as agglomerates, which can be clearly identified by TEM analysis.

References

1. Dierkes, W. K., *Economic mixing of silica-rubber compounds: interaction between the chemistry of the silica-silane reaction and the physics of mixing*. University of Twente: 2005.
2. Rodgers, B., *Rubber compounding: chemistry and applications*. CRC Press: 2015.
3. Mark, J.; Pan, S. J., Reinforcement of polydimethylsiloxane networks by in-situ precipitation of silica: A new method for preparation of filled elastomers. *Die Makromolekulare Chemie, Rapid Communications* 1982, 3 (10), 681-685.
4. Ikeda, Y.; Tanaka, A.; Kohjiya, S., Reinforcement of styrene-butadiene rubber vulcanizate by in situ silica prepared by the sol-gel reaction of tetraethoxysilane. *Journal of Materials Chemistry* 1997, 7 (8), 1497-1503.
5. Tanahashi, H.; Osanai, S.; Shigekuni, M.; Murakami, K.; Ikeda, Y.; Kohjiya, S., Reinforcement of Acrylonitrile-Butadiene Rubber by Silica Generated in situ. *Rubber Chemistry and Technology* 1998, 71 (1), 38-52.
6. Murakami, K.; Osanai, S.; Shigekuni, M.; Iio, S.; Tanahashi, H.; Kohjiya, S.; Ikeda, Y., Silica and Silane Coupling Agent for in Situ Reinforcement of Acrylonitrile-Butadiene Rubber. *Rubber Chemistry and Technology* 1999, 72 (1), 119-129.
7. Kohjiya, S.; Ikeda, Y., Reinforcement of general-purpose grade rubbers by silica generated in situ. *Rubber chemistry and technology* 2000, 73 (3), 534-550.
8. Matějka, L.; Dukh, O.; Kolařík, J., Reinforcement of crosslinked rubbery epoxies by in-situ formed silica. *Polymer* 2000, 41 (4), 1449-1459.
9. Kohjiya, S.; Murakami, K.; Iio, S.; Tanahashi, T.; Ikeda, Y., In situ filling of silica onto "green" natural rubber by the sol-gel process. *Rubber chemistry and technology* 2001, 74 (1), 16-27.
10. Yoshikai, K.; Ohsaki, T.; Furukawa, M., Silica reinforcement of synthetic diene rubbers by sol-gel process in the latex. *Journal of applied polymer science* 2002, 85 (10), 2053-2063.
11. Chen, X.; Wu, L.; Zhou, S.; You, B., In situ polymerization and characterization of polyester-based polyurethane/nano-silica composites. *Polymer International* 2003, 52 (6), 993-998.
12. Ikeda, Y.; Katoh, A.; Shimanuki, J.; Kohjiya, S., Nano-Structural Observation of in situ Silica in Natural Rubber Matrix by Three Dimensional Transmission Electron Microscopy. *Macromolecular Rapid Communications* 2004, 25 (12), 1186-1190.
13. Bandyopadhyay, A.; Bhowmick, A. K.; De Sarkar, M., Synthesis and characterization of acrylic rubber/silica hybrid composites prepared by sol-gel technique. *Journal of Applied Polymer Science* 2004, 93 (6), 2579-2589.
14. Ikeda, Y.; Kameda, Y., Preparation of "green" composites by the sol-gel process: in situ silica filled natural rubber. *Journal of sol-gel science and technology* 2004, 31 (1-3), 137-142.
15. Das, A.; Jurk, R.; Werner Stöckelhuber, K.; Heinrich, G., Silica-Ethylene Propylene Diene Monomer Rubber Networking by In Situ Sol-Gel Method. *Journal of Macromolecular Science, Part A: Pure and Applied Chemistry* 2007, 45 (1), 101-106.

16. Ikeda, Y.; Poompradub, S.; Morita, Y.; Kohjiya, S., Preparation of high performance nanocomposite elastomer: effect of reaction conditions on in situ silica generation of high content in natural rubber. *Journal of Sol-Gel Science and Technology* 2008, 45 (3), 299-306.
17. Kagate, B. P.; Das, C.; Das, A.; Basu, D.; Reuter, U.; Heinrich, G., Effect of sol-gel derived in situ silica on the morphology and mechanical behavior of natural rubber and acrylonitrile butadiene rubber blends. *Journal of Sol-Gel Science and Technology* 2012, 63 (3), 501-509.
18. Wahba, L.; D'Arienzo, M.; Donetti, R.; Hanel, T.; Scotti, R.; Tadiello, L.; Morazzoni, F., In situ sol-gel obtained silica-rubber nanocomposites: influence of the filler precursors on the improvement of the mechanical properties. *RSC Advances* 2013, 3 (17), 5832.
19. Wahba, L.; D'Arienzo, M.; Dire, S.; Donetti, R.; Hanel, T.; Morazzoni, F.; Niederberger, M.; Santo, N.; Tadiello, L.; Scotti, R., A novel non-aqueous sol-gel route for the in situ synthesis of high loaded silica-rubber nanocomposites. *Soft Matter* 2014, 10 (13), 2234-44.
20. Miloskovska, E.; Nies, E.; Hristova-Bogaerds, D.; van Duin, M.; de With, G., Influence of reaction parameters on the structure of in situ rubber/silica compounds synthesized via sol-gel reaction. *Journal of Polymer Science Part B: Polymer Physics* 2014, 52 (14), 967-978.
21. Miloskovska, E.; Hansen, M. R.; Friedrich, C.; Hristova-Bogaerds, D.; van Duin, M.; de With, G., In Situ Silica Nanoparticle Formation in a Rubber Matrix Monitored via Real-Time SAXS and Solid-State NMR Spectroscopy. *Macromolecules* 2014, 47 (15), 5174-5185.
22. Raman, V. S.; Das, A.; Stockelhuber, K. W.; Eshwaran, S. B.; Chanda, J.; Malanin, M.; Reuter, U.; Leuteritz, A.; Boldt, R.; Wie; Heinrich, G., Improvement of mechanical performance of solution styrene butadiene rubber by controlling the concentration and the size of in situ derived sol-gel silica particles. *RSC Advances* 2016, 6 (40), 33643-33655.
23. Litvinov, V. M.; De, P. P., *Spectroscopy of rubbers and rubbery materials*. iSmithers Rapra Publishing: 2002.
24. Socrates, G., Infrared characteristic group frequencies, Tables and charts. *Journal of the American Chemical Society* 1995, 117 (5), 1671-1671.
25. Martinez, J.; Ruiz, F.; Vorobiev, Y. V.; Pérez-Robles, F.; González-Hernández, J., Infrared spectroscopy analysis of the local atomic structure in silica prepared by sol-gel. *Journal of Chemical Physics* 1998, 109 (17), 7511-7514.
26. Kraleovich, M. L.; Koenig, J. L., FTIR Analysis of Silica-Filled Natural Rubber. *Rubber Chemistry and Technology* 1998, 71 (2), 300-309.
27. Beganskienė, A.; Sirutkaitis, V.; Kurtinaitienė, M.; Juškėnas, R.; Kareiva, A., FTIR, TEM and NMR investigations of Stöber silica nanoparticles. *Mater Sci (Medžiagotyra)* 2004, 10, 287-290.
28. Mihara, S.; Datta, R.; Noordermeer, J., Flocculation in silica reinforced rubber compounds. *Rubber Chemistry and Technology* 2009, 82 (5), 524-540.
29. Dutta, N. K.; Tripathy, D., Effects of types of fillers on the molecular relaxation characteristics, dynamic mechanical, and physical properties of rubber vulcanizates. *Journal of applied polymer science* 1992, 44 (9), 1635-1648.
30. Stöckelhuber, K. W.; Svistkov, A. S.; Pelevin, A. G.; Heinrich, G., Impact of Filler Surface Modification on Large Scale Mechanics of Styrene Butadiene/Silica Rubber Composites. *Macromolecules* 2011, 44 (11), 4366-4381.
31. Pal, P.; De, S., Effect of reinforcing silica on vulcanization, network structure, and technical properties of natural rubber. *Rubber Chemistry and Technology* 1982, 55 (5), 1370-1388.

32. Raman, V.; Rooj, S.; Das, A.; Stöckelhuber, K.; Simon, F.; Nando, G.; Heinrich, G., Reinforcement of solution styrene butadiene rubber by silane functionalized halloysite nanotubes. *Journal of Macromolecular Science, Part A* 2013, *50* (11), 1091-1106.
33. Milani, G.; Leroy, E.; Milani, F.; Deterre, R., Mechanistic modeling of reversion phenomenon in sulphur cured natural rubber vulcanization kinetics. *Polymer Testing* 2013, *32* (6), 1052-1063.
34. Aprem, A. S.; Joseph, K.; Thomas, S., Recent Developments in Crosslinking of Elastomers. *Rubber Chemistry and Technology* 2005, *78* (3), 458-488.
35. Hashim, A.; Azahari, B.; Ikeda, Y.; Kohjiya, S., The effect of bis (3-triethoxysilylpropyl) tetrasulfide on silica reinforcement of styrene-butadiene rubber. *Rubber chemistry and technology* 1998, *71* (2), 289-299.
36. Ikeda, Y.; Tanaka, A.; Kohjiya, S., Effect of catalyst on in situ silica reinforcement of styrene-butadiene rubber vulcanizate by the sol-gel reaction of tetraethoxysilane. *J. Mater. Chem.* 1997, *7* (3), 455-458.
37. Tsagaropoulos, G.; Eisenberg, A., Dynamic mechanical study of the factors affecting the two glass transition behavior of filled polymers. Similarities and differences with random ionomers. *Macromolecules* 1995, *28* (18), 6067-6077.
38. Heinrich, G.; Klüppel, M., Recent advances in the theory of filler networking in elastomers. In *Filled Elastomers Drug Delivery Systems*, Springer: 2002, pp 1-44.
39. Das, A.; Stöckelhuber, K.; Jurk, R.; Saphiannikova, M.; Fritzsche, J.; Lorenz, H.; Klüppel, M.; Heinrich, G., Modified and unmodified multiwalled carbon nanotubes in high performance solution-styrene-butadiene and butadiene rubber blends. *Polymer* 2008, *49* (24), 5276-5283.
40. Subramaniam, K.; Das, A.; Heinrich, G., Development of conducting polychloroprene rubber using imidazolium based ionic liquid modified multi-walled carbon nanotubes. *Composites Science and Technology* 2011, *71* (11), 1441-1449.
41. Wagner, M. P., Reinforcing Silicas and Silicates. *Rubber Chemistry and Technology* 1976, *49* (3), 703-774.
42. Park, S.-J.; Cho, K.-S., Filler-elastomer interactions: influence of silane coupling agent on crosslink density and thermal stability of silica/rubber composites. *Journal of colloid and interface science* 2003, *267* (1), 86-91.

Chapter 5

Properties and performance of *in-situ* silica filled SSBR composites with respect to precipitated silica filled SSBR composites

The results of this chapter have been published in *Rubber Chemistry and Technology*, 2017, vol. 90, No. 3, 467 - 486.

5.1 Introduction

The rubber industries are constantly looking for a better material to solve current environmental issues like lower CO₂ emission, lower fuel consumption and safety. Silica reinforced rubbers are one of the important materials playing a major role in the automotive industry due to its versatile functions, in the aspect of lower rolling resistance and wet skid resistance¹⁻². Major issues while using silica as high performance fillers for tyres are poor nanoscale dispersion, higher Payne effect, interrupting vulcanization kinetics and handling issues during compounding. Some of the critical issues have been rectified by using silane coupling agent, improved mixing time and cycles². Anyhow, requirements for silica based rubber products have been not yet been fulfilled and lots of research is going to improve the performance of silica based rubber products. Considering above mentioned issues, we have prepared silica based rubber composites adapting *in-situ* sol-gel method³. In this chapter the properties of developed *in-situ* silica composites are compared with commercial precipitated silica composites in presence and absence of silane coupling agent. 30 phr of silica filled composites and their silane modified composites are taken into study. The fundamental rubber performance analysing instruments along with some new instrumental techniques like tear fatigue analyser and linear friction tester are used to explore the reinforcing nature of silica in rubber.

5.2 Results and discussion

5.2.1 Estimation of amount of silica content

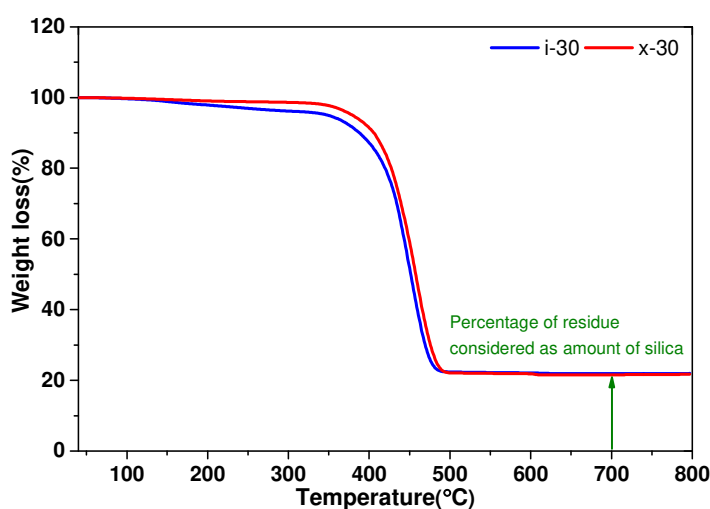


Figure 5.1 Estimation of amount of silica presented in silica-rubber masterbatches by thermogravimetric analysis

The quantitative determination of *in-situ* silica present in silica-rubber masterbatches is estimated by thermogravimetric graphs as depicted in Fig. 5.1 and Eq. 3.1 (in chapter 3). The precipitated silica filled rubber compound does not show any characteristic weight loss in 100 °C to 350 °C regime, whereas, a 5 % weight loss is noticed in the *in-situ* silica compounds. The *in-situ* silica compound might contain traces of volatile substance like catalyst, solvent and unreacted TEOS which evaporates at elevated temperatures⁴. However, the final weight loss obtained at 600 °C to 800 °C is almost equal for both the silica filled compounds. This affirms that the amount of silica presented in rubber is around 30 phr as estimated by thermogravimetric method.

5. 2. 2 Investigation of silica flocculation and network analysis

The flocculation tendency⁵ leading to formation of silica-silica network in the unvulcanized rubber compound is investigated by moving die rheometer. The experimental results from dynamic filler flocculation and strain dependency of silica filled rubber are plotted in Fig. 5.2 and some of the obtained properties are tabulated in Table 5.1.

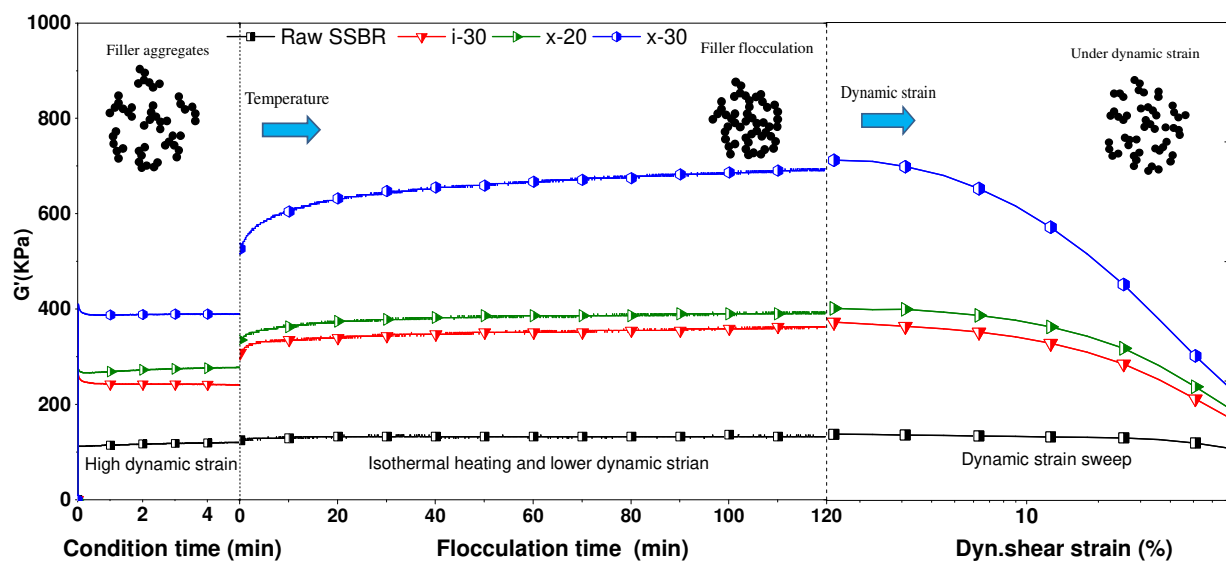


Figure 5.2 Aggregation and reformation of silica network in rubber compound

The raw rubber does not show any increment of the modulus due to the absence of silica. As expected, all silica filled rubber compounds exhibited a time dependent increase in the shear modulus during flocculation experiment at elevated at temperature (120 °C). As in this process the filler-filler network is developed, in the strain sweep experiment a step decrease of the modulus values can be observed from the last step of this experiment. The precipitated

silica filled compound containing 30 phr silica shows maximum modulus values after 120 min flocculation experiment with respect to other composites. A 20 phr precipitated silica filled compound is also analysed and interestingly, the degree of flocculation is found to be higher than 30 phr *in-situ* silica. Therefore, the extent of flocculation for a 30 phr *in-situ* silica filled compound is even lower than 20 phr of precipitated silica. The time taken to achieve 60% filler-filler networks (60% of the developed ultimate torque or maximum modulus) for 30 phr precipitated silica compounds is calculated to be 5.5 min whereas, the 30 phr *in-situ* silica compound took 23 min to achieve the 60% of filler flocculation. These findings point out that *in-situ* silica has relatively less tendency to develop filler-filler agglomerated when compare to precipitated silica. Similarly, the experimental findings with the dynamic strain sweep measurement describe that commercial precipitated silica has a higher tendency to form filler-filler network as it is reflected by showing higher Payne effect⁶. The in current scenario of the SEM images shows that the *in-situ* silica particles are bigger than precipitated silica particles, thus may be a reason that *in-situ* silica compounds exhibit a lower flocculation tendency. Nevertheless, the filler flocculation behaviour in rubber is predominantly depend on the specific surface area, surface functionality and structure of filler particles.

Table 5.1 Flocculation properties of *in-situ* and precipitated silica filled SSBR compounds

Samples	Flocculation				Payne effect		
	G'_{0min} (KPa)	G'_{120min} (KPa)	Flocculation (%)	Time for 60% flocculation (min)	$G'_{0\%}$ (KPa)	$G'_{70\%}$ (KPa)	$\Delta G'_{0min}$ (KPa)
Gum	125	132	0	0	138	108	0
x-20	335	394	17.5	5	401	190	212
x-30	526	694	31.9	5.5	711	232	479
i-30	308	363	17.9	23	372	171	103

5. 2. 3 Rheometric analysis

The vulcanization characteristics of SSBR gum, 30 phr of *in-situ* and 30 phr precipitated silica filled compounds are plotted in Fig. 5.3. From this plot different curing characteristics like minimum torque (S'_{min}), maximum torque (S'_{max}), scorch time (TS2) and optimum cure time (TC90) are calculated and furnished in Table 5.2. As expected the unfilled gum compound shows lower development of torque values as compared with filled system. Precipitated silica (without silane) filled compound exhibits lower S'_{min} and lower S'_{max}

when compared to *in-situ* silica (without silane) compounds. The curing time (TC90) of precipitated silica is longer than gum compound, while *in-situ* silica compound displays even faster cure than the gum compound. This speculates that the cure property of SSBR is adversely affected by the incorporation of precipitated silica but not in the case for *in-situ* silica. The reasons for such an effect are the acidic nature of precipitated silica and adsorption of the curatives on the silica surface which retard vulcanization reaction⁷. In contrast, *in-situ* silica particles are synthesized in the presence of a base catalyst (n-butylamine) and some base molecules can be adsorbed by the surface of the *in-situ* silica that can promote the vulcanization reaction significantly.

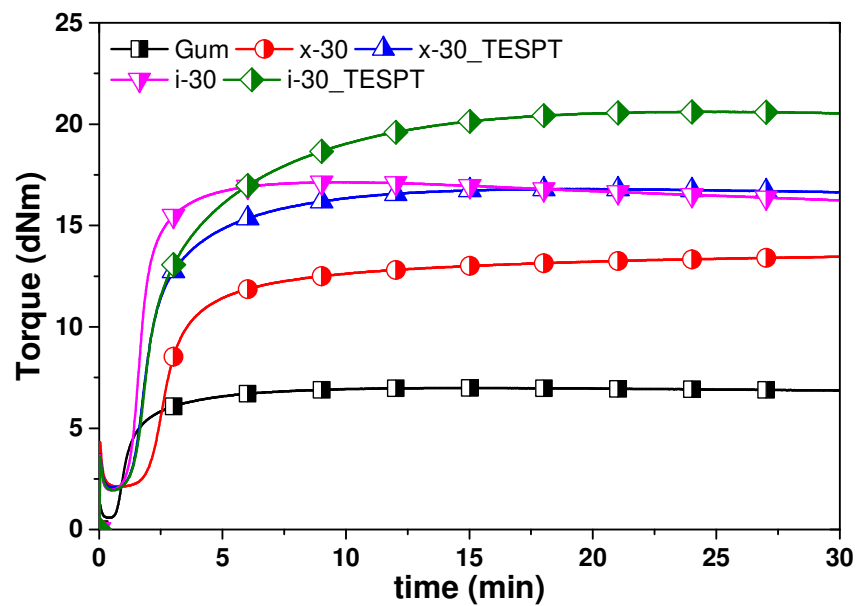


Figure 5.3 Vulcanization characteristics of *in-situ* and precipitated silica filled SSBR compounds

Table 5.2 Vulcanization data of *in-situ* and precipitated silica filled SSBR compounds

Samples	Rheometric torque ($S_{\max} - S_{\min}$) (dNm)	TS2 (min)	TC90 (min)	CRI (min^{-1})
Gum	6.14	1.36	4.26	34.48
x-30	11.34	2.26	18.29	6.58
x-30_TESPT	14.73	1.5	6.35	20.62
i-30	15.18	1.59	4.19	38.46
i-30_TESPT	18.67	2.01	11.12	10.97

Incorporation of silane coupling agent in precipitated silica compound offers faster cure rate; surprisingly, a long cure time is noticed after addition of silane with *in-situ* silica. It can also

be noticed that addition of silane decreased the cure rate index very rapidly with *in-situ* silica⁸. Further chemical studies are required to understand the effect of silane on the curing behaviour of sol-gel silica filled SSBR compound. It is interesting to note that the maximum rheometric torque is found to be highest with silane treated 30 phr of *in-situ* silica indicating a strong reinforcement effect by the fillers. In both silica filled rubber systems, the cure rate index (CRI) is significantly affected by the incorporation of silane coupling agent⁸.

5. 2. 4 Mechanical properties

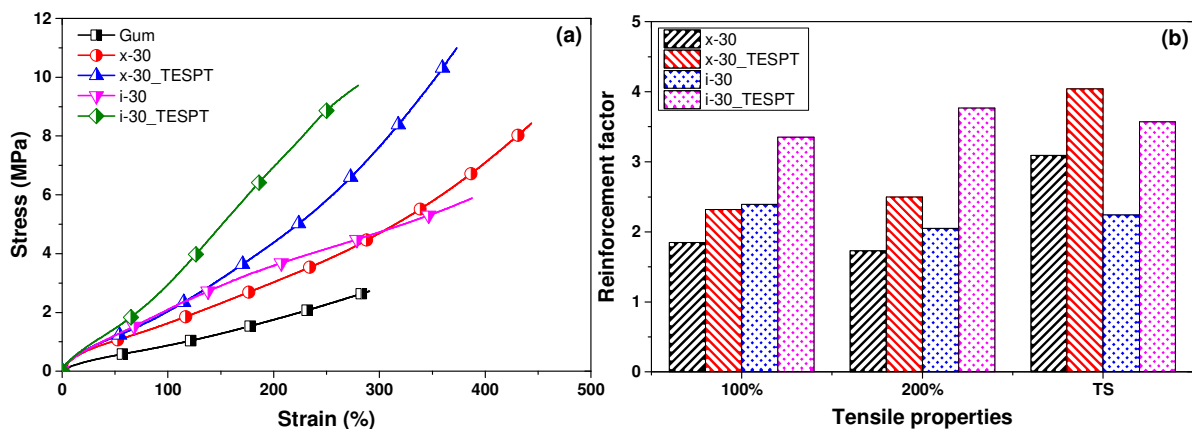


Figure 5.4 (a) Stress-strain properties of 30 phr filled *in-situ* and precipitated silica-SSBR composites (b) reinforcement factor for the silica filled composites calculated from stress-strain plot

The stress-strain properties of SSBR gum and 30 phr silica filled composites are shown in Fig. 5.4a and the reinforcement factors ($RF = \text{Mechanical properties of the composites} / \text{mechanical properties of the gum vulcanizate}$) shown in Fig. 5.4b. Incorporation of silica into the SSBR matrix improves the modulus at different elongations and tensile strength of the composites considerably. *In-situ* silica based composites display higher 100 % and 200 % moduli with a slight compromise on the elongation at break and tensile strength when compared to precipitated silica composites. However, silane modified *in-situ* silica composites exhibit even higher modulus for example, at 100% and 200% elongation, than *in-situ* silica as well as precipitated silica and its silane modified composites. The reinforcement factor⁹ calculated in an effort to understand the silica reinforcement effect on the SSBR rubber is plotted in Fig. 5.4b. The improvement of the modulus values at 100 % and 200 % elongation by *in-situ* silica is much higher than precipitated silica systems, particularly; when silane treated composites are concerned. The observed tensile properties in the presence and absence of silane coupling agent for the *in-situ* silica system describes that the surface chemistry and the nature of filler-polymer interaction of the *in-situ* silica vastly differs from

precipitated silica fillers. Most probably, the *in-situ* silica particles generated in presence of polymer may have trapped some of polymer chains or may be a strong mechanical tethering of rubber chains on the surface of silica particles. By this way, the silica particles are acting as additional crosslinking points and contribute to the final mechanical properties.

5. 2. 5 Dynamic mechanical properties

The dynamic mechanical properties for the gum and 30 phr silica composites are studied over temperatures from -60 °C to 80 °C. The obtained plots are depicted in Fig. 5.5 along with various temperature dependent properties and are furnished in Table 5.3. Fig. 5.5a shows the temperature dependent changes in storage modulus for different silica composites. A higher storage modulus can be observed for the silane modified *in-situ* silica system. A more interesting fact can be observed from the $\tan \delta$ - temperature dependence plot (Fig. 5.5b). Incorporation of silica significantly reduces $\tan \delta$ peak heights ($\tan \delta_{\max}$). Precipitated silica composites display a lower $\tan \delta_{\max}$ than *in-situ* silica. Additionally, incorporation of silane in both systems, further reduces the $\tan \delta_{\max}$ values¹⁰. Compared to precipitated silica composites, *in-situ* silica systems show a bit higher $\tan \delta_{\max}$. The glass transition temperature (T_g) for the composite with *in-situ* silica and silane shifted to higher temperature by ~2°C. The T_g shift could be explained by stronger rubber filler interaction⁹. The $\tan \delta$ values at -10°C, 0°C and 60°C are usually considered to predict the performance of a tyre material in terms of ice grip, wet-skid resistance and rolling resistance¹¹ and the values are given in Table 5.3. The *in-situ* derived silica composite shows improved performance in terms of ice grip, wet-skid resistance and rolling resistance compared to precipitated silica filled composites. The incorporation of silane coupling agent in both silica further improves the ice grip, wet-skid resistance and rolling resistance properties. Fig. 5.5c depicts the frequency dependent $\tan \delta$ values obtained from mastering followed by time temperature superposition principle (WLF principle) of gum and different silica filled composites.

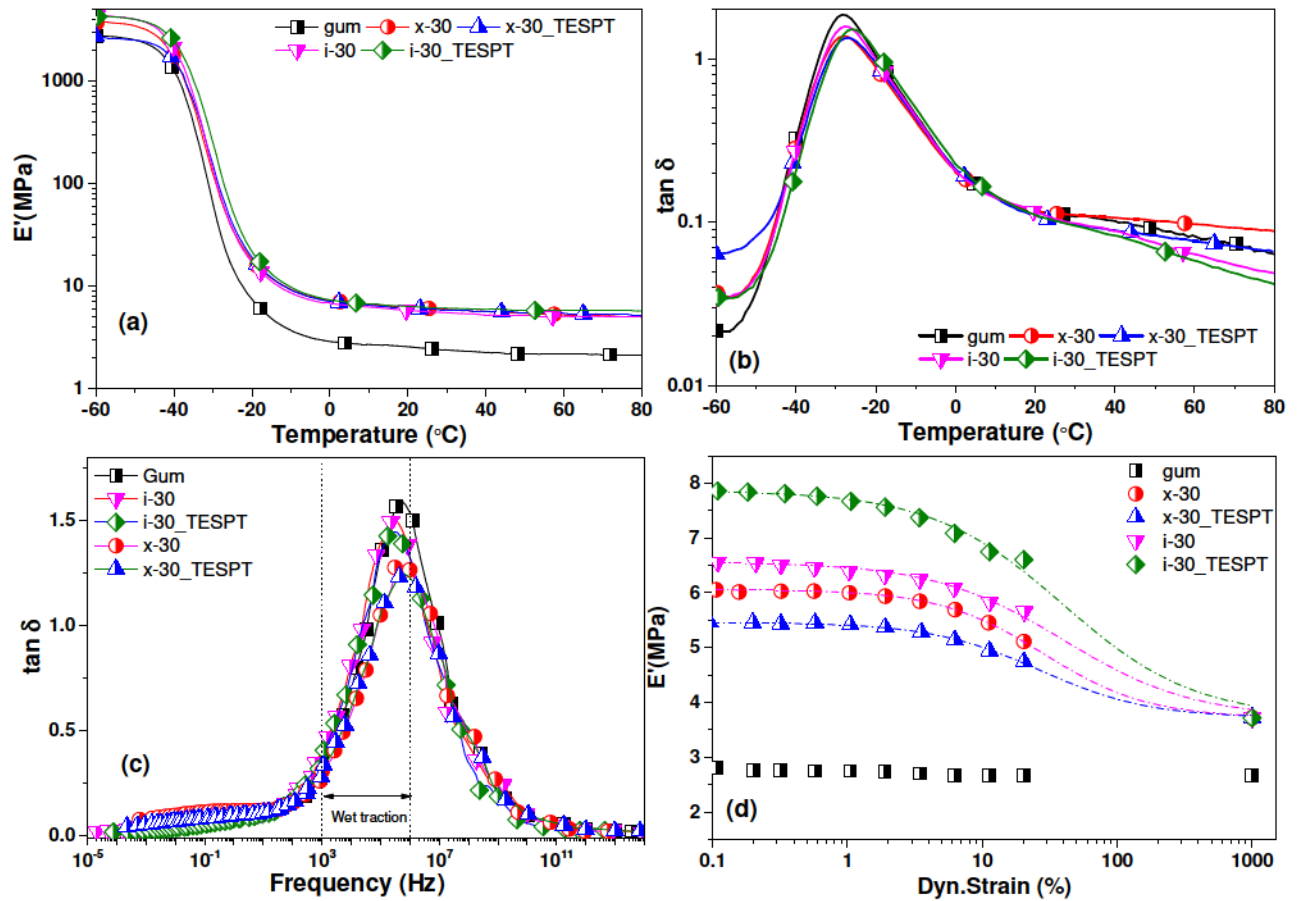


Figure 5.5 Dynamic mechanical performances of *in-situ* and commercial precipitated silica filled SSBR composites (a) dependence of storage modulus (E') on temperature, (b) dependence of loss factor ($\tan \delta$) on temperature, (c) dependence of loss factor ($\tan \delta$) on frequency and (d) dependence of storage modulus (E') on strain (Payne effect measurements)

Table 5.3 Dynamic mechanical behaviour of *in-situ* and commercial silica filled SSBR composites

Samples	E' @	E' @	E' @	\tan	\tan	\tan	\tan	T_g	γ_c	m
	0°C	25°C	60°C	δ @	δ @	δ @	δ_{max}			
				0°C	-10°C	60°C			(%)	
Gum	2.85	2.44	2.14	0.200	0.461	0.0808	1.788	-27.8	-	-
x-30	7.17	6.00	5.22	0.199	0.423	0.0971	1.370	-28.2	28	0.56
X- 30_TESPT	7.04	5.93	5.38	0.209	0.442	0.0761	1.341	-26.8	26	0.54
i-30	6.58	5.58	5.05	0.209	0.467	0.0634	1.575	-27.8	42	0.45
i-30_TESPT	7.20	6.20	5.74	0.229	0.500	0.0573	1.514	-26.0	41	0.44

It is generally accepted that the wet skid resistance of elastomers is a higher frequency phenomenon. A tyre rolling on a road surface comprises of many asperities and irregularities.

When a breaking force is applied, the tyre is pressed against the road and comes in contact with most of the asperities. Considering in numerous of such asperities together, the experienced frequency by a tyre is very high. Usually, properties in the frequency range of 1 kHz to 1MHz obtained from the dynamic mechanical frequency sweep measurement is considered as wet skid properties of tyre¹²⁻¹³. A higher loss modulus in the frequencies range of 10^4 to 10^6 Hz denote better wet traction properties¹⁴. The experimental frequency sweep measurements confirm that *in-situ* silica compounds exhibit higher wet grip properties compared to commercial silica system. The strain dependencies of the dynamic mechanical properties are conducted to investigate the filler-filler interaction and dispersion of silica in the composites. The experimental strain sweep data and the fitted Kraus model is shown in Fig. 5.5d and the obtained important parameters are given in Table 5.3. Experimental results show that incorporation of silane coupling agent in commercial silica system decreases the storage modulus at lower strain region¹⁵. Usually, silane coupling agents assist in silica dispersion, causing a reduction in the overall dynamic modulus¹⁶. The contrary is observed for *in-situ* silica systems, where silane incorporation increases the storage modulus. Similar effect is reported for CNT based rubber composites, improving the state of dispersion leads to increase in the storage modulus of the composites^{17,18}. The estimated critical strain (γ_c) (maximum modulus dropping point) is ~27% for silane modified commercial silica, whereas, *in-situ* silica-silane system displays critical strain values ~41%. This quantitative prediction by model may indicate that commercial silica composites have more filler-filler networks and these networks are more sensitive to dynamic strain amplitude. *In-situ* silica developed composites possess lower filler-filler network which indicates good filler dispersion. The strain amplitude constant (m) lies in between 0.44 to 0.56 and it is common for all the filled rubber systems¹⁹.

5. 2. 6 Other rubber performance properties

The rebound resilience, abrasion and heat build-up properties of SSBR gum, *in-situ* and commercial silica filled composites are summarized in Fig. 5.6. Fig. 5.6a&b shows the resilience of composites are gradually found to reduce with increase in filler content²⁰. At the same time, the resilience characteristics are improved with the addition of silane coupling agent in both silica systems. However, *in-situ* silica based rubber composites shows the better resilience characteristics compared to commercial silica systems²¹.

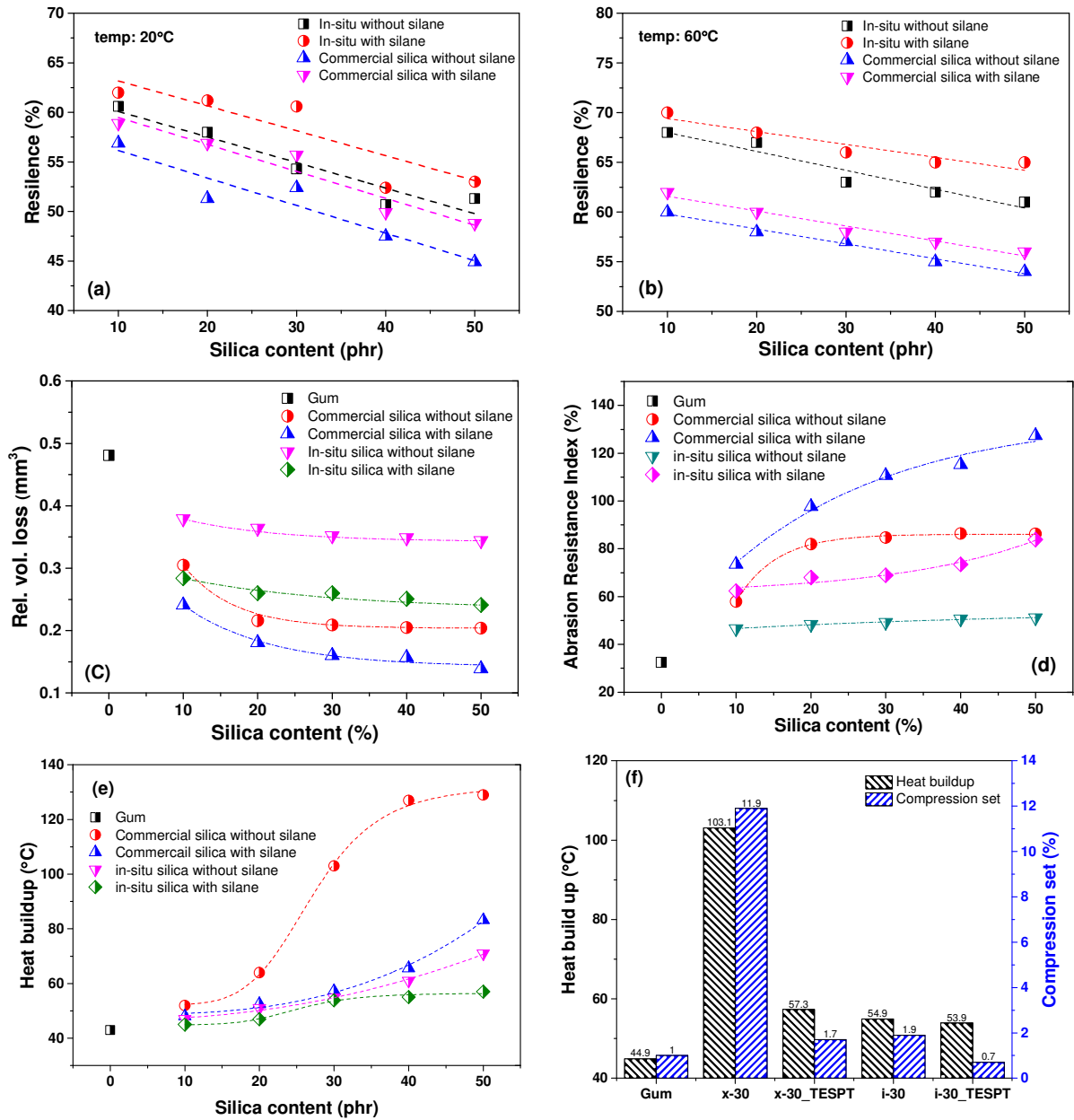


Figure 5.6 Various properties of *in-situ* and commercial silica filled composites (a) rebound resilience at 20 °C, (b) rebound resilience at 60 °C, (c) relative volume loss against abrasion (d) abrasion resistance index (e) amount of heat build-up for different silica concentrations and (f) heat build-up and compression set values for 30 phr of silica

At 60 °C the resilience properties are found to be around 5-10% higher than room temperature experiments. From the results it could be said that *in-situ* silica based composites exhibit better rebound resilience and possess higher elasticity. Fig. 5.6c and Fig. 5.6d depicts the relative volume loss (RV Loss) and abrasion resistance index (ARI) of the composites. The silica filled systems display better RV loss and ARI than gum vulcanizates. Increasing the

amount of silica in rubber gradually reduces the RV loss and improves the ARI values. Eventually, silane addition in silica-rubber system further enhances the abrasion properties.²² The experimental results suggest better abrasion properties for the commercial silica system exhibits than *in-situ* composites.

The heat build-up is one of the important properties for highly filled rubber objects. The amount of heat generated and accumulated inside the composites while dynamic loading is measured and plotted in Fig. 5.6e. Due to the absence of any filler, gum vulcanizates show lower heat build-up and with increase in filler fraction the amount of heat build-up increases. Incorporation of silane coupling agent in *in-situ* and commercial silica systems significantly reduces the amount heat generation. The commercial silica and silane modified composites exhibits higher degree of heat generation when compared to *in-situ* silica composites. Fig. 5.6f summarizes the heat build-up and the corresponding compression set values (calculated after the experiment) for 30 phr silica filled system and gum vulcanizates. 30 phr of commercial silica filled composite exhibits the highest degree of heat build-up of around 103 °C. Interestingly, silane modification on the same system significantly reduces the heat generation from 103 °C to 57 °C. The results clearly indicate that inclusion of commercial silica in rubber increases the internal friction between the silica and rubber, leading to massive heat generation.²³ Eventually the addition of silane coupling agent into silica filled rubber vastly reduces heat generation and improve the heat loss by effective silanization. On the other hand, *in-situ* silica composites without silane coupling agent exhibit even lower heat build-up than commercial silica/silane composites. The addition of silane coupling agents in *in-situ* silica further contributes to the reduction of heat build-up on rubber.

The commercial silica filled composite displays the highest compression set of 11.9 % and is significantly reduced to 1.7 % by silane modification. Meanwhile, *in-situ* silica composite shows a permanent set of around 1.9 % for silica and 0.7 % for silane modified system, which is very low in comparison to commercial silica systems. The results points out that *in-situ* silica composite can offer excellent reinforcement with minimal heat generation even in the absence of silane coupling agent.

5. 2. 7 Hysteresis properties

Fig. 5.7a, b represents the hysteresis plot of *in-situ* and commercial silica filled composites in presence and absence of silane coupling agent. The figures show that hysteresis loss (area inside the hysteresis loop) gradually reduces with increase in number of strain cycles due to stress induced softening effect (Mullins effect) of viscoelastic material²⁴.

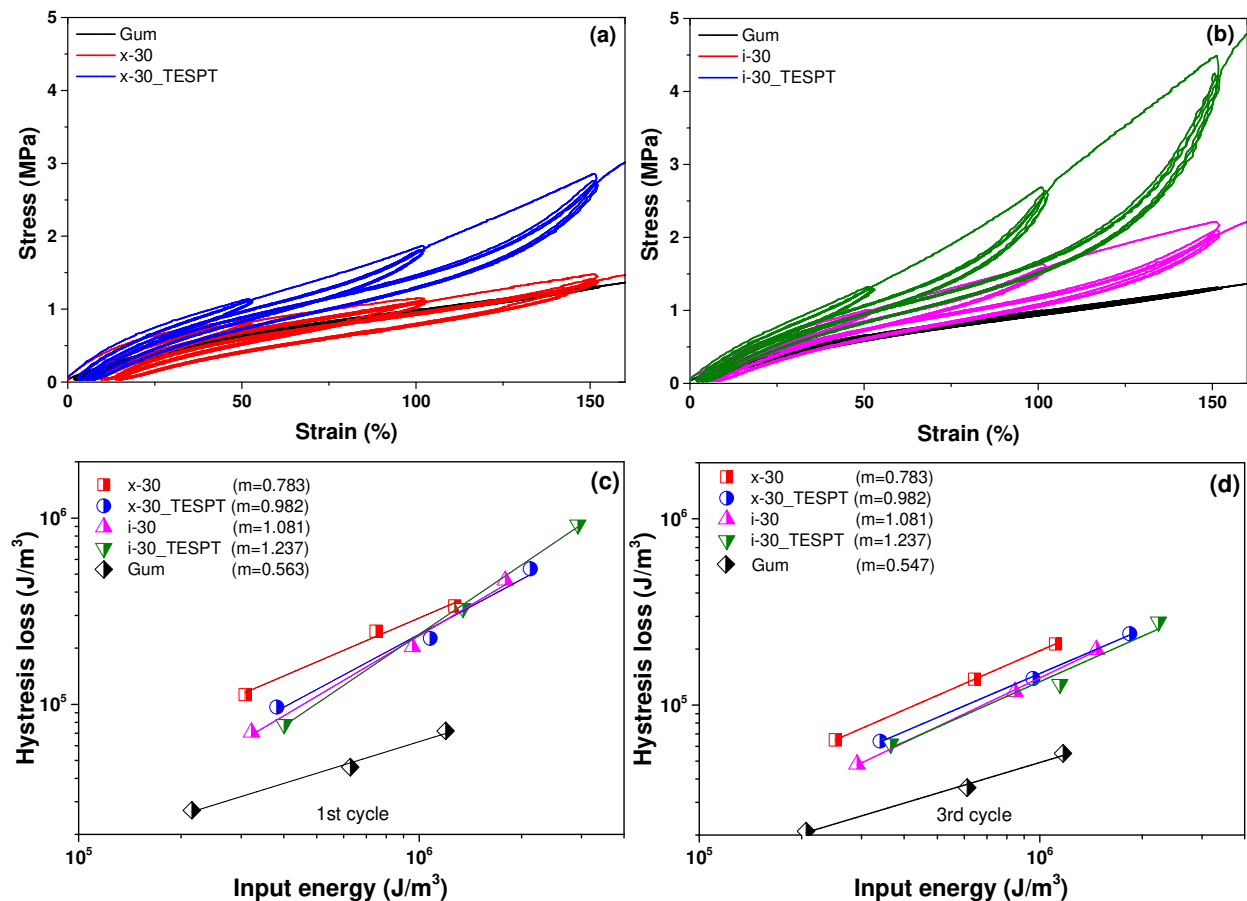


Figure 5.7 Hysteresis plots of (a) *in-situ* and (b) commercial silica filled SSBR composites in presence and absence of silane coupling agent with respect to gum compounds. Plots of hysteresis loss against input energy in (c) 1st cycle and (d) 3rd cycle.

At the same time, area of hysteresis loop increases gradually with respect to applied strain, implying that amount of energy dissipation increases significantly with respect to applied deformation. Addition of silane coupling agent increases the area of hysteresis loop, representing high energy dissipation. The overall results suggest that *in-situ* silica based composites exhibit higher energy loss compared to commercial silica (after the first cycle)⁴.

Fig. 5.7c, d shows hysteresis loss against input energy for different silica filled composites. The 1st and 3rd hysteresis cycles are specifically chosen for the investigation, to understand the stress induced softening effect. Fig. 5.7c indicates the hysteresis loss and input energy for the 1st cyclic of loading for different silica filled SSBR composites. The unfilled gum compound yields a slope of 0.563 and displays least hysteresis loss. Meanwhile, commercial silica filled composite has a slope of 0.783, which is improved to 0.982 with the addition of silane coupling agent. *In-situ* silica filled composites display slopes of 1.021 and 1.237 before and after silanization. A higher hysteresis loss is realized for the *in-situ* silica/silane systems, which is even higher than gum and commercial silica composites. A similar behaviour is also observed in the 3rd loading cycle as plotted in Fig. 5.7d, but the slopes are relatively lower than the 1st cycle, confirming the reduction in loss of energy with multiple cycles. High hysteresis loss is a vital property for a viscoelastic rubber material meant for prolonged dynamic applications. The obtained results from hysteresis loss for different silica filled composites correlate with the findings from dynamic mechanical data and heat build-up values.

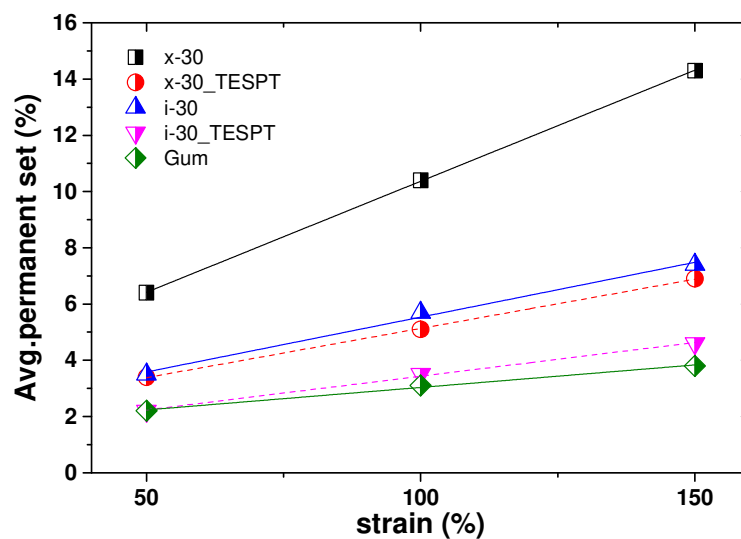


Figure 5.8 Average permanent set of various silica filled composites with respect to given tensile strain

The permanent tensile set of composites are also investigated during each cycle and the average permanent set values at 50 %, 100 % and 150 % strain are calculated and plotted in Fig. 5.8. A lower permanent tensile set is observed for gum vulcanizates and is increasing with respect to the applied strain. Commercial silica filled systems exhibit higher orders of permanent set for a given strain and silane modification helps in achieving lower permanent set values. *In-situ* silica and silane incorporated composites offers even lower permanent set

values than commercial silane modified silica composites. The experimental results confirm that *in-situ* silica based composites possess good dynamic stress-strain properties, better hysteresis loss and low hysteresis²⁵. Incorporation of silane in both silica systems, contribute towards the low hysteresis properties via improved silica-rubber interaction.

5. 2. 8 Scanning electron microscopy

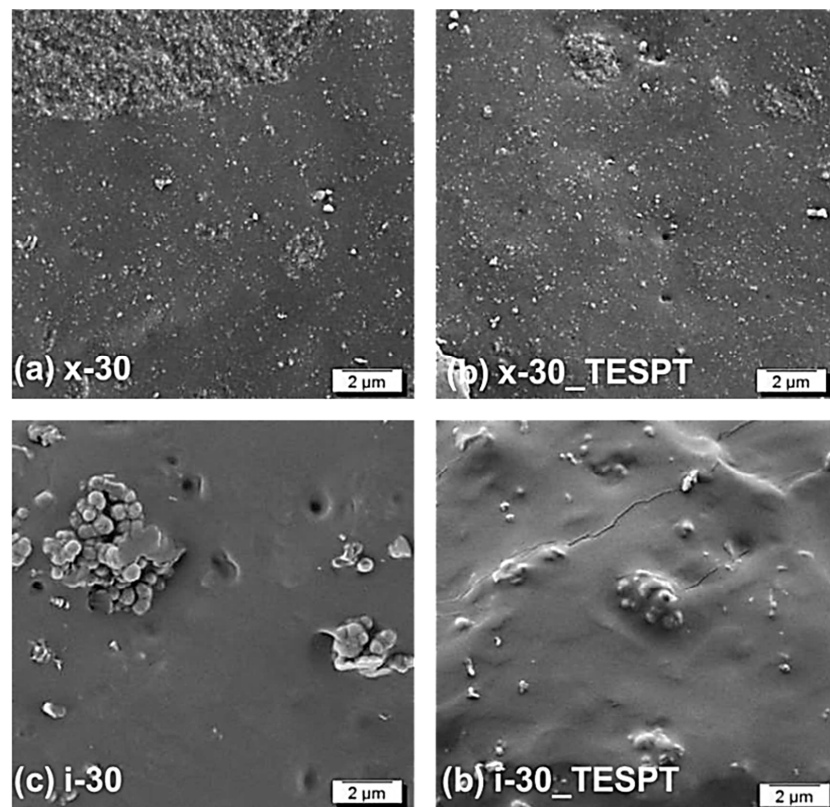


Figure 5.9 SEM images of fracture surface of (a) commercial silica without silane coupling agent (b) commercial silica with silane coupling agent (c) *in-situ* silica without silane coupling agent (d) *in-situ* silica with silane coupling agent

To understand the silica - rubber interaction and interfacial adhesion in the presence and absence of silane coupling agent, the brittle fractured composite surface is analysed by SEM. The SEM micrographs in Fig. 5.9 shows 30 phr of commercial and *in-situ* silica filled rubber composites. Commercial silica composites display some agglomerated particles and after silane treatment the aggregated morphology is reduced significantly. The *in-situ* silica composites without silane coupling agent have very few agglomerates with bigger particles morphology. This agglomerate seems to be comprised of a large number of individual small spherical particles. The average size of the small spheres was found to be in the range of 150-200 nm. Most probably, some of the polymer chains are trapped by the grown silica particles

(see chapter 8 for schematic representation). These free particles, being loosely bound, are also pulled out from the matrix. Therefore, micro size holes are observed on the fracture surface. In case of silane modification, the *in-situ* silica particles are completely covered by a thin rubber layer, affirming significant improvements in interfacial bonding between silica and rubber.

5. 2. 9 Friction co-efficient and friction master curves

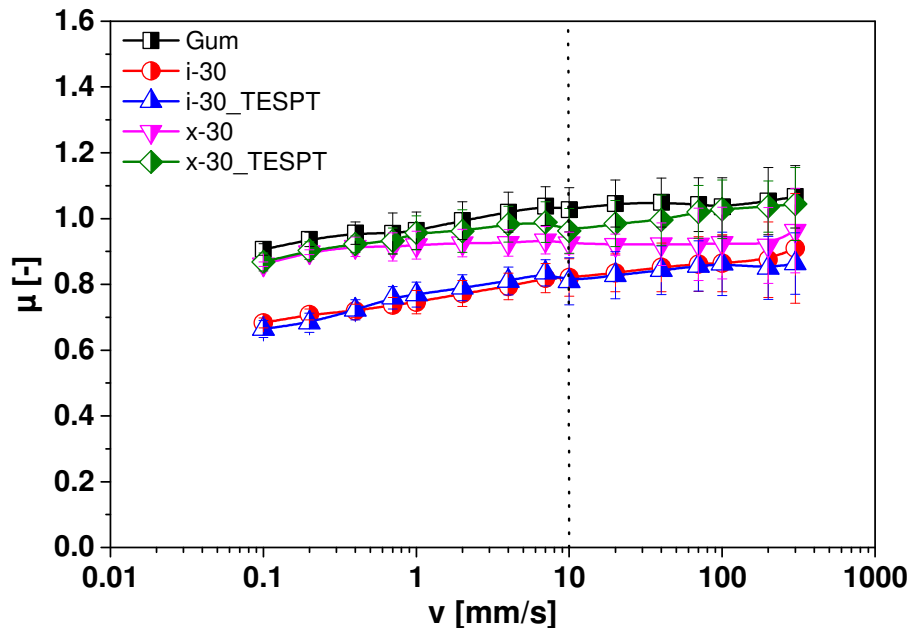


Figure 5.10. Friction master curves for gum, *in-situ* silica and commercial silica in presence and absence of silane coupling agent. The dotted line represents the friction co-efficient value measured by experimentally remaining data points are predicted by using WLF equation

Fig. 5.10 shows the experimental friction results measured at the velocity of 10 mm/sec at 15 °C and obtained experimental result is extrapolated using by WLF equation. The experimental result shows that the unfilled rubber vulcanizates exhibits higher coefficient of friction. The incorporation silica in SSBR slightly reduces the friction co-efficient. The commercial silica without silane exhibits lower co-efficient of friction compare to silane modified commercial system. However the addition of silane coupling agent in commercial silica system significantly improved the friction properties at higher friction velocity. On the other hand the *in-situ* generated silica in SSBR showed that least friction coefficient when compared to commercial silica systems. An interesting remark is the incorporation of silane coupling agent in *in-situ* silica system do not change the friction behaviour of the material. This result is further evidence that *in-situ* silica can be reinforcing the matrix without any

silane and it is reported in chapter 4. Apart from good traction properties a lower friction coefficient is also an interesting property. From this perspective to achieve better rolling resistance rubber compounds the rubber compound needed lower hysteresis, lower $\tan \delta$ at high temperature as well as with lower rolling friction. For this purpose *in-situ* silica system is fulfilling the requirement, which is reported previously²⁶. According to the estimated friction co-efficient, the friction rating for different silica filled SSBR rubber is given below.

$$\mathbf{x-30_TESPT < x-30 < i-30_TESPT \text{ and } i-30}$$

5. 2. 10 Tear fatigue analyzer (TFA)-Crack propagation measurements

TFA tests are carried out to understand the crack propagation behaviour of silica filled SSBR composites and the effect of silane coupling agent in silica-rubber composites. The logarithmic plot of crack growth rate (da/dn) against tearing energy (T), which is usually known as ‘Paris-Erdogan plot’ is given in Fig. 5.11. The rate of crack propagation is directly proportional to the tearing energy of the material at a certain tear energy regime. As expected, a gum vulcanizate exhibits lower tearing energy and faster crack formation compared to a filled system. The incorporation of both, *in-situ* silica and commercial silica, significantly improves the crack propagation behaviour of vulcanized rubber. The main mechanism proposed for the addition of filler particles in rubber prevent the crack propagation by resisting the crack tip growing²⁷. Nevertheless, the crack propagation rate is greatly changed with similar amount of silica loading in both cases. Also the silane modification of silica in both cases increased the crack propagation behaviour. However, *in-situ* silica filled system exhibits faster crack propagation behaviour than commercial silica system. These results are states that the state of silica dispersion is not only a critical parameter deciding the crack propagation behaviour of filled rubber system. Equally particle size, particle morphology, crosslink density and filler polymer interfaces are playing major part on the crack. The SEM analysis states that the particle size and morphology of commercial and *in-situ* silica is entirely different. Also the amount of estimated crosslink density is nearly higher for *in-situ* silica composites, when compared with commercial silica filled composites.

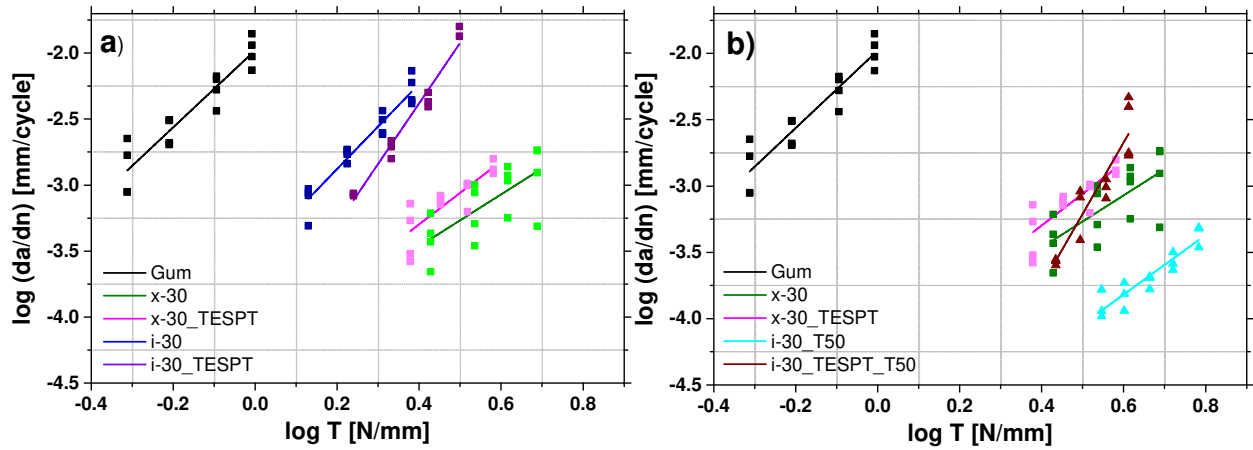


Figure 5.11.a) Crack growth rate as a function of tearing energy for *in-situ* silica and commercial silica filled composites **b)** crack behaviour of equally adjusted crosslink density of *in-situ* silica and commercial silica composites

Table 5.4. The crack propagation behaviour of silica filled SSBR composites with respect to crosslink density.

Sample	Crosslink density ($\times 10^{-4}$ g/cc)	Slope
SSBR-Gum	1.463	2.9
x-30	1.571	3.2
x-30s	2.202	4.6
i-30	2.128	2.4
i-30s	2.718	1.9
i-30-TC ₅₀	1.677	2.2
i-30s-TC ₅₀	2.232	5.4

To ensure the effect of crosslink density on the crack propagation behaviour of silica filled SSBR composites, the crosslink density of *in-situ* samples are reduced and matched with commercial silica composites by modifying the rate of cure from TC₉₀ to TC₅₀. The amount of crosslinks density estimated by swelling experiments with modified Flory-Rhener equation²⁸ is given in Table 5.4. After changing the crosslink density of *in-situ* silica composites, it is found that crack propagation behaviour is completely different than previous experimental results. The new experimental results are plotted in Fig. 5.11b and it clearly stated that the crack propagation behaviour of *in-situ* silica is significantly improved. And the rate of crack growth is lower or better than commercial silica filled composites without any silane modification. However the addition silane coupling agent in both silica systems slightly reduces the crack propagation properties.

5.3 Conclusions

The performance of silica synthesized via *in-situ* sol-gel route was compared with commercial precipitated silica composites in presence and absence of TESPT silane coupling agent. The superior mechanical performance of the *in-situ* silica rubber composites were supported by various mechanical and dynamic mechanical characterizations. From the dynamic mechanical temperature sweep measurement, higher $\tan \delta$ at 0 °C and -10 °C and lower $\tan \delta$ at 60 °C were observed for *in-situ* silane modified composites, which is related to a higher wet skid resistance and lower resistance properties. The strain sweep measurements fitted with Kraus model show *in-situ* silica composites exhibiting higher critical strain values. This represents that *in-situ* silica compounds were less sensitive to dynamic strain and possess less filler-filler networks. Higher rebound resilience, lower heat build-up, lower hysteresis and lower friction co-efficient were observed for *in-situ* silica composites, which are very essential to achieve high performance in rubber products during service, especially for tyres. With further addition of TESPT silane in *in-situ* silica composites, even better performance was observed. Commercial precipitated silica composites exhibited better abrasion properties because of their small particle morphology. Nevertheless, it generally implied that to achieve (low) better rolling resistance, it is necessary to compromise on the abrasion properties²⁹. Generation of silica particles in the rubber by sol-gel route could be a better way to develop high performance tyre compounds.

References

1. ten Brinke, A. Silica reinforced tyre rubbers. PhD Thesis. Twente University, The Netherlands, 2002.
2. Kaewsakul, W.; Sahakaro, K.; Dierkes, W.; Noordermeer, J., Optimization of mixing conditions for silica-reinforced natural rubber tire tread compounds. *Rubber chemistry and technology* 2012, 85 (2), 277-294.
3. Raman, V. S.; Das, A.; Stockelhuber, K. W.; Eshwaran, S. B.; Chanda, J.; Malanin, M.; Reuter, U.; Leuteritz, A.; Boldt, R.; Wie; Heinrich, G., Improvement of mechanical performance of solution styrene butadiene rubber by controlling the concentration and the size of in situ derived sol-gel silica particles. *RSC Advances* 2016, 6 (40), 33643-33655.
4. Kohjiya, S.; Murakami, K.; Iio, S.; Tanahashi, T.; Ikeda, Y., In situ filling of silica onto "green" natural rubber by the sol-gel process. *Rubber chemistry and technology* 2001, 74 (1), 16-27.
5. Stöckelhuber, K. W.; Svistkov, A. S.; Pelevin, A. G.; Heinrich, G., Impact of Filler Surface Modification on Large Scale Mechanics of Styrene Butadiene/Silica Rubber Composites. *Macromolecules* 2011, 44 (11), 4366-4381.

6. Mihara, S.; Datta, R.; Noordermeer, J., Flocculation in silica reinforced rubber compounds. *Rubber Chemistry and Technology* 2009, *82* (5), 524-540.
7. Pal, P.; De, S., Effect of reinforcing silica on vulcanization, network structure, and technical properties of natural rubber. *Rubber Chemistry and Technology* 1982, *55* (5), 1370-1388.
8. Raman, V.; Rooj, S.; Das, A.; Stöckelhuber, K.; Simon, F.; Nando, G.; Heinrich, G., Reinforcement of solution styrene butadiene rubber by silane functionalized halloysite nanotubes. *Journal of Macromolecular Science, Part A* 2013, *50* (11), 1091-1106.
9. Hashim, A.; Azahari, B.; Ikeda, Y.; Kohjiya, S., The effect of bis (3-triethoxysilylpropyl) tetrasulfide on silica reinforcement of styrene-butadiene rubber. *Rubber chemistry and technology* 1998, *71* (2), 289-299.
10. Ikeda, Y.; Kohjiya, S., In situ formed silica particles in rubber vulcanizate by the sol-gel method. *Polymer* 1997, *38* (17), 4417-4423.
11. Evans, M. S., *Tyre compounding for improved performance*. iSmithers Rapra Publishing: 2002; Vol. 12, p112.
12. Rahalkar, R., Dependence of wet skid resistance upon the entanglement density and chain mobility according to the Rouse theory of viscoelasticity. *Rubber chemistry and technology* 1989, *62* (2), 246-271.
13. Heinrich, G.; Dumler, H. B., Wet Skid Properties of Filled Rubbers and the Rubber—Glass Transition. *Rubber Chemistry and Technology* 1998, *71* (1), 53-61.
14. Mouri, H.; Akutagawa, K., Improved Tire Wet Traction through the Use of Mineral Fillers. *Rubber Chemistry and Technology* 1999, *72* (5), 960-968.
15. Ramier, J.; Gauthier, C.; Chazeau, L.; Stelandre, L.; Guy, L., Payne effect in silica-filled styrene-butadiene rubber: Influence of surface treatment. *Journal of Polymer Science Part B: Polymer Physics* 2007, *45* (3), 286-298.
16. Sahakaro, K.; Beraheng, S., Reinforcement of maleated natural rubber by precipitated silica. *Journal of applied polymer science* 2008, *109* (6), 3839-3848.
17. Subramaniam, K.; Das, A.; Heinrich, G., Development of conducting polychloroprene rubber using imidazolium based ionic liquid modified multi-walled carbon nanotubes. *Composites Science and Technology* 2011, *71* (11), 1441-1449.
18. Das, A.; Stöckelhuber, K.; Jurk, R.; Saphiannikova, M.; Fritzsche, J.; Lorenz, H.; Klüppel, M.; Heinrich, G., Modified and unmodified multiwalled carbon nanotubes in high performance solution-styrene-butadiene and butadiene rubber blends. *Polymer* 2008, *49* (24), 5276-5283.
19. Heinrich, G.; Klüppel, M., Recent advances in the theory of filler networking in elastomers. In *Filled Elastomers Drug Delivery Systems*, Springer: 2002, pp 1-44.
20. Reincke, K.; Grellmann, W.; Heinrich, G., Investigation of Mechanical and Fracture Mechanical Properties of Elastomers Filled with Precipitated Silica and Nanofillers Based upon Layered Silicates. *Rubber Chemistry and Technology* 2004, *77* (4), 662-677.
21. Murakami, K.; Iio, S.; Ikeda, Y.; Ito, H.; Tosaka, M.; Kohjiya, S., Effect of silane-coupling agent on natural rubber filled with silica generated in situ. *Journal of materials science* 2003, *38* (7), 1447-1455.
22. Nayek, S.; Bhowmick, A. K.; Pal, S. K.; Chandra, A. K., Wear Behavior of Silica Filled Tire Tread Compounds by Various Rock Surfaces. *Rubber Chemistry and Technology* 2005, *78* (4), 705-723.
23. Wagner, M. P., Reinforcing Silicas and Silicates. *Rubber Chemistry and Technology* 1976, *49* (3), 703-774.

24. Kar, K. K.; Bhowmick, A. K., High Strain Hysteresis Loss of Rubber Vulcanizates under Pure Shear and Constrained Extension and Influence of Filler. *Rubber Chemistry and Technology* 2000, 73 (1), 56-73.
25. Kohjiya, S.; Katoh, A.; Shimanuki, J.; Hasegawa, T.; Ikeda, Y., Three-dimensional nano-structure of in situ silica in natural rubber as revealed by 3D-TEM/electron tomography. *Polymer* 2005, 46 (12), 4440-4446.
26. Vaikuntam, S. R.; Bhagavatheswaran, E. S.; Stöckelhuber, K. W.; Wießner, S.; Heinrich, G.; Das, A., DEVELOPMENT OF HIGH PERFORMANCE RUBBER COMPOSITES FROM ALKOXIDE-BASED SILICA AND SOLUTION STYRENE–BUTADIENE RUBBER. *Rubber Chemistry and Technology* 2016.
27. Persson, B. N. J.; Albohr, O.; Heinrich, G.; Ueba, H., Crack propagation in rubber-like materials. *Journal of Physics: Condensed Matter* 2005, 17 (44), R1071.
28. Sankar Raman, V.; Das, A.; Stockelhuber, K. W.; Eshwaran, S. B.; Chanda, J.; Malanin, M.; Reuter, U.; Leuteritz, A.; Boldt, R.; Wiessner, S.; Heinrich, G., Improvement of mechanical performance of solution styrene butadiene rubber by controlling the concentration and the size of in-situ derived sol-gel silica particles. *RSC Advances* 2016.
29. Baker, C.; Gelling, I.; Newell, R., Epoxidized natural rubber. *Rubber chemistry and Technology* 1985, 58 (1), 67-85.

Chapter 6

Influence of silica-silane interaction and silica-rubber interfaces on the microscopic properties of rubber

The results of this chapter have been published in “The Journal of Physical Chemistry Part - B, 2018, 122, 2010-2022”.

6.1 Introduction

Understanding the concept of rubber reinforcement by fillers is one of the major challenges in the field of rubber science and technology. Several rubber fillers like carbon black, precipitated silica, fumed silica, clay and talc have taken over the rubber industry from the very beginning. Carbon black is one of the vastly used and well known rubber reinforcing agents for all general and special purpose rubber products. The rubber reinforcement by carbon black is mainly determined by the surface area, structure, particle size and surface activity¹⁻². On the same context, for the past two decades, silica based reinforcement of tyres are gaining more importance due to its versatile functional properties on lower rolling resistance, wet skid resistance and abrasion resistance³. Some of the major issues encountered while using silica as reinforcing filler are poor nano scale dispersion, higher Payne effect, interrupting on vulcanization kinetics⁴ and processing⁵. Some of these issues have been addressed by the addition of different silane coupling agent and optimized the mixing cycles. In case of silica filled rubber systems, major part of reinforcement and the improvement in dynamic mechanical properties depend on the type of silica-rubber coupling used and the state of silica dispersion. Anyhow, the need for improving silica dispersion and properties are increasing day-by-day, due to the environmental issues like lower CO₂ emission, lower fuel consumption and safety aspects. Therefore, *in-situ* silica prepared from sol-gel process gained much attention in rubber reinforcement⁶. The *in-situ* derived silica particles in rubber offers excellent reinforcement, good dispersion and also solved the environmental issues to an extent. However, understanding the characteristics of *in-situ* silica is more important to ensure better performance in rubber composites. There have been several investigations and models developed to understand the interaction of silica-rubber and the enhanced reinforcement by silane incorporation. Many articles have been published till now on *in-situ* silica generation in rubber⁷⁻²¹, but detailed investigations of rubber reinforcement by *in-situ* generated silica are scarce.

In this chapter, efforts have been placed to investigate the mechanism of *in-situ* silica and their reinforcement on solution styrene butadiene rubber. For a better understanding of reinforcement effect by *in-situ* silica, a commercial precipitated silica system is mutually considered and compared. The study has been elaborated to effect of silica loading, influence of silica-silane interaction and influence of different silane coupling agents. This allows a more systematic investigation of the filler system and their chemical properties in rubber, role

of silane coupling agent in silica filled system influences on the microscopic properties of the vulcanized rubber network.

6. 2 Results and discussions

6. 2. 1 Silica particle investigation

Fig 6.1 shows the x-ray diffraction (XRD) analysis of *in-situ* and commercial silica powder samples. The broad XRD band is observed on the 2 theta region of 15 to 40. Thus state that physical state of silica is completely amorphous²² and there is no difference in the crystalline structure.

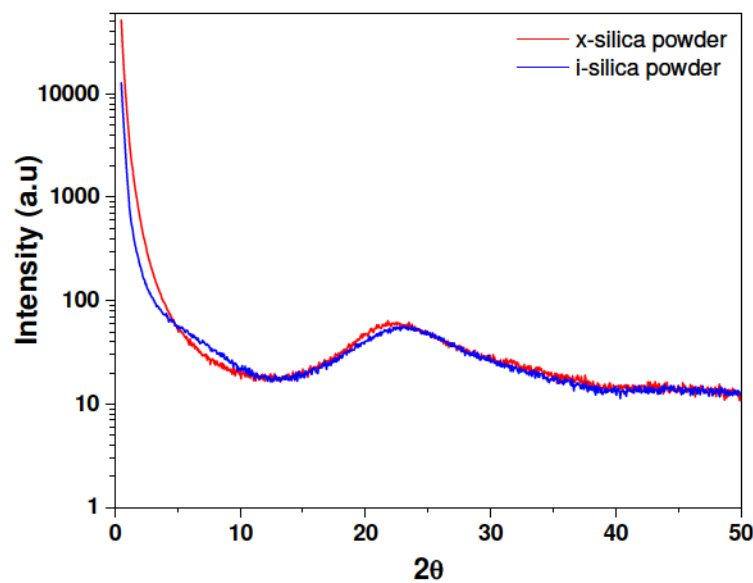


Figure 6.1 The X-ray diffraction patterns of *in-situ* silica and commercial silica powder particles

The dynamic light scattering measurement (DLS) is performed to understand the diameter (hydrodynamic diameter) silica particle size and structure. The commercial precipitated ULTRASIL VN3 silica particles in Fig. 6.2a show a bimodal distribution with broad range of particle sizes. The commercial silica particles are aggregated and the aggregate diameter sizes range from 150 to 1500 nm. The DLS results from Fig. 6.2b state an average diameter of around 200-500 nm for the *in-situ* derived silica particles. The *in-situ* silica particles are more over monodisperse or unimodal narrow particle distribution, which is further confirmed by transmission electron microscopy (TEM) images in Fig. 6.2d. Fig. 6.3 shows the typical morphology of pristine powders and composites of *in-situ* and commercial silica system.

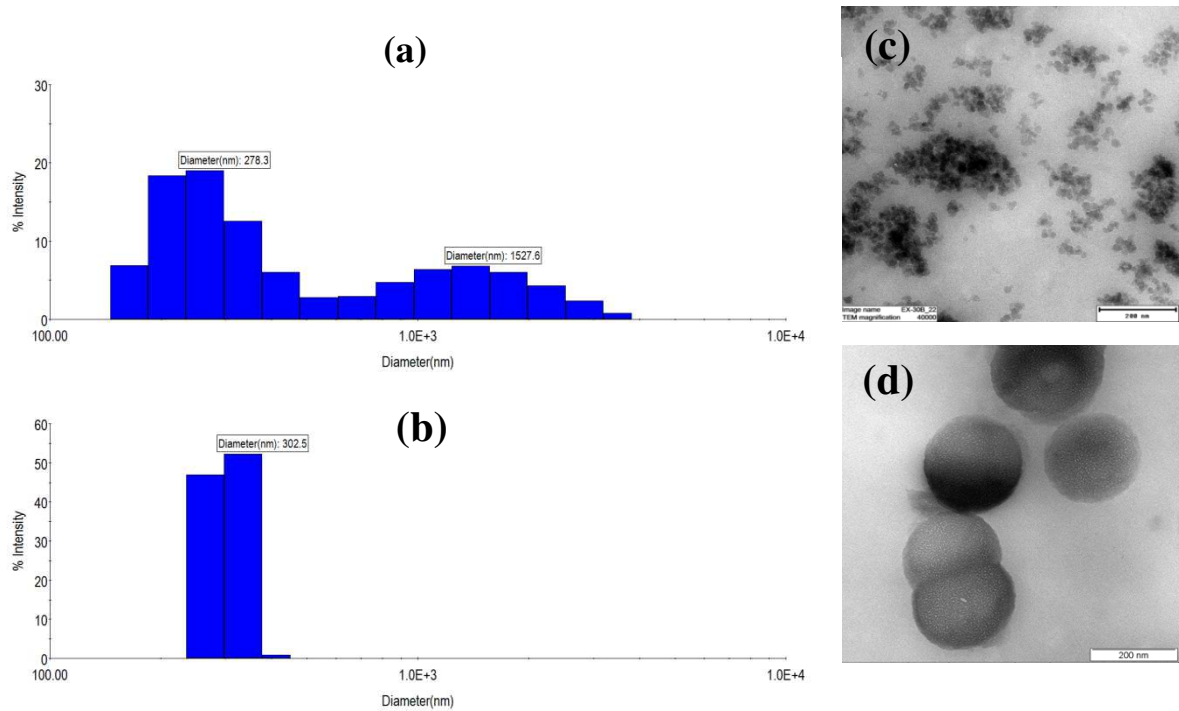


Figure 6.2 Particle size and distributions of (a) commercial ULTRASIL VN3 precipitated silica and (b) *in-situ* derived silica measured by DLS method. Morphology of (c) commercial ULTRASIL VN3 precipitated silica and (d) *in-situ* silica particles analyzed by TEM

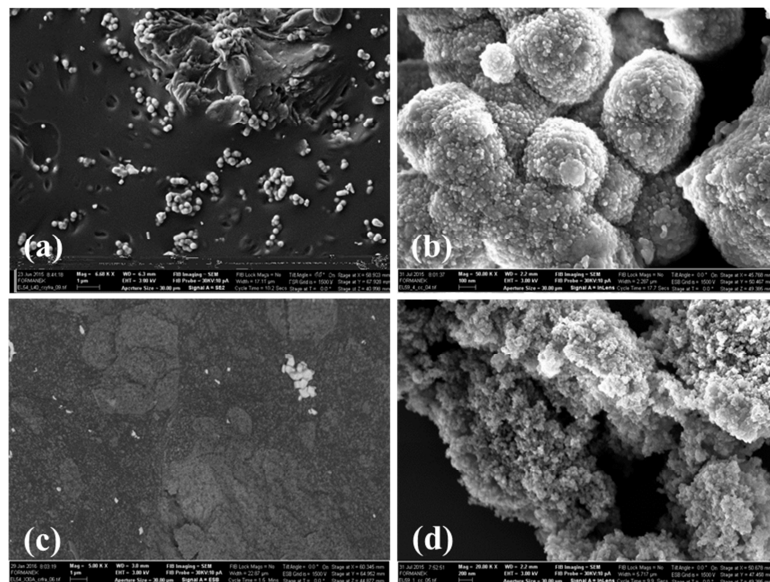


Figure 6.3 SEM fracture images of (a) 30 phr of *in-situ* silica composite (b) *in-situ* silica powder removed from the un-crosslinked rubber after sol-gel synthesis (c) 30 phr of commercial ULTRASIL VN3 silica composite (30 phr) (d) pristine commercial ULTRASIL VN3 silica powder

6. 2. 2 Estimation of crosslink density and rubber-silica interaction by Multiple Quantum NMR experiments

6. 2. 2. 1 Unfilled SSBR vulcanizates

The correlation between crosslink density of unfilled SSBR with different amounts of sulphur, measured by DQ-NMR experiments, equilibrium swelling method and the actual Double Quantum build-up curves are given in Fig 6.4a&b. Fig. 6.4a shows the linear relationships between the NMR observances and equilibrium swelling results while increasing the amount of sulphur content in SSBR rubber. The correlation between NMR and swelling results demonstrates that D_{res} (residual dipolar coupling constant) is directly proportional to the molecular weight between successive crosslinks ($1/M_c$). Nevertheless, equilibrium swelling is a quantitative technique, it includes the physical constraints (entanglements) as well as chemical constraints (chemical bridges contributed by sulphur in our case). Swelling of crosslinked rubber networks is an inhomogeneous complex process due to the contributions by non-elastic components, sub-affine local deformation and topological reorganization of non-trapped entanglements. It is important to note that DQ-NMR experiments are sensitive to both physical and chemical constraints, which means that it can distinguish the different topologically constrained rubber networks. The intercept at Y-axis in Fig. 6.4a relates to the network density by entanglement contribution or other topological constraints as detected from NMR measurements²³. The intercept at Y-axis quantitatively defines that crosslinked rubber networks consists of elastically active rubber chains as well as non-elastic defects. Unlike natural rubber, which has a residual dipolar coupling constant of 617 Hz, SBR and other copolymer systems cannot yield the actual crosslink density value, because there are no reasonable reference coupling values available²⁴. Also natural rubber (NR) vulcanizates have more physical entanglements than synthetic solution styrene butadiene rubber (SSBR) which is polymerized by anionic polymerization with narrow molecular weight distribution²⁵.

6. 2. 2. 2 Silica filled composites

The effect of silica filler loading on crosslinking density of rubber matrix and the interfacial interaction between silica and rubber with presence and absence of TESPT silane coupling is also investigated by DQ-NMR experiments and correlated with equilibrium swelling measurements. As mentioned earlier, unfilled vulcanizates with different sulphur content show a linear relationship between the crosslink density values by swelling and NMR measurements.

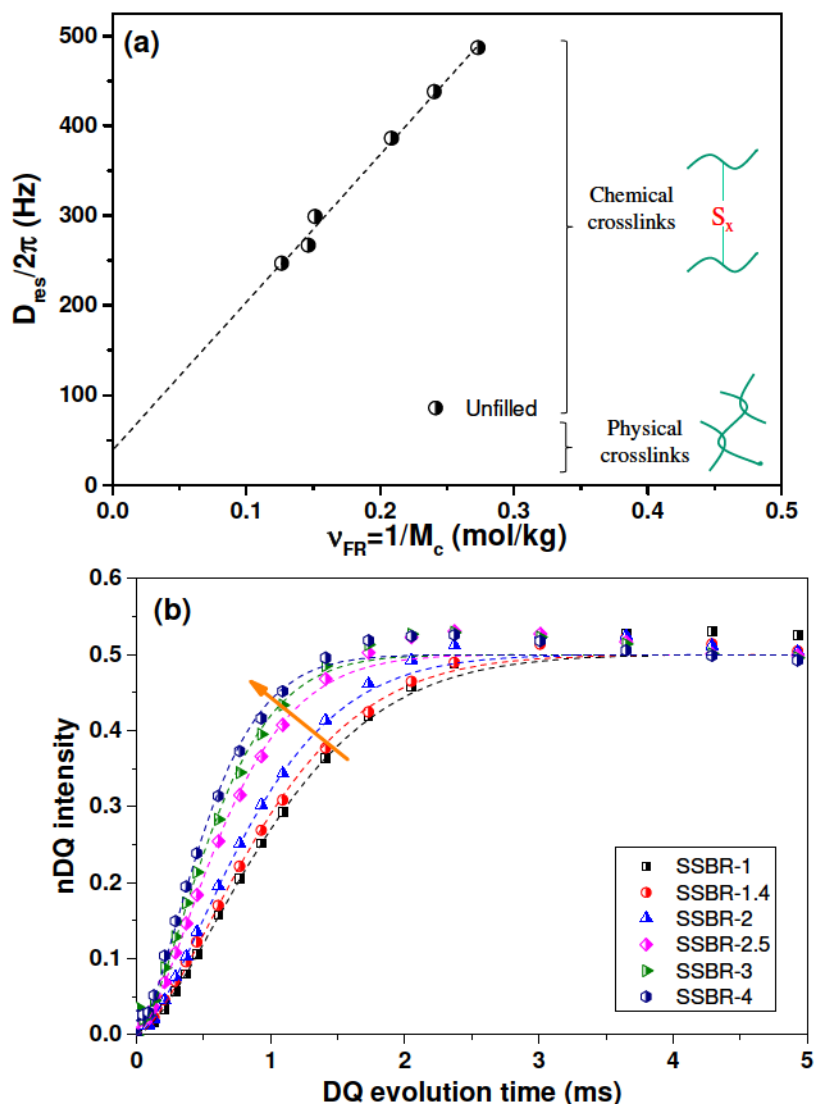


Figure 6.4 a) The correlation between crosslink density of unfilled SSBR with different amounts of sulphur (SSBR vulcanized with 1, 1.4, 2, 2.5, 3 and 4 phr of sulphur), measured by DQ-NMR experiments and equilibrium swelling method based Flory-Rehner b) the actual Double Quantum build-up curves of various amount of sulphur contain SSBR vulcanizates

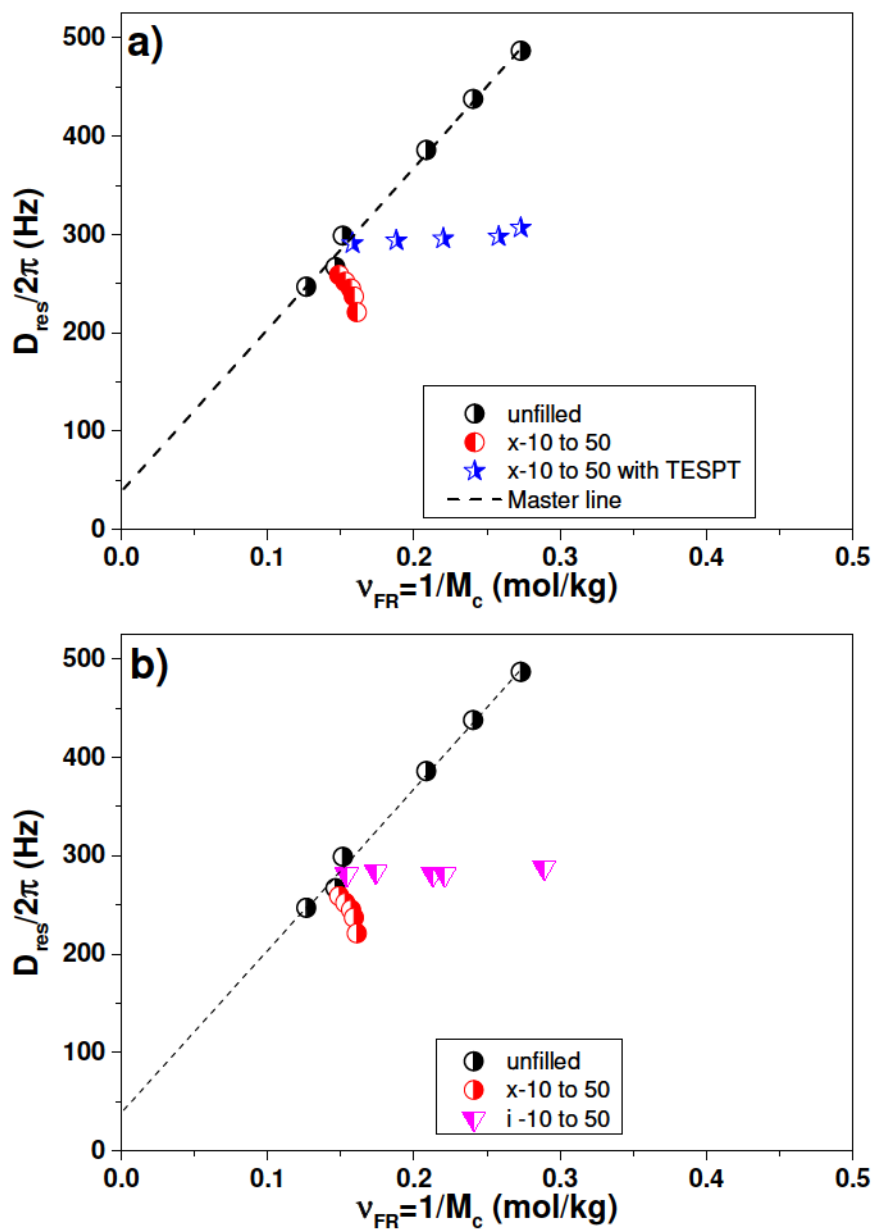
Silica filled compounds display four different scenarios in our study, namely, when (a) there is no filler-polymer interaction, (b) filler-polymer (physical) interaction by virtue of fillers being generated inside the elastomer, (c) an enhanced filler-polymer interaction using TESPT (bi-functional) silane coupling agent and (d) a filler-polymer interaction influenced by physical coupling as well as chemical coupling between the silica and rubber. To highlight these points, our study mainly focuses on SSBR rubber filled with commercial precipitated silica and *in-situ* sol-gel derived silica along with the effect of incorporating TESPT silane coupling agents.

6. 2. 2. 2. 1 Commercial precipitated silica filled composites

Unfilled vulcanizates with different sulphur contents from Fig. 6.4 are set as reference and the linear fit is assumed to be the master line. The incorporation of precipitated silica into SSBR tends to reduce the crosslink density, as indicated in Fig. 6.5a by the gradual decrease of $D_{res}/2\pi$ and $1/M_c$ values as evaluated by NMR and swelling measurements. The phenomenon is well-known and is attributed to the adsorption of vulcanizing chemicals like zinc salts (zinc oxide and stearic acid mixture) and DPG on the filler surface, inhibiting the curing process⁴. The effects are more pronounced when increasing the volume fraction of precipitated silica (ULTRASIL VN3) in the rubber matrix. The samples $x-10$ to $x-50$ (samples filled with 10 to 50 phr of precipitated silica) show significant reduction in crosslink density (downwards shifts) with increasing volume fraction of silica. The deviating data points ($D_{res}/2\pi$ VS $1/M_c$) from the master line indicate the filler induced effect as well as the improved filler-polymer interfacial interactions on the crosslink density²⁶. TESPT is a well-known bifunctional silane coupling agent widely used in the tyre industry. It is also one of important silica surface modifier, through its silanization reaction of hydroxyl group situated on the silica surface and the ethoxy groups of the coupling agent. The silane contains sulphur bridges (S: ~4) which can participate in the crosslinking of rubber chains during the vulcanization process. Addition of such bi-functional coupling agents facilitates interfacial bonding between the silica filler and rubber and one can expect significantly higher crosslinks²⁷. In Fig. 6.5a, with the incorporation of TESPT silane coupling agent into the commercial silica system, a horizontal shift (shift towards right) in the values from the master line is observed. Therefore, the DQ-NMR display negligible increment in the $D_{res}/2\pi$ values, while the $1/M_c$ values from the swelling measurements are found to be increasing. The additional crosslink provided by the TESPT coupling agent must be closer to the silica surface and therefore, the contribution to the bulk polymer phase is lower. Perhaps, the improved rubber-silica interface could also result in a lower degree of swelling for the silane incorporated samples. It is however clear that commercial silica has weak interactions with the rubber matrix without coupling agent²⁸.

6. 2. 2. 2 *In-situ* sol-gel derived silica composites

In Fig. 6.5b, interesting observations are found for silica particles generated by sol-gel reaction²⁹. The values are found to shift horizontally towards to the right with increasing *in-situ* silica content. These *in-situ* silica particles yield no change in the number of chemical crosslinks as indicated by the NMR measurements. Such an effect from the *in-situ* silica composites clearly explains the higher interaction between rubber chains and the silica filler, even with the absence of TESPT coupling agent or may be a reduced activator and accelerator adsorption on the catalyst (n-butylamine) modified silica surface.



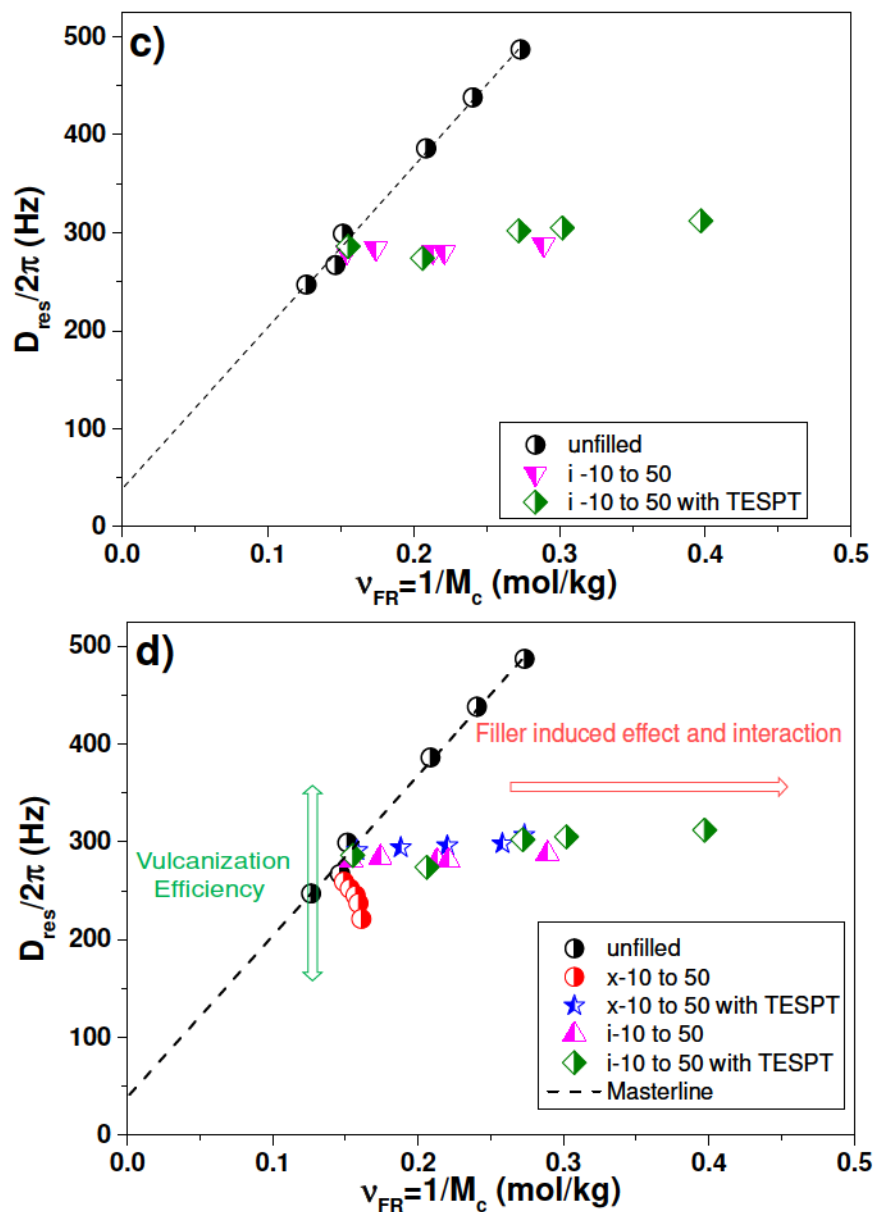


Figure 6.5 Plots of crosslink density by DQ-NMR as a function of Flory-Rehner based equilibrium swelling method for (a) Commercial ULTRASIL VN3 silica composites contain 10 to 50 phr of silica with and without TESPT coupling agent (b) Commercial ULTRASIL VN3 and *in-situ* silica system contain 10 to 50 phr of silica without TESPT coupling agent (c) *in-situ* sol-gel derived silica contain 10 to 50 phr of silica with and without TESPT coupling agent (d) summary of all the composites. The linear fitted line (master line) represents unfilled rubber samples vulcanized with different amounts of sulphur

The chemical properties and synthesis conditions of the *in-situ* silica particles are entirely different from commercial precipitated silica. The *in-situ* silica are prepared under alkaline condition using n-butylamine catalyst, which is basic in nature, could immensely influence

the surface and interaction properties of silica as well as the rate of the vulcanization reaction³⁰. The findings are therefore different to commercial silica composites, which show a reduction in the crosslink density but similar to that of silane modified commercial silica composites. The drift from the master line for the *in-situ* silica samples is, however, less than the silane coupled commercial silica composites. This behaviour may be explained by the inhomogeneity in swelling, possibly due to the elastomer chains being tethered onto the surface or entrapped inside the *in-situ* silica particles²⁰. Meanwhile, the small vertical shift observed for the *in-situ* silica composites from NMR measurements, indicates higher crosslink density values, probably due to the rubber chain entrapment or the filler surfaces acting as macro crosslink junctions²⁷.

Table 6.1 Crosslink densities of different silica filled SSBR composites estimated by NMR and swelling method

Silica (in phr)	$D_{res}/2\pi$ (kHz)				V_{FR} (mol/kg)			
	i	i_TESPT	x	x_TESPT	i	i_TESPT	x	x_TESPT
gum	0.268				0.146			
10	0.281	0.286	0.259	0.291	0.154	0.155	0.149	0.158
20	0.284	0.274	0.252	0.294	0.174	0.206	0.153	0.188
30	0.281	0.302	0.245	0.296	0.213	0.272	0.157	0.220
40	0.281	0.305	0.237	0.298	0.221	0.302	0.159	0.258
50	0.288	0.312	0.221	0.307	0.289	0.397	0.161	0.273

An addition of TESPT silane coupling agents to *in-situ* silica shows significant increase in the crosslink density of the rubber matrix (Fig. 6.5c). The vertical shift from the master line indicates that D_{res} values are increasing with TESPT modified *in-situ* silica content. Presence of TESPT has increased the crosslink density, due to better interaction with the active silica filler surface, modified by n-butylamine catalyst used during the synthesis. In our previous study we found that amine modified *in-situ* silica can enhance the vulcanization efficiency and cleave the sulphur molecules (-S, -S₂), providing additional crosslinks to the rubber²⁹. This phenomenon would result in a huge significant horizontal shift in $1/M_c$ values after silanization of *in-situ* silica composites. One could therefore expect the additional crosslinks as a) cumulative effects from effective tethering of elastomer chains on the surface of *in-situ* silica by TESPT coupling agent, b) entrapment of the rubber chains inside the *in-situ* silica particles, c) excess sulphur donation by the silane coupling agent and cleavage of sulphur molecules.

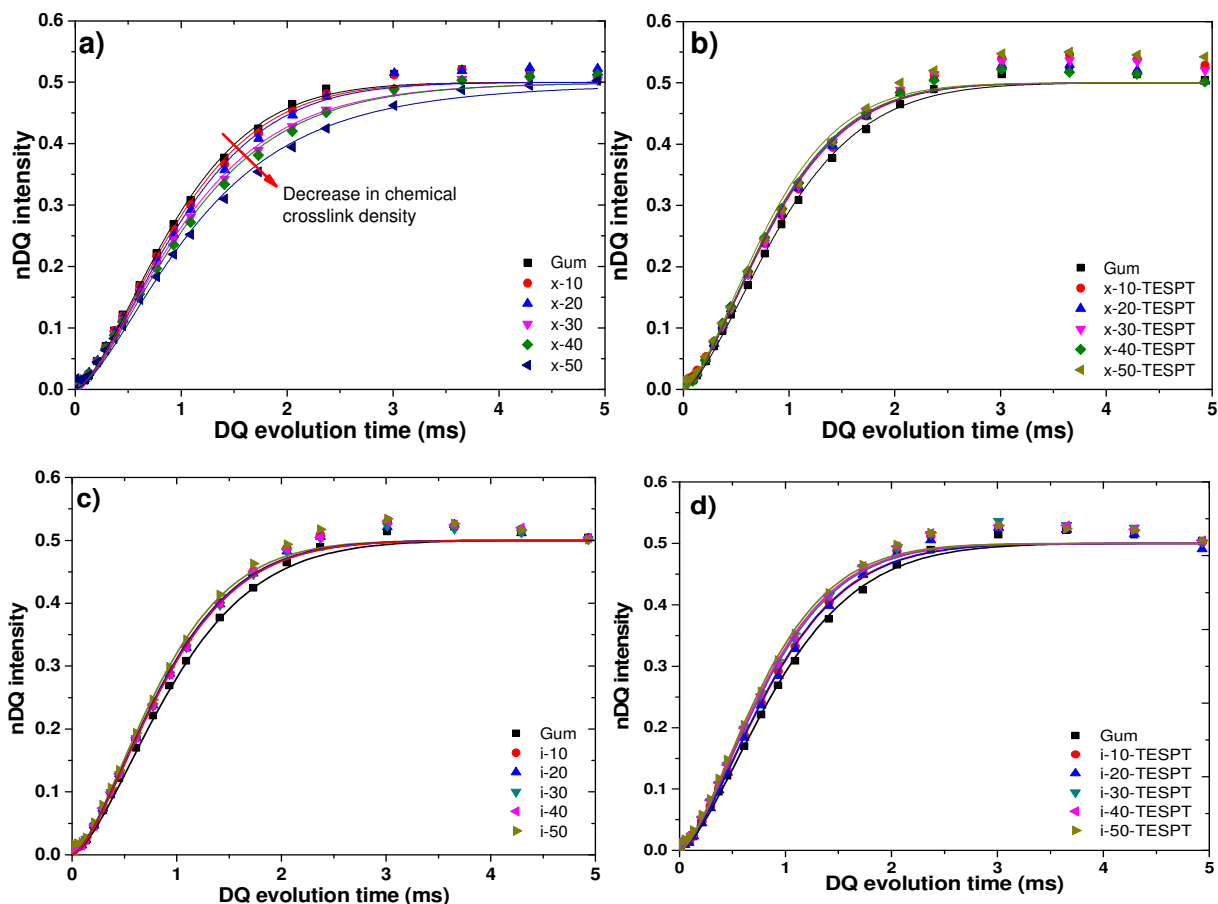


Figure 6.6 The plot normalized Double Quantum intensity versus Double quantum evolution time a) commercial precipitated silica b) silane modified commercial precipitated silica c) *in-situ* silica d) silane modified *in-situ* silica of 10 to 50 phr filled SSBR composites

Fig. 6.5d and Table 6.1 summarize all the *in-situ* and commercial silica composites, with and without TESPT silane coupling agent. The plot correlates the NMR crosslink density ($D_{res}/2\pi$, vertical shifts) with the vulcanization efficiency as well as the influence of silica chemistry (acidic or alkaline) on the crosslink density of the rubber matrix²⁷. Consequently, the crosslink density values by swelling ($1/M_c$, horizontal shift) depict the filler induced effects as well as filler-polymer interaction aided by the silane coupling agents²⁴. The plot normalized Double Quantum intensity versus Double quantum evolution time of commercial precipitated silica, *in-situ* silica and their silane modified 10 to 50 phr of SSBR composites are given in Figure 6.6.

6. 2. 3 Physical estimation of silanol groups situated on the surface of silica particle

To the understanding of the reactivity of silica surface, the amount of silanol groups present on the silica surface are calculated by Eq. 3.22 (in chapter 3) and the physical properties of the silica powders are enumerated in Table 6.2. The silica surface usually tends to adsorb significant amount of moisture due to its hygroscopic nature. According to the chemical structure of silica, it contains three different chemical structures namely isolated, vicinal and geminal silanols (see chapter 2). The silanol type and density would vary according to the preparation condition and the amount of water being used during synthesis. By knowing the thermal degradation behaviour and the specific surface area (BET- nitrogen adsorption number), one could roughly estimate the number of silanol groups³¹. The estimated silanol density for in-situ silica is higher as compared to the precipitated silica powder. This may be due to the higher amount of bound moisture and the higher final weight loss because of the entrapped polymer chains³⁷. However, the physical estimation of silanol groups for in-situ silica is not valid due to the absence of purity. Scientifically the calculated amount of Si-OH of 34 OH/nm² is sterically inconceivable^{38,40} and the estimation of silanol density using physical equation is not an accurate method for in-situ silica system³⁹.

Table 6.2 Determined properties of different silica materials and silanol density

Type of silica	Final weight loss (%)	Amount of moisture (%)110°C for 2hrs	BET (N ₂) surface (m ² /g)	Si-OH per nm ²
Commercial Precipitated	7	4.6	175	9.2
<i>In-situ</i> sol-gel	12	9.4	32*	≈34

*The measured BET - N₂ surface area of in-situ silica is around 32m²/g, which is considerably lower than commercial silica. It is found that after separation of in-situ silica particles from the rubber by solvent dilution technique, trace rubber exist and the presence of these trace rubber inhibits N₂ adsorption on silica surface, resulting in lower BET numbers. However, the given BET surface is an approximate value.

6. 2. 4 ^{29}Si -Solid state NMR investigation of silica and silica composites

6. 2. 4. 1 ^{29}Si -MAS NMR experiments

Fig. 6.7 depicts the direct excited ^{29}Si magic angle spinning spectrum (MAS) of two silica powders. The chemical structure of two given silica are different as evident from the MAS spectra. The chemical structure of silica particles are defined by the different silanols groups namely isolated, vicinal, geminal silanols and silica di-oxide⁴. Both silica powders are expected to display two important peaks at -103 ppm and -113 ppm, corresponding to mono-silanols and silica oxide respectively³². In commercial silica samples, these two main peaks are found at -103 ppm attributed to the mono-silanol group of Si-OH (Q^3) and at -113 ppm attributed to the SiO_2 (Q^4). The peak at -93 ppm of the geminal silanols Si-(OH)₂ (Q^2) is not detected because of its lower count. In the case of *in-situ* silica powder, the peak at -103 ppm is much stronger and the line width is nearly two times than commercial silica powders. This explains that *in-situ* silica surface consists of many mono-silanol groups Si-OH (Q^3)³³⁻³⁴. From the direct excited spectrum of two silica powders, Q^4 and Q^3 groups are estimated by peak integral analysis to get quantitative information on the chemical structure of in silica powders. Commercial silica powder consists 92% of Q^4 and 8% of Q^3 , whereas, *in-situ* silica consists 57% of Q^4 and 43% of Q^3 . Both the silica powders possess negligible geminal silanol (Q^2) groups. These findings correlate well with the physically estimated silanol density by thermogravimetric analysis and BET surface (in Table 6.2).

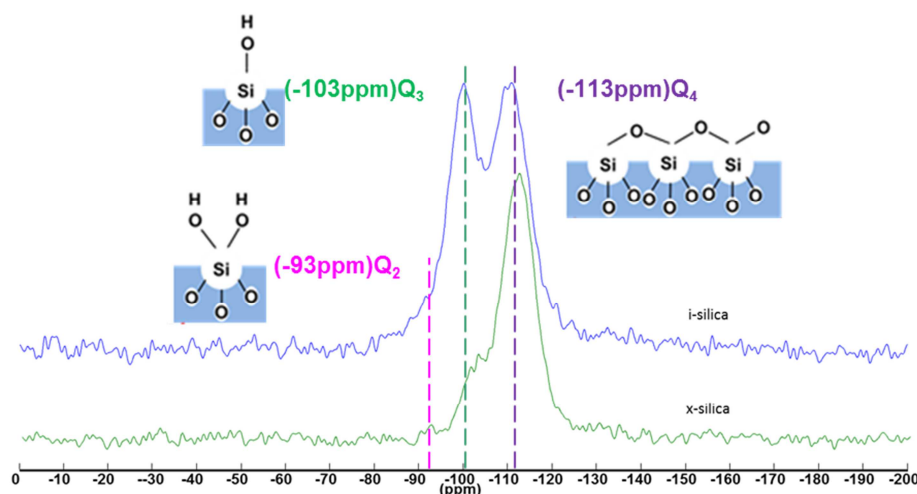


Figure 6.7 Direct excited ^{29}Si MAS spectrum for *in-situ* and commercial silica powers

6. 2. 4. 2 ^{29}Si - ^1H Cross polarization experiments

To understand the changes in proton density on silica surface in the presence of rubber and silane coupling agents, ^{29}Si - ^1H cross polarization experiments are performed. Fig. 6.8 shows the ^{29}Si - ^1H cross polarization spectra for SSBR/*in-situ* and commercial silica composites. The cross polarization spectra indicate minor amounts of Q^2 groups, which are expected to be present on the surface of the particles.

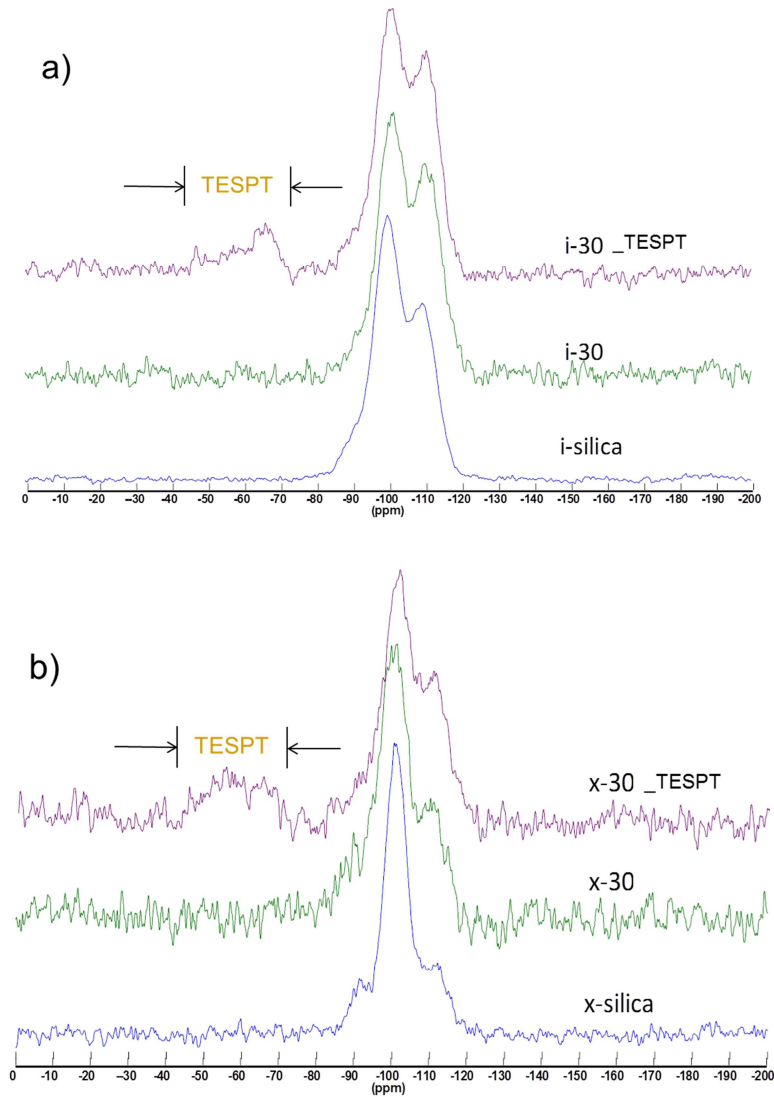


Figure 6.8 ^{29}Si - ^1H cross polarization spectrum for SSBR / (a) *in-situ* and (b) commercial silica composites

From Table 6.3, the quantitative peak intensity estimates around about 21.69% of Q^3 and 78.31% of Q^4 groups for the *x*-silica and around 42.98% of Q^3 and 57.02% of Q^4 for the *in-situ* silica powders. With the incorporation of *in-situ* silica and commercial silica into rubbers, the intensity of the Q^3 and Q^4 reduces significantly. This is a consequence of increase

in magnetization transfer to the non-hydrogenated Q⁴ and Q³ groups due to the presence of protons from the rubber molecules on the silica surface. Due to these effects, the Q³ intensity has reduced from 42.98 (*in-situ* silica powders) to 27.76% for the *in-situ* silica composites. In the case of commercial silica powders, there is a reduction from 21.69% to 20.44%. The values indicate that the surface chemistry and interaction of silica to rubber changes after mixing. This could be due to the higher mechanical energy applied during the mixing process for commercial silica systems³³ and the particle growth during *in-situ* sol-gel generation for the *in-situ* silica composites. The Q³ intensity is further reduced for the silane modified silica composites. The reduction in Q³ is around 2.27% for *in-situ* silane modified system and 0.14% for the commercial silane modified system, which indicates that the extent of silanization is high for *in-situ* silica than commercial silica systems. T-groups indicating the covalent bonds between silica and silane coupling agent is observed in the cross polarization spectra of the compounds. These signals are in the chemical shift range of -40 to -70 ppm³⁵⁻³⁶.

Table 6.3 Estimated peak integral from ²⁹Si-¹H cross polarization experiments

Materials	Q ³ integral (%)	Q ⁴ integral (%)
<i>In-situ</i> silica powder	42.98	57.02
i-30	27.76	72.24
i-30_TESPT	25.49	74.51
Commercial silica powder	21.69	78.31
x-30	20.44	79.56
x-30_TESPT	20.30	79.70

6. 2. 5 Energy dispersive X-ray spectroscopy (EDX) analysis

Fig. 6.9a shows a normalized EDX spectrum with respect to Si- peak acquired from 30 x 40 μm² samples (see chapter 3). The elemental mapping of silane modified silica particles exhibit five different traces of elements like silicon, carbon, oxygen, sodium and sulphur. The average of two scanned areas and the detected elemental composition is summarized in Table 6.4. The determined average quantitative amount of elements states that the reactivity of silane coupling agent with either of the silica is different. The commercial silane modified silica yields a lower carbon trace, while is higher for the *in-situ* silica. At the same time, sulphur traces on the silica surface confirm that both silica surfaces are modified by TESPT silane coupling agent. However, from quantitative determination, sulphur content is higher in the case of *in-situ* silica around 0.4 % and is only 0.2 % for commercial silica system.

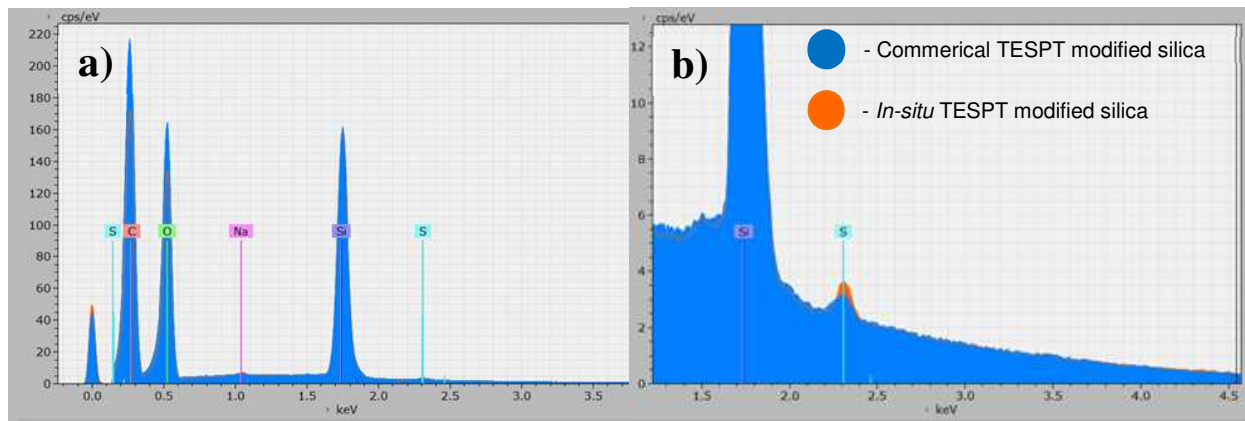


Figure 6.9 (a) EDX core spectrum of two silane modified silica particles separated from the rubber matrix (b) Detected sulphur peak on the surface of the precipitated and *in-situ* silica powder by EDX analysis

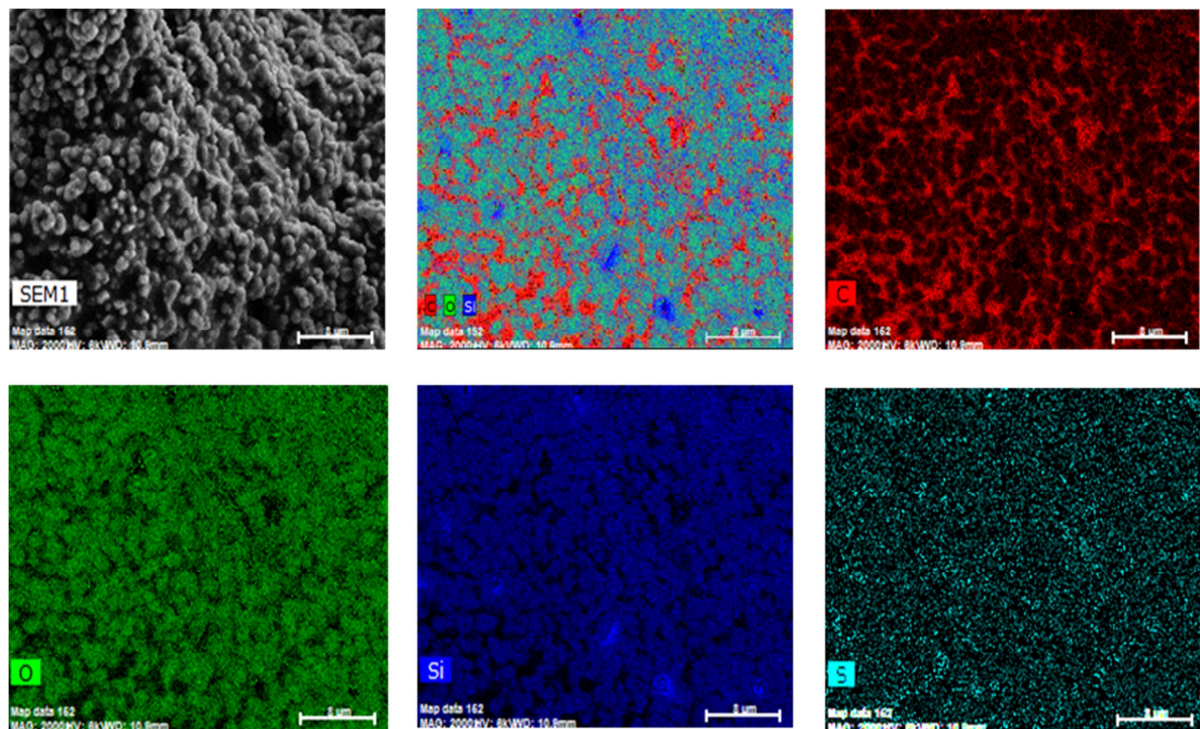


Figure 6.10 (a) Normal SEM image (b) SEM image with color overlay of C, O, Si distribution and elemental distribution maps of (c) Carbon (d) Oxygen (e) Silica (f) Sulfur of *i*-30_TESPT commercial silica composite

The higher amount of sulfur atoms detected on the *in-situ* silica surface further confirms its higher reactivity with the silane coupling agent, because of its active and ample hydroxyl groups. The small sodium peak observed in the case of *in-situ* silica and commercial silica might be due to the presence of impurities from the precursor. Fig. 6.10 and Fig. 6.11 show the distribution of different elements of samples *i*-30_TESPT and *x*-30_TESPT respectively.

The apparent non-uniformity of element distribution in specimen *x-30_TESPT* is found due to the inhomogeneous topography of the specimen. For specimen *i-30_TESPT* the silica particles are surrounded by rich carbon layer probably is a strong thin film of rubber covering the silica surface along with sulphur.

Table 6.4 Average composition in weight (%) derived from EDX spectra

Element	<i>x-30_TESPT</i>	<i>i-30_TESPT</i>
C	32 ± 10	36.5 ± 10
Si	33 ± 4	31 ± 7
O	34 ± 10	32.5 ± 7
S	0.2 ± 0.1	0.4 ± 0.1

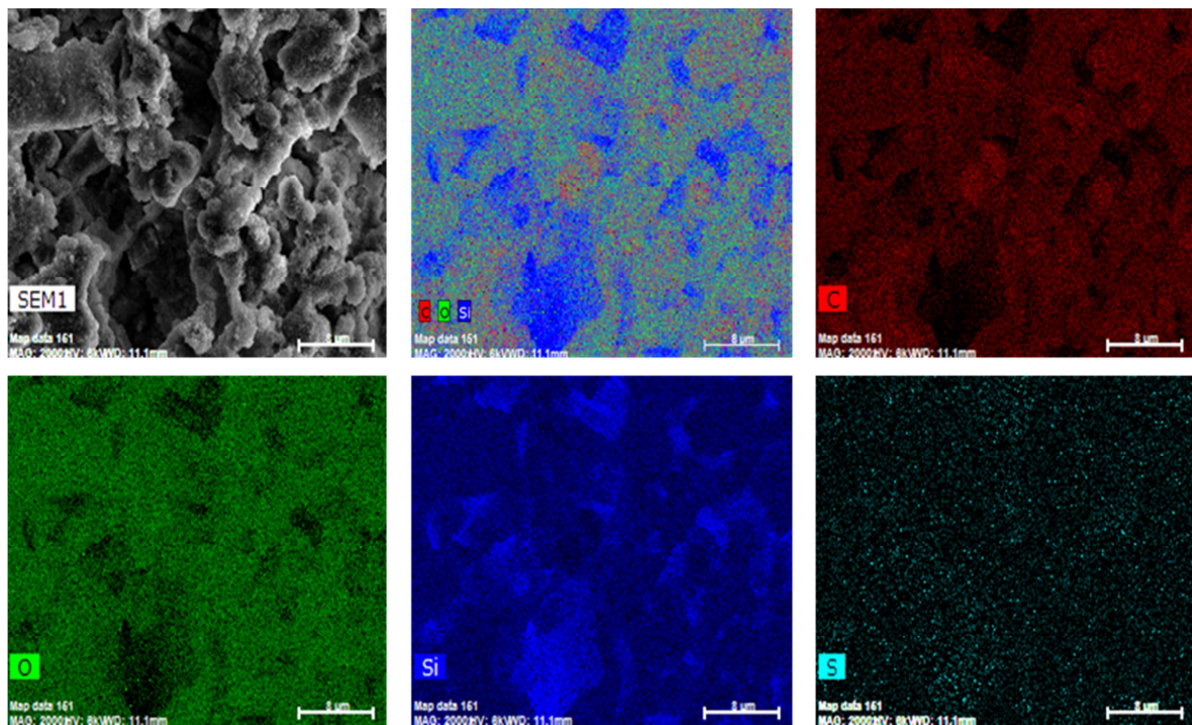


Figure 6.11 (a) Normal SEM image (b) SEM image with color overlay of C, O, Si distribution and elemental distribution maps of (c) Carbon (d) Oxygen (e) Silica (f) Sulfur of *x-30_TESPT* commercial silica composite

6.3 Conclusions

In this chapter, detailed studies were done to understand the reinforcement of SSBR by two different silica fillers *in-situ* sol-gel silica and precipitated commercial silica. The main challenge was to study the effects of silica generation and incorporation into rubber, along with the influence of surface chemistry, rubber-filler interactions in presence and absence of silane on reinforcement. Low field proton NMR investigations emphasized that the surface functionality and alkaline or acidic nature of silica influenced on the crosslink density of rubber. The DQ-NMR versus equilibrium swelling experiments correlations evidenced that generation of silica inside the rubber matrix can reinforce significantly better than incorporation of silica into the rubber. The type of filler-rubber interaction (physical or chemical) was scientifically distinguished from DQ-NMR versus swelling correlation plots. The interaction mechanism of *in-situ* silica with the rubber was unique, which reinforced the rubber without any silane coupling agent. Entrapment of rubber chains inside the silica particles as well as strong mechanical tethering of rubber chains onto the surface of the *in-situ* silica particles were the most plausible reasons for the enhanced rubber/*in-situ* silica filler interactions. The solid state ^{29}Si NMR MAS investigations depict different chemical structures for commercial silica and *in-situ* silica powders; a higher silanol density was also observed for *in-situ* silica. The solid state ^{29}Si - ^1H cross polarization experiments highlighted that around 2% of silanol groups were modified by TESPT coupling agent in *in-situ* silica composites and was rather only 0.2% in the case of ppt. silica composites. The EDX investigations affirmed both the silica surfaces being modified by TESPT silane, however the extent silane modification was higher for *in-situ* silica. Finally, it could be concluded that silanization efficiency not only depends on the processing temperature and time, rather also on the reactive hydroxyl density of silica fillers.

References

1. Morton, M., Rubber Technology, Springer science and business media, 2013, 523.
2. Hofmann, W., *Rubber technology handbook*. Hanser Publishers. Distributed in the USA by Oxford University Press: 1989, ISBN 3446148957, 574.
3. Evans, M. S., *Tyre compounding for improved performance*. iSmithers Rapra Publishing: 2002, (12), 112.

4. Hewitt, N.; Ciullo, P., *Compounding precipitated silica in elastomers: theory and practice*. William Andrew: 2007.
5. Nakajima, N.; Shieh, W. J.; Wang, Z. G., Mixing and Extrusion of High Silica and all Silica-natural Rubber Compounds. *International Polymer Processing* 1991, 6 (4), 290-296.
6. Mark, J.; Pan, S. J., Reinforcement of polydimethylsiloxane networks by in situ precipitation of silica: A new method for preparation of filled elastomers. *Die Makromolekulare Chemie, Rapid Communications* 1982, 3 (10), 681-685.
7. Ikeda, Y.; Kohjiya, S., In situ formed silica particles in rubber vulcanizate by the sol-gel method. *Polymer* 1997, 38 (17), 4417-4423.
8. Ikeda, Y.; Tanaka, A.; Kohjiya, S., Effect of catalyst on in situ silica reinforcement of styrene-butadiene rubber vulcanizate by the sol-gel reaction of tetraethoxysilane. *J. Mater. Chem.* 1997, 7 (3), 455-458.
9. Ikeda, Y.; Tanaka, A.; Kohjiya, S., Reinforcement of styrene-butadiene rubber vulcanizate by in situ silica prepared by the sol-gel reaction of tetraethoxysilane. *Journal of Materials Chemistry* 1997, 7 (8), 1497-1503.
10. Hashim, A.; Azahari, B.; Ikeda, Y.; Kohjiya, S., The effect of bis (3-triethoxysilylpropyl) tetrasulfide on silica reinforcement of styrene-butadiene rubber. *Rubber chemistry and technology* 1998, 71 (2), 289-299.
11. Tanahashi, H.; Osanai, S.; Shigekuni, M.; Murakami, K.; Ikeda, Y.; Kohjiya, S., Reinforcement of Acrylonitrile-Butadiene Rubber by Silica Generated in situ. *Rubber Chemistry and Technology* 1998, 71 (1), 38-52.
12. Murakami, K.; Osanai, S.; Shigekuni, M.; Iio, S.; Tanahashi, H.; Kohjiya, S.; Ikeda, Y., Silica and Silane Coupling Agent for in Situ Reinforcement of Acrylonitrile-Butadiene Rubber. *Rubber Chemistry and Technology* 1999, 72 (1), 119-129.
13. Kohjiya, S.; Ikeda, Y., Reinforcement of general-purpose grade rubbers by silica generated in situ. *Rubber chemistry and technology* 2000, 73 (3), 534-550.
14. Matějka, L.; Dukh, O.; Kolařík, J., Reinforcement of crosslinked rubbery epoxies by in-situ formed silica. *Polymer* 2000, 41 (4), 1449-1459.
15. Kohjiya, S.; Murakami, K.; Iio, S.; Tanahashi, T.; Ikeda, Y., In situ filling of silica onto “green” natural rubber by the sol-gel process. *Rubber chemistry and technology* 2001, 74 (1), 16-27.
16. Yoshikai, K.; Ohsaki, T.; Furukawa, M., Silica reinforcement of synthetic diene rubbers by sol-gel process in the latex. *Journal of applied polymer science* 2002, 85 (10), 2053-2063.
17. Murakami, K.; Iio, S.; Ikeda, Y.; Ito, H.; Tosaka, M.; Kohjiya, S., Effect of silane-coupling agent on natural rubber filled with silica generated in situ. *Journal of materials science* 2003, 38 (7), 1447-1455.
18. Ikeda, Y.; Kameda, Y., Preparation of “green” composites by the sol-gel process: in situ silica filled natural rubber. *Journal of sol-gel science and technology* 2004, 31 (1-3), 137-142.
19. Das, A.; Jurk, R.; Werner Stöckelhuber, K.; Heinrich, G., Silica-Ethylene Propylene Diene Monomer Rubber Networking by In Situ Sol-Gel Method. *Journal of Macromolecular Science, Part A: Pure and Applied Chemistry* 2007, 45 (1), 101-106.
20. Miloskovska, E.; Friedrichs, C.; Hristova-Bogaerds, D.; Persenair, O.; van Duin, M.; Hansen, M. R.; de With, G., Chemical Mapping of Silica Prepared via Sol-Gel Reaction in Rubber Nanocomposites. *Macromolecules* 2015, 48 (4), 1093-1103.
21. Miloskovska, E.; Hansen, M. R.; Friedrich, C.; Hristova-Bogaerds, D.; van Duin, M.; de With, G., In Situ Silica Nanoparticle Formation in a Rubber Matrix Monitored via Real-Time SAXS and Solid-State NMR Spectroscopy. *Macromolecules* 2014, 47 (15), 5174-5185.
22. Iler, R. K., *The chemistry of silica: solubility, polymerization, colloid and surface properties, and biochemistry*. Wiley: 1979.

23. Syed, I. H.; Stratmann, P.; Hempel, G.; Klüppel, M.; Saalwächter, K., Entanglements, Defects, and Inhomogeneities in Nitrile Butadiene Rubbers: Macroscopic versus Microscopic Properties. *Macromolecules* 2016, *49* (23), 9004-9016.
24. Saalwächter, K., Proton multiple-quantum NMR for the study of chain dynamics and structural constraints in polymeric soft materials. *Progress in Nuclear Magnetic Resonance Spectroscopy* 2007, *51* (1), 1-35.
25. Valentín, J. L.; Mora-Barrantes, I.; Carretero-González, J.; López-Manchado, M. A.; Sotta, P.; Long, D. R.; Saalwächter, K., Novel Experimental Approach To Evaluate Filler–Elastomer Interactions. *Macromolecules* 2010, *43* (1), 334-346.
26. Pérez-Aparicio, R.; Schiewek, M.; Valentín, J. L.; Schneider, H.; Long, D. R.; Saphiannikova, M.; Sotta, P.; Saalwächter, K.; Ott, M., Local Chain Deformation and Overstrain in Reinforced Elastomers: An NMR Study. *Macromolecules* 2013, *46* (14), 5549-5560.
27. Valentín, J. L.; Mora-Barrantes, I.; Carretero-González, J.; López-Manchado, M. A.; Sotta, P.; Long, D. R.; Saalwächter, K., Novel Experimental Approach To Evaluate Filler–Elastomer Interactions. *Macromolecules* 2010, *43* (1), 334-346.
28. Mujtaba, A.; Keller, M.; Iisch, S.; Radosch, H.-J.; Beiner, M.; Thurn-Albrecht, T.; Saalwächter, K., Detection of Surface-Immobilized Components and Their Role in Viscoelastic Reinforcement of Rubber–Silica Nanocomposites. *ACS Macro Letters* 2014, *3* (5), 481-485.
29. Raman, V. S.; Das, A.; Stockelhuber, K. W.; Eshwaran, S. B.; Chanda, J.; Malanin, M.; Reuter, U.; Leuteritz, A.; Boldt, R.; Wie; Heinrich, G., Improvement of mechanical performance of solution styrene butadiene rubber by controlling the concentration and the size of in situ derived sol-gel silica particles. *RSC Advances* 2016, *6* (40), 33643-33655.
30. Krejsa, M. R.; Koenig, J. L., A Review of Sulfur Crosslinking Fundamentals for Accelerated and Unaccelerated Vulcanization. *Rubber Chemistry and Technology* 1993, *66* (3), 376-410.
31. Meier, J. G.; Fritzsche, J.; Guy, L.; Bomal, Y.; Klüppel, M., Relaxation Dynamics of Hydration Water at Activated Silica Interfaces in High-Performance Elastomer Composites. *Macromolecules* 2009, *42* (6), 2127-2134.
32. Ye, G.; Hayden, C. A.; Goward, G. R., Proton Dynamics of Nafion and Nafion/SiO₂ Composites by Solid State NMR and Pulse Field Gradient NMR. *Macromolecules* 2007, *40* (5), 1529-1537.
33. Simonutti, R.; Comotti, A.; Negroni, F.; Sozzani, P., ¹³C and ²⁹Si Solid-State NMR of rubber-silica composite materials. *Chemistry of materials* 1999, *11* (3), 822-828.
34. Xie, X.-Q.; Ranade, S.; DiBenedetto, A., A solid state NMR study of polycarbonate oligomer grafted onto the surface of amorphous silica. *Polymer* 1999, *40* (23), 6297-6306.
35. Hoh, K. P.; Ishida, H.; Koenig, J. L., Silicon-²⁹ solid-state nuclear magnetic resonance spectroscopy of composite interfaces. *Polymer composites* 1990, *11* (2), 121-125.
36. Mora-Barrantes, I.; Valentín, J. L.; Rodríguez, A.; Quijada-Garrido, I.; Paris, R., Poly (styrene)/silica hybrid nanoparticles prepared via ATRP as high-quality fillers in elastomeric composites. *Journal of Materials Chemistry* 2012, *22* (4), 1403-1410.
37. Vaikuntam, S. R.; Stockelhuber, K. W.; Bhagavatheswaran, E. S.; Wiessner, S.; Scheler, U.; Saalwächter, K.; Formanek, P.; Heinrich, G.; Das, A., Entrapped styrene butadiene polymer chains by sol-gel derived silica nanoparticles with hierarchical raspberry structures. *The journal of physical chemistry B*, 2018, *122*, 2010-2022.
38. L. T. Zhuravlev., Concentration of hydroxyl groups on the surface of amorphous silicas. *Langmuir* 1987, *3* (3), 316-318.

39. Mueller, R., Hendrik K. Kammler, Wegner, K., and Sotiris E. Pratsinis., OH Surface Density of SiO₂ and TiO₂ by Thermogravimetric Analysis, *Langmuir* 2003, 19, 1, 160-165.
40. Zhuravlev, L.T. & Potapov, V.V. Density of silanol groups on the surface of silica precipitated from a hydrothermal solution, *Russian Journal of Physical Chemistry* 2006, 80, 1119.

Chapter 7

Effect of silica-silane interaction on the mechanical performance of silica filled solution styrene butadiene rubber

7.1 Introduction

Silane coupling agents are one of the important rubber ingredients and playing a major role in manufacturing silica filled tyres¹⁻². Plenty of silane coupling agent are commercially available in the market. However, according to the reactivity between rubber and silica, the silane coupling agents are generally divided into two, namely, mono-functional silanes and bi-functional silanes³. Similarly, according to the type of molecular interaction between rubber and silica, they are further classified into physically (physically coupled with rubber chains) or chemically (covalently coupled with rubber chains) interacting coupling agents. Nevertheless, the bi-functional silane or sulphur containing silane coupling agents are primarily considered and are more important in the field of rubber science and technology. The proper selection of silane coupling agent is one of the critical parameters in rubber product manufacturing and decides the final performance of the rubber-silica composite⁴. In the previous chapters, the reinforcement effects observed for the *in-situ* and precipitated silica composites are explained to be entirely different because of their particle sizes, state of dispersion and filler-polymer interaction. The silica particles developed by the *in-situ* method were found to be relatively bigger around 200~400 nm⁵. In this chapter, attention is paid to understand the reinforcing effect achieved by the incorporation of different silane coupling agents like Diethoxydimethylsilane (DMS), (3-Aminopropyl)triethoxysilane (APTES), n-Octadecyltriethoxysilane (ODTES), 3-Octanoylthio-1-propyltriethoxysilane (NXT), (3-Mercaptopropyl)trimethoxysilane (MPTES), Bis[3-(triethoxysilyl)propyl]disulfide (TESPD) and Bis[3-(triethoxysilyl)propyl]tetrasulfide (TESPT) into *in-situ* silica composites. The study is further extended and compared with commercial precipitated silica composites. The influence of silica dispersion, filler-filler interaction, filler-polymer interaction, filler-polymer interfaces, type of interaction between the rubber and silica and finally the crosslink density of the composites on the reinforcement of rubber are investigated in detail.

7.2 Results and discussion

7.2.1 Mechanical properties

The stress-strain properties of SSBR gum and 30 phr silica filled composites are shown in Fig. 7.1. *In-situ* silica based composites display higher 100% and 200% moduli with slight compromise in elongation at break and tensile strength, when compared to precipitated silica composites. All silane modified *in-situ* silica composites exhibit higher modulus (i.e. at 100% and 200% elongation) than *in-situ* silica without any silane. This trend can also be

found at precipitated silica and their silane modified composites. The improvement in mechanical strength by silanes for the *in-situ* silica composites is much higher than in precipitated silica systems. The observed tensile properties in presence and absence of silane coupling agents for the *in-situ* silica system illustrates that the surface chemistry and the nature of filler-polymer interaction is different from the precipitated silica fillers⁴. The numerical order of mechanical reinforcement with respect to increase in 100% and 200% modulus offered by various silanes could be summarized as:

for *in-situ* silica: ODTES < Pristine < APTES < DMS < NXT < TESPDP < MPTES < TESPT

for precipitated silica: ODTES < DMS < Pristine < APTES < NXT < TESPDP < TESPT < MPTES

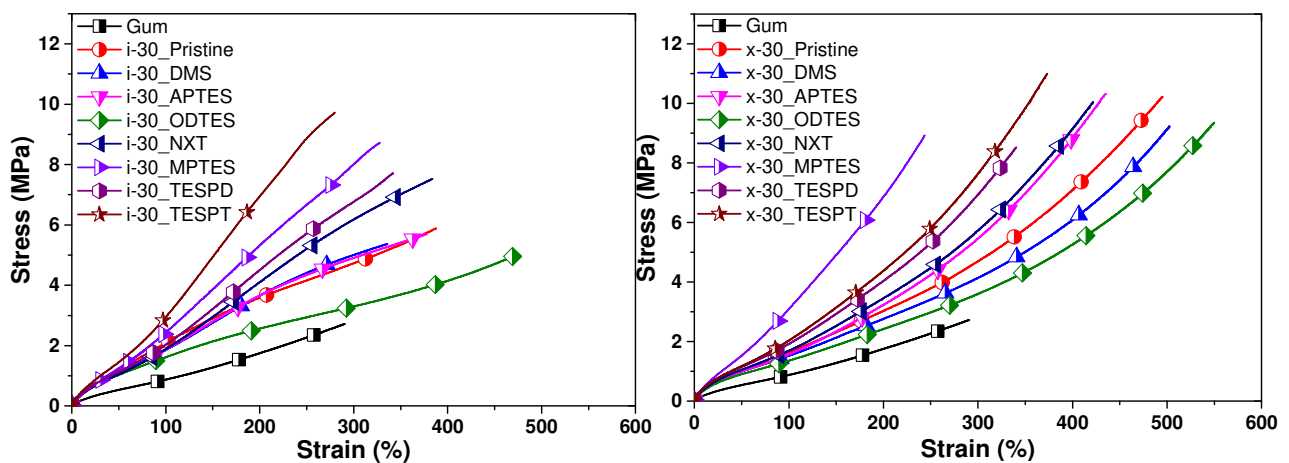


Figure 7.1: Stress-strain properties of different silanes in 30 phr (a) *in-situ* silica and (b) precipitated silica filled SSBR composites

The reinforcement effect of *in-situ* and precipitated silica using different silane coupling agents varies due to several factors. Some of the possible reasons are like, 1) a different pH of the rubber system depending on the fillers (*in-situ* silica is synthesised in an alkaline medium and precipitated silica has an acidic surface), 2) the different coupling efficiencies of silanes to the silica and polymer, 3) different reactivities of silanes under alkaline and acidic atmosphere (for example: TESPT silane is able to donate the sulphur atoms to the rubber matrix in highly alkaline condition and mercapto silane may be sensitive to react faster in acidic atmosphere), 4) a plasticizing effect by DMS, ODTES and APTES due to mono functionality. However, further investigations are necessary to understand the mechanical reinforcement of rubber by different silane coupling agents in the *in-situ* silica system.

7. 2. 2 Dynamic mechanical properties

7. 2. 2. 1 Strain sweep measurements

The dynamic mechanical strain dependent properties are studied to investigate the filler-filler interaction and dispersion of silica in the composites. The experimental strain sweeps along with extrapolated hydrodynamic reinforcement (Chen-Acrivos model)⁶ data are fitted with the Kraus model ($E'(\gamma_c) = E'_\infty + (E'_i - E'_\infty)/(1 + (\gamma/\gamma_c)^{2m})$) and shown in Fig. 7.2 and the obtained parameters are summarized in Table 7.1. Experimental results show that incorporation of silane coupling agents in precipitated silica filled systems decrease the storage modulus in the lower strain regime⁷⁻⁸. Usually, silane coupling agents assist in silica dispersion, causing an overall reduction in the dynamic modulus⁹.

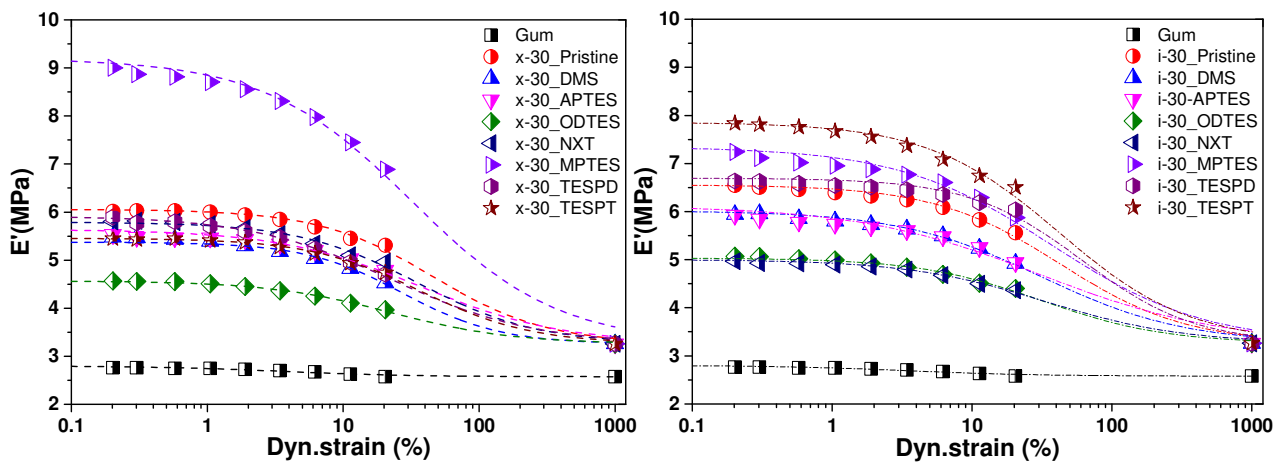


Figure 7.2 Strain dependency of dynamic elastic modulus for the SSBR/*in-situ* silica composites (symbols represent experimental data and lines represent the fitted Kraus equation (chapter-3, equation 3.6))

A contrary effect is observed with the addition of MP TES silane in the precipitated silica system, where the dynamic modulus of rubber increased. Generally, MP TES silane is considered to be highly reactive with precipitated silica facilitating improved silanization reaction. This coupling agent is so reactive that the crosslinking reactions (scorch) are partially taken place and increase the viscosity of rubber compound during the mixing process of the silica in the internal mixer¹⁰⁻¹¹. Interesting scenarios are observed for *in-situ* silica systems, where silane incorporation increases as well as decreases the storage modulus. Addition of sulphur containing silanes like MP TES, TESP D and TESPT displays higher storage modulus than the pristine *in-situ* silica composites.

Table 7.1 Calculated strain dependent dynamic properties of composites by Kraus function

30 phr of silica	Critical strain (%)		Strain amplitude constant (m)	
	<i>In-situ</i>	Precipitated	<i>In-situ</i>	Precipitated
Pristine	42	39	0.47	0.51
DMS	31	27	0.42	0.51
APTES	30	37	0.33	0.41
ODTES	31	22	0.49	0.47
NXT	33	35	0.43	0.49
MPTES	37	31	0.39	0.40
TESPD	41	33	0.53	0.41
TESPT	41	37	0.46	0.52

7. 2. 2. 2 Temperature sweep measurements

Table 7.2 Important dynamic mechanical properties of various silane modified silica-SSBR composites

Samples	E'@	E'@	E'@	tan δ @	tan	tan δ @	tan	T _g
	0°C	25°C	60°C	0°C	δ @	60°C	δ_{\max}	
					-10°C			
gum	2.85	2.44	2.14	0.200	0.461	0.080	1.788	-27.8
x-30	7.17	6.00	5.22	0.199	0.423	0.097	1.370	-28.2
x-30 DMS	7.59	6.02	5.07	0.246	0.468	0.106	1.314	-27.0
x-30 APTES	6.72	5.59	4.78	0.205	0.420	0.114	1.387	-27.8
x-30 ODTES	5.76	4.79	4.13	0.200	0.395	0.109	1.413	-29.2
x-30 NXT	6.86	5.71	4.82	0.200	0.408	0.101	1.353	-28.4
x-30 MPTES	9.38	7.87	6.83	0.201	0.397	0.093	1.304	-28.1
x-30 TESP	7.95	6.48	5.51	0.216	0.443	0.098	1.304	-28.2
x-30 TESPT	7.04	5.93	5.38	0.209	0.442	0.076	1.341	-26.8
i-30	6.58	5.58	5.05	0.209	0.467	0.063	1.575	-27.8
i-30 DMS	6.64	5.41	4.64	0.218	0.429	0.103	1.542	-28.6
i-30 APTES	6.24	5.19	4.43	0.191	0.404	0.111	1.618	-28.7
i-30 ODTES	5.57	4.46	3.97	0.190	0.384	0.100	1.604	-29.7
i-30 NXT	5.79	4.79	4.18	0.203	0.405	0.100	1.602	-27.8
i-30 MPTES	6.67	5.50	4.93	0.200	0.426	0.090	1.569	-28.0
i-30 TESP	6.47	5.31	4.77	0.212	0.458	0.085	1.559	-28.0
i-30 TESPT	7.20	6.20	5.74	0.229	0.500	0.057	1.514	-26.0

The physical coupling agents DMS, APTES and ODTES show a reduction in the dynamic modulus of the *in-situ* silica composites⁷. To further understand the filler-filler interaction effect, the strain sweep data are fitted with Kraus model and the results are given in Table 7.1.

The estimated critical strain values are different for all composites. It is generally believed that high critical strain represents lower filler-filler interaction, higher filler dispersion and the composites are less sensitive to dynamic strains. The results show that in average the *in-situ* silica contributes higher critical strain values as compared with the corresponding precipitated silica. This quantitative prediction indicates that precipitated silica composites have more filler-filler networks and these networks are more susceptible to dynamic strains¹². *In-situ* derived silica composites possess lower filler-filler network, which indicates good filler dispersion⁵. The SEM investigation show that the *in-situ* silica particles are bigger in size as compared to precipitated silica system. In this scenario, one could also consider that at the equal amount of *in-situ* and precipitated concentration (volume fraction of silica) in rubber, *in-situ* silica system exhibit a lower particle to particle distance when compared to precipitated silica. The strain amplitude constant (m) lies in between 0.33 to 0.53 and is common for all silica filled rubber systems¹³.

The dynamic mechanical time dependent properties for the gum and 30 phr silica filled composites are studied over temperatures from -60°C to 80°C , the obtained plots are depicted in Fig. 7.3 and specific properties are summarized in Table 7.2. Fig. 7.3a and 7.3c show the temperature dependent changes in the storage moduli for different silica composites. The storage modulus behaviour for the filled composites with increasing temperature is almost similar to gum vulcanizates. Storage modulus of the composites changes significantly with respect to the type of silane coupling agent used. The mono-functional silane modified composites exhibit lower high temperature modulus compared to bi-functional silane modified composites. This higher storage modulus is mainly due to the improved filler-polymer interaction and the additional sulphur in the rubber matrix. Interesting facts are observed from the $\tan \delta$ - temperature plots. Incorporation of silica significantly reduces the $\tan \delta$ peak height ($\tan \delta_{max}$). Precipitated silica composites display lower $\tan \delta_{max}$ than *in-situ* silica systems. Additionally, incorporation of silanes in both the systems further reduces the $\tan \delta_{max}$ values¹⁴. The glass transition temperature (T_g) for the *in-situ* and precipitated silica modified by ODTES silane display a negative T_g shift of $\sim 2^{\circ}\text{C}$. The ODTES silane is a linear long chain aliphatic silane, which could acts as a plasticizing agent and the T_g of composites are therefore lower. Whereas, with the addition of bi-functional silanes, *in-situ* silica composites shows a slight increase in T_g . The T_g shift in this case could be explained by the stronger rubber-filler interaction¹⁵ and the additional crosslinks formed¹⁶ in the rubber matrix. The $\tan \delta$ values at -10°C , 0°C and 60°C are generally considered to predict the performance

of tyre treads in terms of ice grip, wet grip and rolling resistance¹⁷ respectively; values are given in Table 7.2.

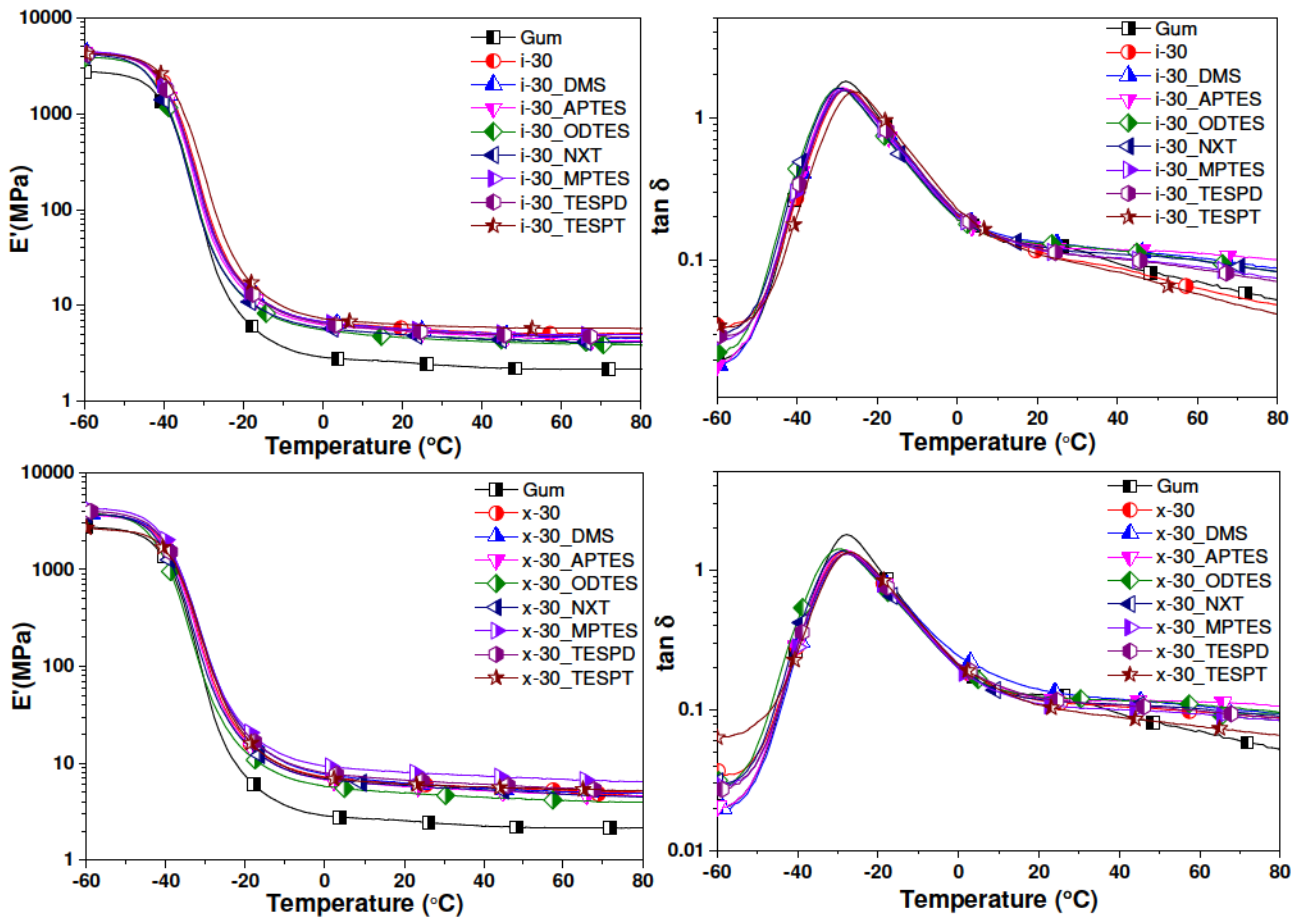


Figure 7.3 Dynamic mechanical temperature sweep analysis of different silane modified *in-situ* silica and ppt. silica based SSBR nanocomposites (a) & (c) temperature dependent changes in storage modulus and (b) & (d) temperature dependent changes in $\tan \delta$

TESPT modified silica composites exhibit improved ice grip, wet grip and rolling resistance properties. Furthermore, TESPT modified *in-situ* silica composite shows better performance than precipitated silica filled composites.

7. 2. 3 Heat build-up properties

The amount of heat generated and accumulated inside the composites under a dynamic load is measured and the corresponding compression-set values (calculated after the experiment) are plotted in Fig 7.4. In Fig 7.4a, due to the absence of any filler, the gum vulcanizate shows a lower heat build-up and with the incorporation of silica, heat build-up increases. Incorporation of silane coupling agent in *in-situ* and precipitated silica systems, significantly suppress the amount of heat generation. The silane modification by a chemical coupling agent shows lower heat build-up than physical coupling agents. For physically coupled systems, it is observed that an increase in aliphatic chain length decreases the heat build-up. The precipitated silica and their silane modified composites display higher heat build-up than *in-situ* silica systems.

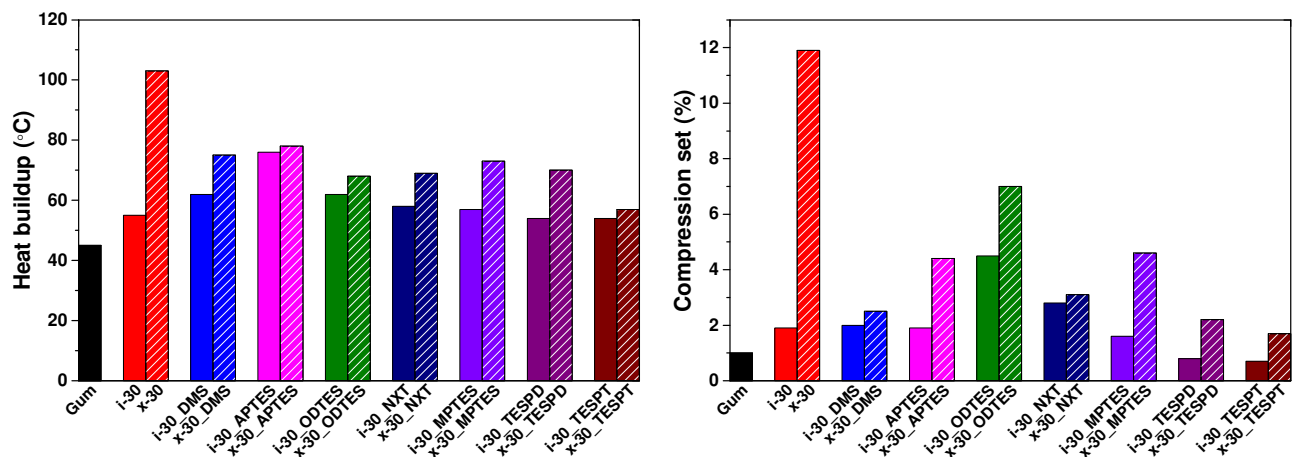


Figure 7.4 (a) Heat build-up properties and (b) compression set values (after heat build-up experiments) for various 30 phr *in-situ* and ppt. silica filled composites

Fig.7.4b summarizes the compression set values after the heat build-up experiments. The pristine ppt. silica system exhibits the highest compression set compared to gum and other silane modified systems. The physical modification of silica by DMS, APTES and ODTES results in larger compression set compared to other bi-functional silanes. The chemical modification however offers lower compression set, especially TESPT. The results clearly show that inclusion of precipitated silica increases the internal friction between the silica and rubber, leading to massive heat generation¹⁸ and results in a higher compression set.

7. 2. 4 Rebound resilience

The rebound resilience properties of SSBR gum, *in-situ* and precipitated silica filled composites are summarized in Fig 7.5. The resilience of rubber is found to be reduced with the addition of filler¹⁹. However, the resilience characteristics are improved with the addition of all type of silane coupling agent in both the silica systems. The physical and chemical silane modification of silica in the rubber improves the resilience characteristics significantly. Chemically modified silica composites exhibit better resilience properties than physically modified systems. However, *in-situ* silica based rubber composites shows better resilience characteristics in comparison to precipitated silica systems²⁰ and possess high elasticity than the reference compound (gum vulcanizate).

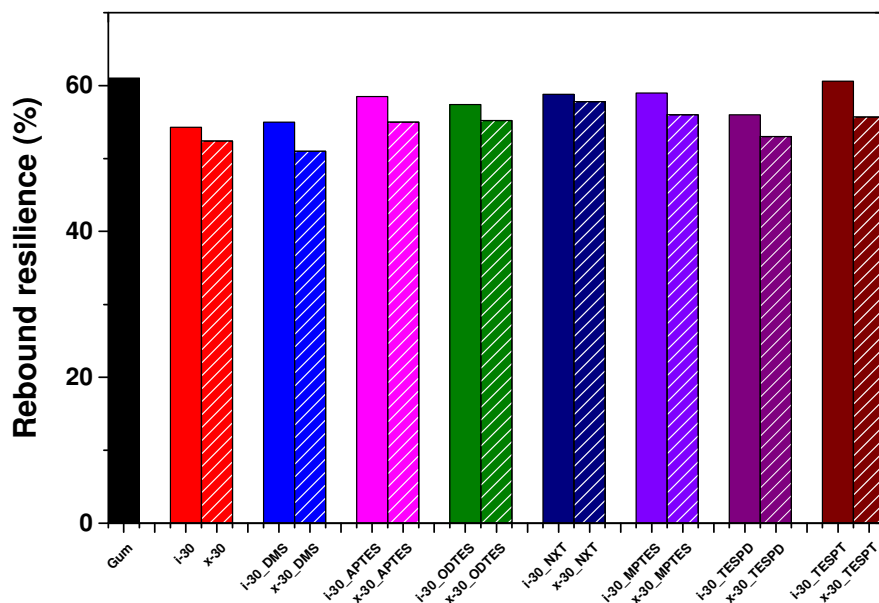


Figure 7.5. Rebound resilience properties of 30 phr different silane modified in-situ and precipitated silica filled SSBR composites

7. 2. 5 Abrasion properties (DIN 53516)

Fig.7.6 depicts the abrasion resistance index (ARI) of gum and 30 phr silica filled silane modified SSBR composites. The incorporation of silica and silane significantly improves the abrasion resistance of the rubber composites. The abrasion properties are however dependent on the type and nature of silane coupling agent²¹. In precipitated silica systems, physical modification by APTES and ODTES improve the ARI compared to DMS modification. In *in-situ* silica systems, all physical silane modifications increase the ARI values significantly compared to the pristine *in-situ* silica system. The chemical modification of silica by the bi-

functional silanes exhibits even higher resistance to abrasion with respect to physical silanes, in both *in-situ* as well as precipitated. silica systems. The NXT silane modified precipitated silica composite exhibits the highest ARI value than other sulphur based silanes like MPTES, TESP and TESPT. Experimental results suggest better abrasion properties for the ppt. silica systems.

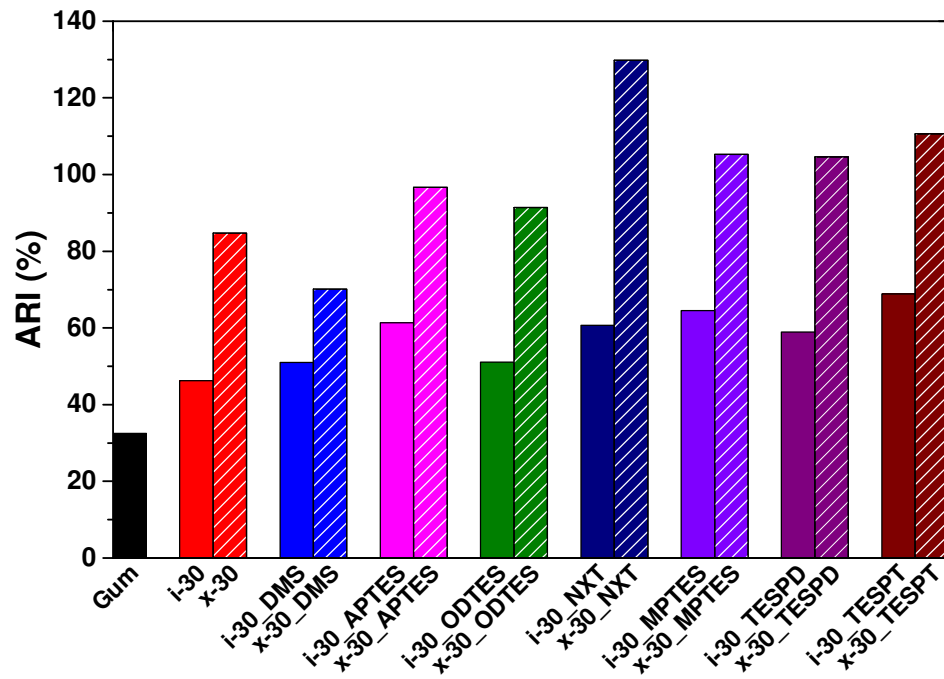


Figure 7.6 Abrasion resistance index of gum and 30 phr silica filled different silane modified composites

7.2.6 Molecular interpretation of silica-silica network and desorption of rubber chains from the silica surface by temperature dependent-strain sweep measurements

From the perspective of adsorption, the polymer chains are attached onto the filler surface in two different ways, namely physical adsorption (physisorption) and chemical adsorption (chemisorption)²². In chemisorption process, the polymer molecules strongly adhere onto the surface by chemical bonding. Removal of such chemisorbed layer is more difficult and it is non-reversible process. In physisorption process, there are attractive Van-der-Waals forces acting between the polymer chains and the filler surface. Physisorption enables both adsorption and desorption and is also a reversible process. Physical adsorption involves the formation of successive multi-molecular layers and desorption can take place from top to bottom of the multiple physisorption layer. But, chemisorption is always restricted to a single layer. In some cases, physical adsorption may take place on the top of a chemisorbed layer²³⁻²⁴. Maier and Göritz model²⁵ is mainly based on temperature dependent

strain sweep (Payne effect) measurements. The model describes that rubber chains come closer and interact with the filler surface and the density of adsorption and desorption of rubber chains are temperature and strain dependent.

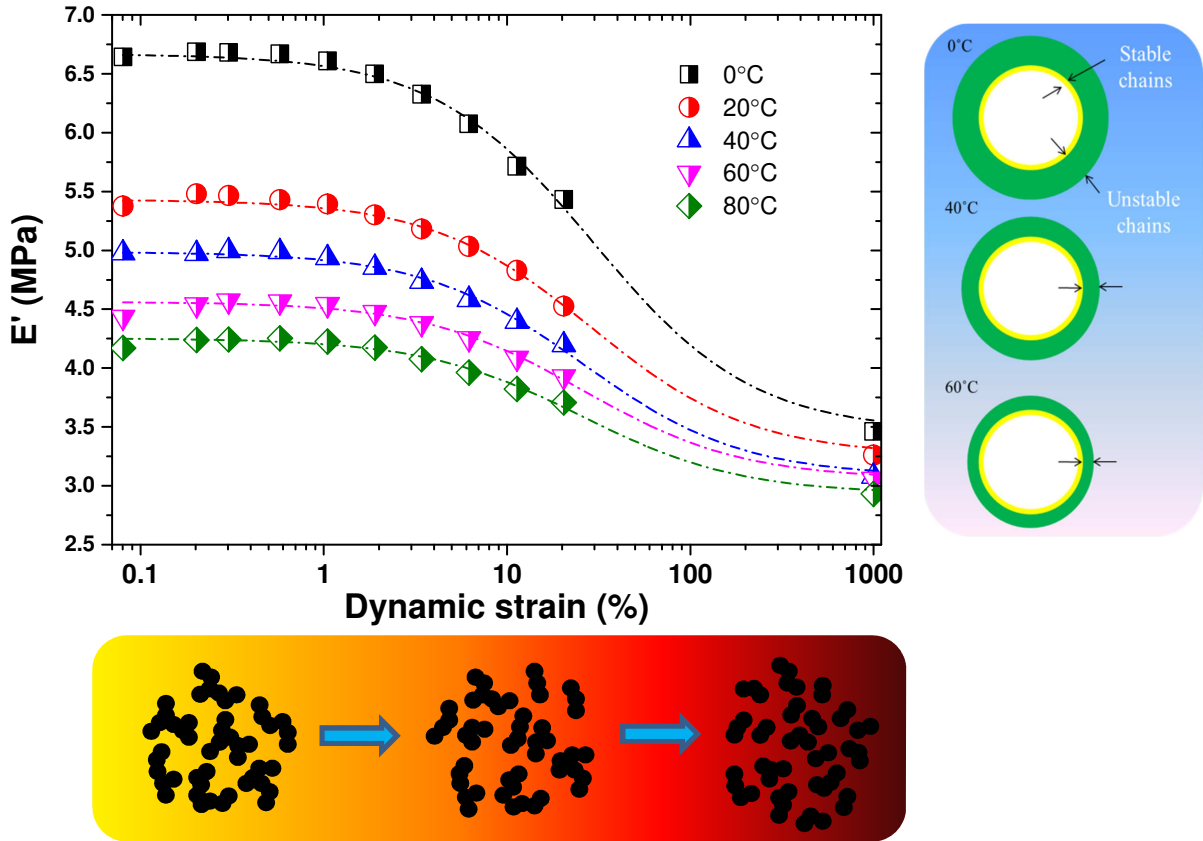


Figure 7.7 Strain sweep experiments performed at different temperatures on a 30phr *in-situ* silica filled silane modified system, extrapolated to 1000% modulus estimated from hydrodynamic Chen-Acrivos equation and fitted with Maier-Göritz model (dashed lines). The scheme in bottom shows the impact of strain amplitude and the scheme on the right depicts the effect of temperature on the silica filled rubber composites

The basic principle of the model is derived from the theory of entropy elasticity of rubbers.

$$E' = NK_B T \quad (7.1)$$

where E' is the storage modulus of filled system, N is the network density, K_B is the Boltzmann constant and T is the absolute temperature. According to the theory of reinforcement, the network density of filled rubber is contributed by three different parts

$$N = N_{Cr} + N_{St} + N_{un} \quad (7.2)$$

where N_{Cr} is chemical network density, N_{st} is density of stable bonds strongly attached (immobilized rubber chains) at filler surface and N_{un} is density of unstable bonds between chains and filler. When the dynamic strain is increased, more unstable rubber chains are torn off from their bonds. Therefore, the storage modulus of the material is strongly dependent on the strain amplitude (γ) and the strain dependent entropy elasticity of rubber material is therefore,

$$E'(\gamma) = (N_{Cr} + N_{st} + N_{un}(\gamma))K_B T \quad (7.3)$$

With this relationship, it is easy to describe the strain dependent modulus contribution by means of entropy elasticity.

As per the basic Langmuir adsorption theory, the adsorption and desorption of molecules on the surface come to equilibrium after a certain period of time. In the case of Langmuir's model the adsorption is determined by a function of pressure. According to Maier-Göriz model, 'the adsorption rate of rubber chains is constant, because the number of chains segments in the range of free isolated interaction position and the pressure is constant'²⁵. On the other hand, the rate of desorption is strongly dependent on the magnitude of dynamic strain deformation. Therefore, with the increase in dynamic strain amplitude, more rubber chains are separated from the filler surface. The desorption rate is proportional to the dynamic strain amplitude, i.e., $\Phi_{de} = \varphi\gamma$ where Φ_{de} is desorption rate, φ is a constant. The maximum possible interaction sites per volume which are able to develop a bond to a segment

$$N_{un}(\gamma) = \frac{N_{iso}}{1+c\gamma} \quad (7.4)$$

Here N_{iso} is number of isolated interaction sites per volume. From Eq.3 and Eq.4 the following equation is obtain

$$E'(\gamma) = (N_{Cr} + N_{st} + \frac{N_{iso}}{1+c\gamma})K_B T \quad (7.5)$$

So the strain dependent storage modulus of filled rubber system can be related to the variation of the network density and the Eq.5 can be written as²⁵

$$E'(\gamma) = E'_{st} + \frac{E'_{un}}{1+c\gamma} \quad (7.6)$$

Where $E'_{st} = (N_{cr} + N_{st})K_B T$ and $E'_{un} = N_{iso}K_B T$. The parameter 'c' is approximately constant.

Temperature has a great influence on the modulus of a rubber material according to theory of rubber elasticity. It is also well known that the storage modulus at small deformation is lower at high temperatures and the Payne effect is also reduced. The stable network density contributed by $N_{cr} + N_{st}$ is therefore assumed to be less influenced by temperature, whereas, the amount of unstable network (Eq.4) is strongly reduced. The model describes that desorption of unstable chains from the filler surface is responsible for the strong decrease in dynamic storage modulus with increasing the temperature. Desorption of rubber chains from the filler surface is a temperature activated process and the temperature dependence of the number unstable bonded chains $N_{un}(T)$ is explained as an Arrhenius equation.

$$N_{un}(T) = N_{\infty} e^{-E_a/K_B T} \quad (7.7)$$

where, N_{∞} is a constant representing the density of unstable bonds independent of temperature or deformation amplitude and E_a is the activation energy.

Fig.7.7 shows the temperature and strain dependent Payne effect experiments of a 30 phr *in-situ* silica filled TESPT modified rubber composite. The amplitude of the Payne effect decreases gradually with temperature. According to the theory of rubber elasticity, the modulus of a rubber material should increase linearly with respect to temperature. At the same time, it is well accepted that the storage modulus at small deformations is lower at high temperatures and the Payne effect diminishes with increasing temperatures. The observations confirm that the decrease of dynamic moduli in filled rubber composites is not only contributed by the filler-filler interaction, but rather also by the polymer chains. To understand desorption of rubber chains from the immobilized layer (chemisorbed layer), three different silica systems have been chosen and given in Fig 7.8. The three systems are chosen according to the nature of interaction between silica and rubber i.e., chemical interaction by TESPT, physical interaction by DMS and between unmodified silica and rubber. Figure 7.8 also shows the linear Arrhenius fits for estimation of unstable bonds for the 30 phr *in-situ* and ppt. silica filled composites, modified by various silane coupling agents along with an unfilled gum vulcanizate. Obtained slope values and the calculated activation energies are given in Table 7.8. The number of unstable rubber chains (physically adsorbed on the filler surface) is strongly influenced by the filler content, as can be seen from Table 7.3. The model equally applies to unfilled systems and suggests that a part of the entangled networks have longer

relaxation times than the experiment. Unfilled vulcanizates display the highest slope of ~ 1059 . From the perspective of Payne effect, an unfilled system does not exhibit any strain dependency. However, temperature induced softening of the crosslinked rubber network as well as disentanglement or entanglement relaxation in the rubber chains might occur. The silica filled silane modified systems show lower slope values than the gum vulcanizate, effects attributing to silica and silane coupling. When the composites are subjected to temperature, one could expect contributions from polymer, filler as well as from the immobilized and loosely bounded rubber chains.

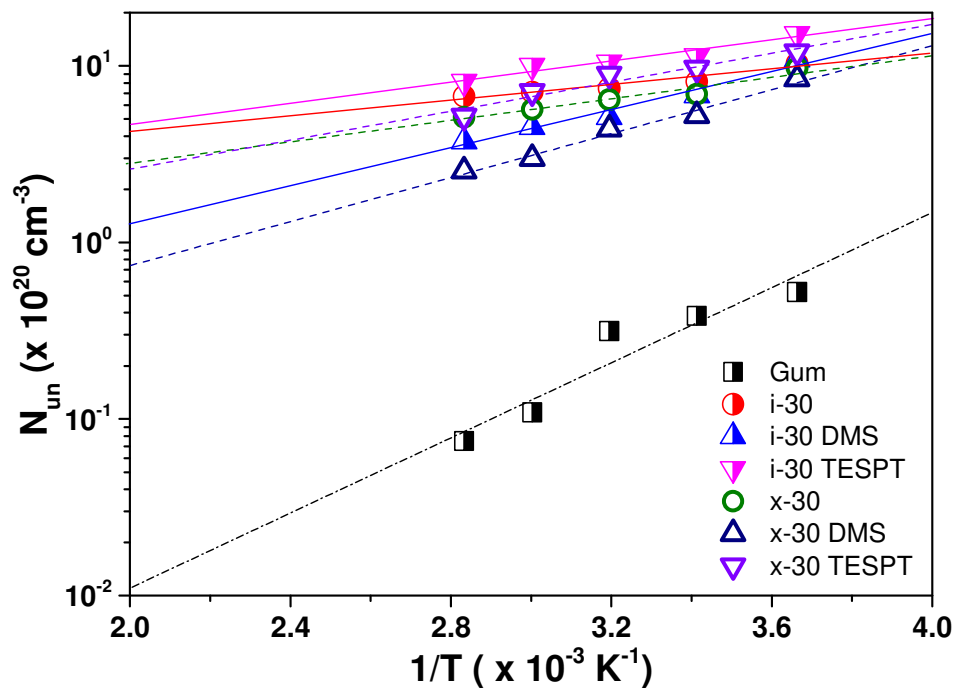


Figure 7.8 Arrhenius plot of temperature and strain dependent desorption of unstable rubber chains from silica particles predicted by Maier-Görizt model²⁵

The Arrhenius slopes are changing with respect to the nature of silica and the silane coupling agent, implying different silica-rubber interactions. Therefore, the estimated activation energies are different for *in-situ* and precipitated silica systems that are filled with the same volume fraction and modified by the same silane. It is observed that both stable and unstable bonds in the network simultaneously reduce with an increase in temperature from 273 to 353 K. This huge change in the number stable bonds arise questions, since stable bonds are described as tightly bounded chains in the vicinity of the filler surface. Some NMR investigations state that the stable immobilized layer thickness in silica filled composites is nearly 1-5 nm at 350 K²⁶⁻²⁸. However, if the rubber-filler interface adherence is poor, it would account for the sharp decrease in the number of stable bonds at high temperatures.

The Maier and Göritz model is mainly developed for carbon black filled systems; where polymer chains adhere strongly onto the filler, by virtue of their high interaction with rubbers. Whereas, in case of silica filled systems, the rubber chains sparingly adhere on the filler surface and the silane coupling agents tether the rubber chains with the silica. This makes silica filled systems to have both stable and unstable bonds. Some of the stable bonds may also be connected through glassy bridges (between the silica particles), which would cause a reduction in the modulus as suggested by Merabia *et.al.*²⁹. To further analyse the results, the temperature dependence of the density of unstably bonded chains is written as an Arrhenius law:

$$N_{un}(T) = N_{un}e^{-E_a/RT} \quad (7.8)$$

Where, N_{un} is a constant characterizing the density of unstable bonds independent of temperature or deformation amplitude and E_a is the activation energy.

From the plot of the logarithm of the density of unstable chains against the inverse of temperature shown in Figure 7.8, the activation energy can be calculated and is found to be in between 0.0913 to 0.0184 eV for different silane modified SSBR composites filled with 30phr of *in-situ* and commercial precipitated silica³⁰⁻³¹. This value is within the range of the van der Waal's interaction. The rate of desorption is directly proportional to the number of unstable chains at the filler surface. Hence it is concluded that the number of unstable fixed chains adsorbed on the filler surface contributes to the reduction of modulus with increase in temperature. Nevertheless, the prediction of stable and unstable polymer chains²⁵ on silica surface are also depend on the specific surface area of silica, the amount of silanol groups situated on the surface, the size of primary-secondary particles and the functionality of silane coupling agent.

Table 7.3 The stable chains and unstable chains predicted from the Payne effect measurements

	1/T (K ⁻¹)	Stable chains [N _{st} x 10 ²⁰] (1/cm ³)		Unstable chains [N _{un} x 10 ²⁰] (1/cm ³)	
		<i>In-situ</i>	Precipitated	<i>In-situ</i>	Precipitated
Gum	0.00366	7.57		0.52	
	0.00341	6.92		0.38	
	0.00319	6.01		0.31	
	0.00300	5.32		0.10	
	0.00283	4.86		0.07	
Pristine	0.00366	19.51	18.92	10.32	9.74
	0.00341	16.21	14.97	8.15	6.91
	0.00319	14.58	13.56	7.45	6.44
	0.00300	13.75	11.9	7.1	5.67
	0.00283	12.73	11.13	6.72	5.12
DMS	0.00366	20.01	17.62	10.88	8.44
	0.00341	14.87	13.29	6.81	5.23
	0.00319	12.24	11.51	5.11	4.39
	0.00300	11.15	9.64	4.5	2.99
	0.00283	9.75	8.55	3.74	2.54
APTES	0.00366	18.1	17.21	8.92	8.02
	0.00341	15.13	13.94	7.08	5.88
	0.00319	13.02	12.22	5.89	5.10
	0.00300	11.33	11.37	4.68	4.72
	0.00283	9.86	9.07	3.85	3.06
ODTES	0.00366	14.87	12.31	5.68	3.23
	0.00341	12.43	11.29	4.38	3.12
	0.00319	10.58	9.87	3.46	2.75
	0.00300	9.55	8.04	2.91	1.5
	0.00283	8.88	7.51	2.87	1.39
NXT	0.00366	13.92	16.73	4.73	7.55
	0.00341	12.36	14.31	4.3	6.26
	0.00319	10.19	11.34	3.06	4.21
	0.00300	9.49	9.97	2.84	3.32
	0.00283	8.33	9.13	2.32	3.11
MPTES	0.00366	26.59	26.05	17.4	16.87
	0.00341	18.65	22.73	10.6	14.67
	0.00319	16.41	19.18	9.28	12.05
	0.00300	14.42	16.19	7.77	9.54
	0.00283	11.87	13.88	5.86	7.87
TESPD	0.00366	18.59	21.73	9.41	12.55
	0.00341	15.31	15.75	7.25	7.69
	0.00319	13.14	14.17	6.01	7.04
	0.00300	11.81	12.57	5.16	5.93
	0.00283	10.79	10.2	4.78	4.19
TESPT	0.00366	24.33	21.2	15.15	12.01
	0.00341	19.42	17.78	11.36	9.72
	0.00319	17.56	16.08	10.44	8.96
	0.00300	16.66	13.79	10.01	7.14
	0.00283	14.13	11.19	8.12	5.18

Table 7.4 Crosslink density of different silane modified silica filled SSBR composites estimated by NMR and swelling method as well as the desorption of activation energy and slope estimated by the Maier-Görizt model²⁵

30 phr of silica	$D_{res}/2\pi$ (kHz)		V_{FR} (mol/kg)		Desorption activation energy (10^{-2} eV)		Slope	
	<i>In-situ</i>	Precipitated	<i>In-situ</i>	Precipitated	<i>In-situ</i>	Precipitated	<i>In-situ</i>	Precipitated
Gum		0.268		0.146		9.13		1059
Pristine	0.281	0.245	0.212	0.157	1.84	2.71	213	315
DMS	0.277	0.258	0.209	0.144	4.66	5.37	541	623
APTES	0.252	0.263	0.200	0.155	3.77	3.83	437	445
ODTES	0.255	0.253	0.207	0.185	3.25	4.08	377	474
MPTES	0.280	0.275	0.252	0.206	3.52	3.49	524	405
NXT	0.262	0.259	0.251	0.207	3.31	4.37	384	507
TESPD	0.282	0.293	0.264	0.203	3.09	4.44	358	515
TESPT	0.303	0.296	0.272	0.220	2.49	3.53	289	410

7. 2. 7 Effect of physical and chemical interfaces on crosslink density of rubber

Filler-polymer interaction is considerably a major factor deciding the mechanical properties. Major properties of a silica filled composite depend on the type of silane coupling agent being used as well as the nature of interaction (physical or chemical) between rubber and silica. The final crosslink density of rubber matrix is also influenced by type of functional groups present in the silane coupling agent and their functionality (mono- or bi-functional)³². Fig.7.9a&b and Table 7.4 depict the influence of various silane coupling agents on the crosslink density of the SSBR matrix based on the DQ-NMR and equilibrium swelling measurements. The grey dashed line represents the unfilled system vulcanized with 1.4 phr sulphur to understand the changes in chemical crosslinks. Values above and below the grey line distinguishes the change in network density by physical and chemical coupling of silanes. The effect of mono functional silanes (data within the red circle) and bi-functional silanes (data within the blue circle) on the physical and chemical crosslink densities are apparent from the plots. Addition of mono functional coupling agents like DMS, APTES, and ODTES in precipitated silica composites exhibits a slight increase in the chemical crosslink. It reveals the inferior effect (reduction in chemical crosslink) of precipitated silica in rubber is defeated by physical modification.

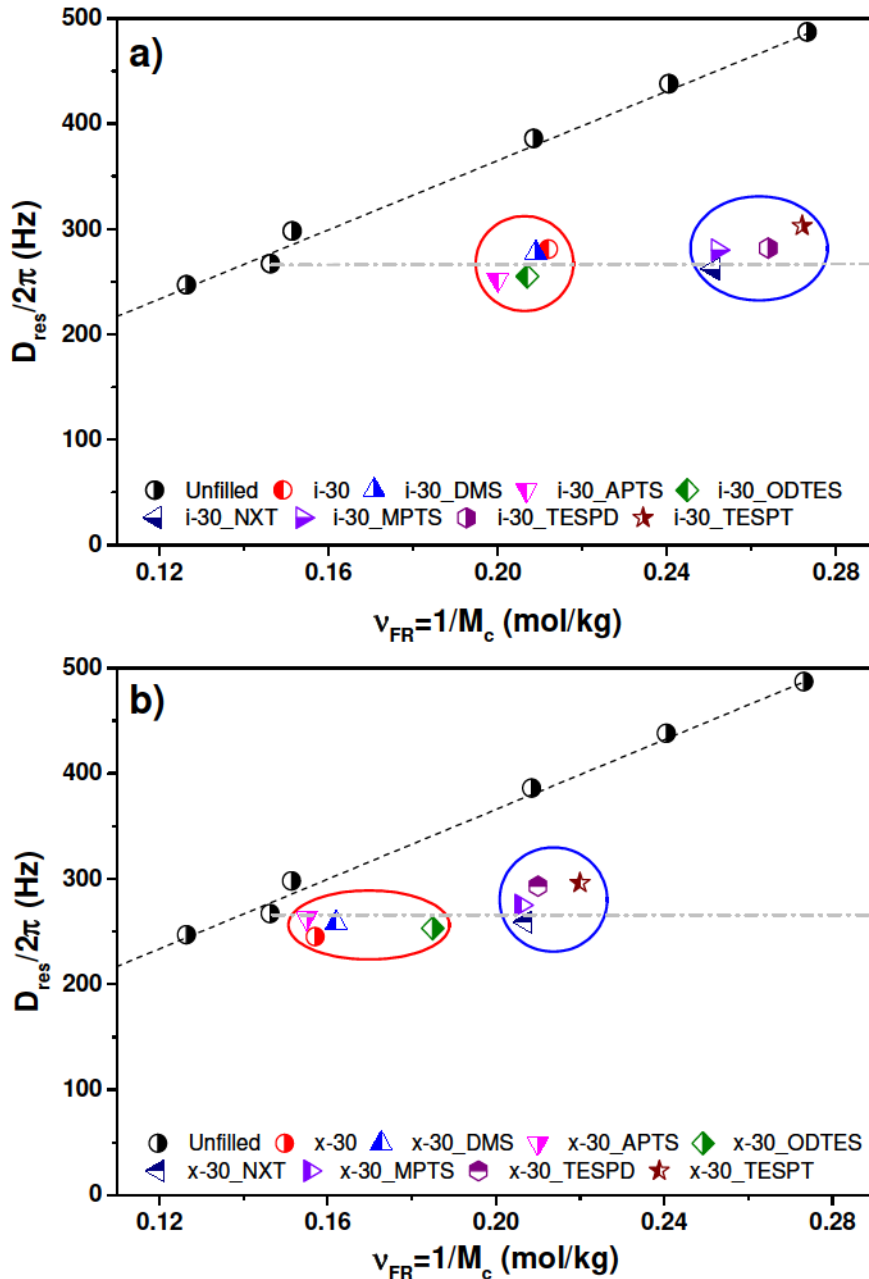


Figure 7.9 Type of coupling agent on the crosslink density of SSBR measured by NMR as a function of Flory-Rehner based equilibrium swelling method. 30 phr of a) *in-situ* and b) ppt. silica filled elastomers with different silane coupling agent

In the case of *in-situ* silica composites the physical modification by DMS, APTES, and ODTES tend to slight reduction in amount of final crosslinks. On the other hand, bi-functional silanes like NXT, MPTES, TESPD and TESPT show significant improvements in amount of chemical crosslinks (larger horizontal shift)¹¹. The vertical deviation from the master line (the vertical shift) of red and blue circles signifies that *in-situ* silica has better filler-polymer

interaction than precipitated silica filled system. The plots affirm that the additional crosslinks are mainly contributed by the sulphur present in the silane coupling agent and are also directly related to the chemical interfacial changes between silica and rubber³³.

7.3 Conclusions

The effects of incorporating different silane coupling agents on the performance and properties of *in-situ* derived and commercial precipitated silica based rubber composites were investigated in details in this chapter. The mechanical reinforcement in terms of improvement in tensile modulus offer by the *in-situ* silica was higher compared to precipitated silica composites. The elongation at break and tensile strength were slightly compromised for the *in-situ* composites. Payne effect measurements showed that filler-filler network break down and effect of silanes on the dynamic storage modulus were entirely different for *in-situ* and precipitated silica composites. The physical and chemical modification of silica and the reactivity of silanes were some of the parameters that influenced the filler-filler interaction. The temperature sweep measurement showed that the storage modulus above room temperature was unaffected with respect to different silanes, except TESPT and ODTES. TESPT showed slightly higher and ODTES showed slightly lower storage moduli. The TESPT silane shows an enhanced interaction with the rubber, while ODTES have a plasticizing effect, as observed from the high temperature storage modulus of the composites. The rolling resistance predicted from $\tan \delta$ plots indicated that the TESPT modified *in-situ* and precipitated silica composites display low $\tan \delta$ at 60 °C compared to other silane modified silica composites. The heat build-up studies revealed that *in-situ* silica and their all their silane modified composites exhibit lower heat build-up and lower dynamic compression set. The rebound resilience was reduced with the addition *in-situ* and precipitated silica and the silane modification further improved the resilience properties. However, the chemical interaction between silica-rubber by NXT, MPTES, TESP and TESPT showed higher resilience compared to physical interaction by DMS, APTES and ODTES. The abrasion experiments showed the precipitated silica composites offered higher abrasion resistance compared to *in-situ* silica systems. The addition of silane coupling agents significantly improved the abrasion resistance index, however chemically modified silica composites showed better abrasion resistance than physically modified silica composites. The molecular interpretation of Payne effect studies showed that the number of unstable chains adsorbed on the silica surface contributes to the reduction of modulus with increase in temperature. The crosslink density study revealed that the bi-functional silanes like NXT, MPTS, TESP and

TESPT show significantly higher amounts of chemical crosslinks due to enhanced silica-rubber interaction. Finally, the nature of silane interaction (physical or chemical) with rubber and silica mainly decided the reinforcement and performance of silica-rubber composites.

References

1. Ten Brinke, J.; Debnath, S.; Reuvekamp, L.; Noordermeer, J., Mechanistic aspects of the role of coupling agents in silica–rubber composites. *Composites Science and Technology* 2003, 63 (8), 1165-1174.
2. Heinrich, G.; Vilgis, T., Why Silica Technology Needs S-SBR in High Performance Tires?: The Physics of Confined Polymers in Filled Rubbers. *KGK. Kautschuk, Gummi, Kunststoffe* 2008, (61) 7-8.
3. Visakh, P.; Thomas, S.; Chandra, A. K.; Mathew, A. P., *Advances in elastomers I: blends and interpenetrating networks*. Springer Science & Business Media, 2013, 1-200.
4. Rodgers, B., *Rubber compounding: chemistry and applications*. CRC Press: 2015.
5. Raman, V. S.; Das, A.; Stockelhuber, K. W.; Eshwaran, S. B.; Chanda, J.; Malanin, M.; Reuter, U.; Leuteritz, A.; Boldt, R.; Wie; Heinrich, G., Improvement of mechanical performance of solution styrene butadiene rubber by controlling the concentration and the size of in situ derived sol-gel silica particles. *RSC Advances* 2016, 6 (40), 33643-33655.
6. Hsiao-Sheng, C.; Acrivos, A., The effective elastic moduli of composite materials containing spherical inclusions at non-dilute concentrations. *International Journal of Solids and Structures* 1978, 14 (5), 349-364.
7. Ramier, J.; Gauthier, C.; Chazeau, L.; Stelandre, L.; Guy, L., Payne effect in silica filled styrene–butadiene rubber: Influence of surface treatment. *Journal of Polymer Science Part B: Polymer Physics* 2007, 45 (3), 286-298.
8. Sarkawi, S. S.; Dierkes, W. K.; Noordermeer, J. W. M., MORPHOLOGY OF SILICA-REINFORCED NATURAL RUBBER: THE EFFECT OF SILANE COUPLING AGENT. *Rubber Chemistry and Technology* 2015, 88 (3), 359-372.
9. Sahakaro, K.; Beraheng, S., Reinforcement of maleated natural rubber by precipitated silica. *Journal of applied polymer science* 2008, 109 (6), 3839-3848.
10. Lin, C.-C.; Hergenrother, W. L., Silica-reinforced rubber compounded with mercaptosilanes and alkyl alkoxysilanes, 2002, US6453065B1.
11. ten Brinke, A. Silica reinforced tyre rubbers. PhD Thesis. Twente University, The Netherlands, 2002.
12. Vaikuntam, S. R.; Bhagavatheswaran, E. S.; Stöckelhuber, K. W.; Wießner, S.; Heinrich, G.; Das, A., DEVELOPMENT OF HIGH PERFORMANCE RUBBER COMPOSITES FROM ALKOXIDE-BASED SILICA AND SOLUTION STYRENE–BUTADIENE RUBBER. *Rubber Chemistry and Technology* 2017, 90(3), 467-486.
13. Heinrich, G.; Klüppel, M., Recent advances in the theory of filler networking in elastomers. In *Filled Elastomers Drug Delivery Systems*, Springer: 2002; 1-44.
14. Ikeda, Y.; Kohjiya, S., In situ formed silica particles in rubber vulcanizate by the sol-gel method. *Polymer* 1997, 38 (17), 4417-4423.
15. Hashim, A.; Azahari, B.; Ikeda, Y.; Kohjiya, S., The effect of bis (3-triethoxysilylpropyl) tetrasulfide on silica reinforcement of styrene-butadiene rubber. *Rubber chemistry and technology* 1998, 71 (2), 289-299.
16. Sankar Raman, V.; Das, A.; Stockelhuber, K. W.; Eshwaran, S. B.; Chanda, J.; Malanin, M.; Reuter, U.; Leuteritz, A.; Boldt, R.; Wiessner, S.; Heinrich, G., Improvement of mechanical performance of solution styrene butadiene rubber by controlling the concentration and the size of in-situ derived sol-gel silica particles. *RSC Advances* 2016.

17. Evans, M. S., *Tyre compounding for improved performance*. iSmithers Rapra Publishing: 2002; (12), 112.
18. Wagner, M. P., Reinforcing Silicas and Silicates. *Rubber Chemistry and Technology* 1976, 49 (3), 703-774.
19. Reincke, K.; Grellmann, W.; Heinrich, G., Investigation of Mechanical and Fracture Mechanical Properties of Elastomers Filled with Precipitated Silica and Nanofillers Based upon Layered Silicates. *Rubber Chemistry and Technology* 2004, 77 (4), 662-677.
20. Murakami, K.; Iio, S.; Ikeda, Y.; Ito, H.; Tosaka, M.; Kohjiya, S., Effect of silane-coupling agent on natural rubber filled with silica generated in situ. *Journal of materials science* 2003, 38 (7), 1447-1455.
21. Nayek, S.; Bhowmick, A. K.; Pal, S. K.; Chandra, A. K., Wear Behavior of Silica Filled Tire Tread Compounds by Various Rock Surfaces. *Rubber Chemistry and Technology* 2005, 78 (4), 705-723.
22. Gaspard, J., Physisorption and Chemisorption. In *Interfacial Aspects of Phase Transformations*, Springer: 1982; 103-118.
23. Wolff, S.; Wang, M.-J., Filler-elastomer interactions. Part IV. The effect of the surface energies of fillers on elastomer reinforcement. *Rubber chemistry and technology* 1992, 65 (2), 329-342.
24. Dannenberg, E. M., The Effects of Surface Chemical Interactions on the Properties of Filler-Reinforced Rubbers. *Rubber Chemistry and Technology* 1975, 48 (3), 410-444.
25. Maier, P.; Goeritz, D., Molecular interpretation of the Payne effect. *Kautschuk Gummi Kunststoffe* 1996, 49 (1), 18-21.
26. Saalwächter, K., Microstructure and Molecular Dynamics of Elastomers as Studied by Advanced Low-Resolution Nuclear Magnetic Resonance Methods. *Rubber Chemistry and Technology* 2012, 85 (3), 350-386.
27. Papon, A.; Saalwächter, K.; Schäler, K.; Guy, L.; Lequeux, F.; Montes, H., Low-Field NMR Investigations of Nanocomposites: Polymer Dynamics and Network Effects. *Macromolecules* 2011, 44 (4), 913-922.
28. Mujtaba, A.; Keller, M.; Ilisch, S.; Radosch, H.-J.; Beiner, M.; Thurn-Albrecht, T.; Saalwächter, K., Detection of Surface-Immobilized Components and Their Role in Viscoelastic Reinforcement of Rubber-Silica Nanocomposites. *ACS Macro Letters* 2014, 3 (5), 481-485.
29. Merabia, S.; Sotta, P.; Long, D. R., A Microscopic Model for the Reinforcement and the Nonlinear Behavior of Filled Elastomers and Thermoplastic Elastomers (Payne and Mullins Effects). *Macromolecules* 2008, 41 (21), 8252-8266.
30. Meera, A.; Said, S.; Grohens, Y.; Thomas, S., Nonlinear viscoelastic behavior of silica-filled natural rubber nanocomposites. *The Journal of Physical Chemistry C* 2009, 113 (42), 17997-18002.
31. Simha, R.; Frisch, H.; Eirich, F., The adsorption of flexible macromolecules. *The Journal of Physical Chemistry* 1953, 57 (6), 584-589.
32. Valentín, J. L.; Mora-Barrantes, I.; Carretero-González, J.; López-Manchado, M. A.; Sotta, P.; Long, D. R.; Saalwächter, K., Novel Experimental Approach To Evaluate Filler-Elastomer Interactions. *Macromolecules* 2010, 43 (1), 334-346.
33. Mora-Barrantes, I.; Rodríguez, A.; Ibarra, L.; González, L.; Valentín, J. L., Overcoming the disadvantages of fumed silica as filler in elastomer composites. *Journal of Materials Chemistry* 2011, 21 (20), 7381.

Chapter 8

Conclusions and outlooks

8 Conclusions and outlook

Synthesis of silica nanoparticles in SSBR matrix was done successfully by sol-gel method using tetraethoxyorthosilicate (TEOS) as silica precursor in presence of alkaline medium (n-butylamine). The TEOS and water ratio (1:2), amount of catalyst and solvent were kept constant and by changing the amount of TEOS and water in rubber solution the content of silica in rubber was controlled in scientific manner. The silica formed inside the rubber was measured by thermogravimetric analysis and the amount of ash after 600 °C was considered as amount of silica presented in rubber¹. The *in-situ* derived silica composites offered an improved mechanical and dynamic mechanical properties, lower heat build-up, higher rebound resilience, better processability and abrasion characteristics in the presence and absence of silane coupling agent as compared to precipitated silica composites². The maximum silica yield obtained by the current technique is approximately 98 %. The prepared in-situ silica particles are around 200-400 nm range.

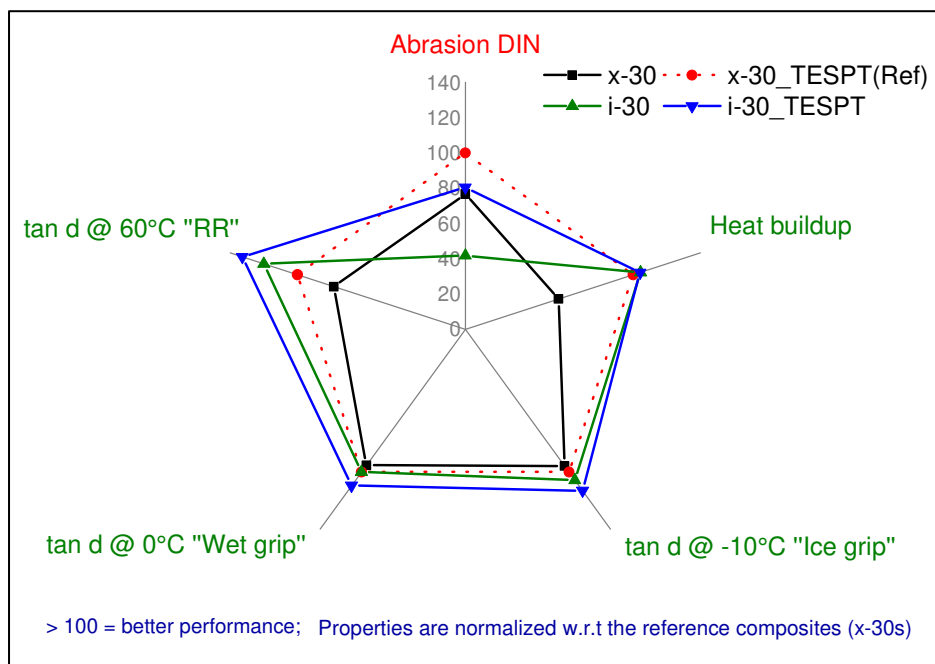


Figure 8.1 Magic pentagon for tyre related properties

Similarly, the performance of silica synthesized by in-situ sol-gel route is compared with precipitated silica composites, and superior mechanical performance of the in-situ silica rubber composites are supported by various mechanical characterizations. To compare the performance of various silica filled composites in the perspective of tire applications, the tire performance magic pentagon is constructed and depicted in the following fig. 8.1. The

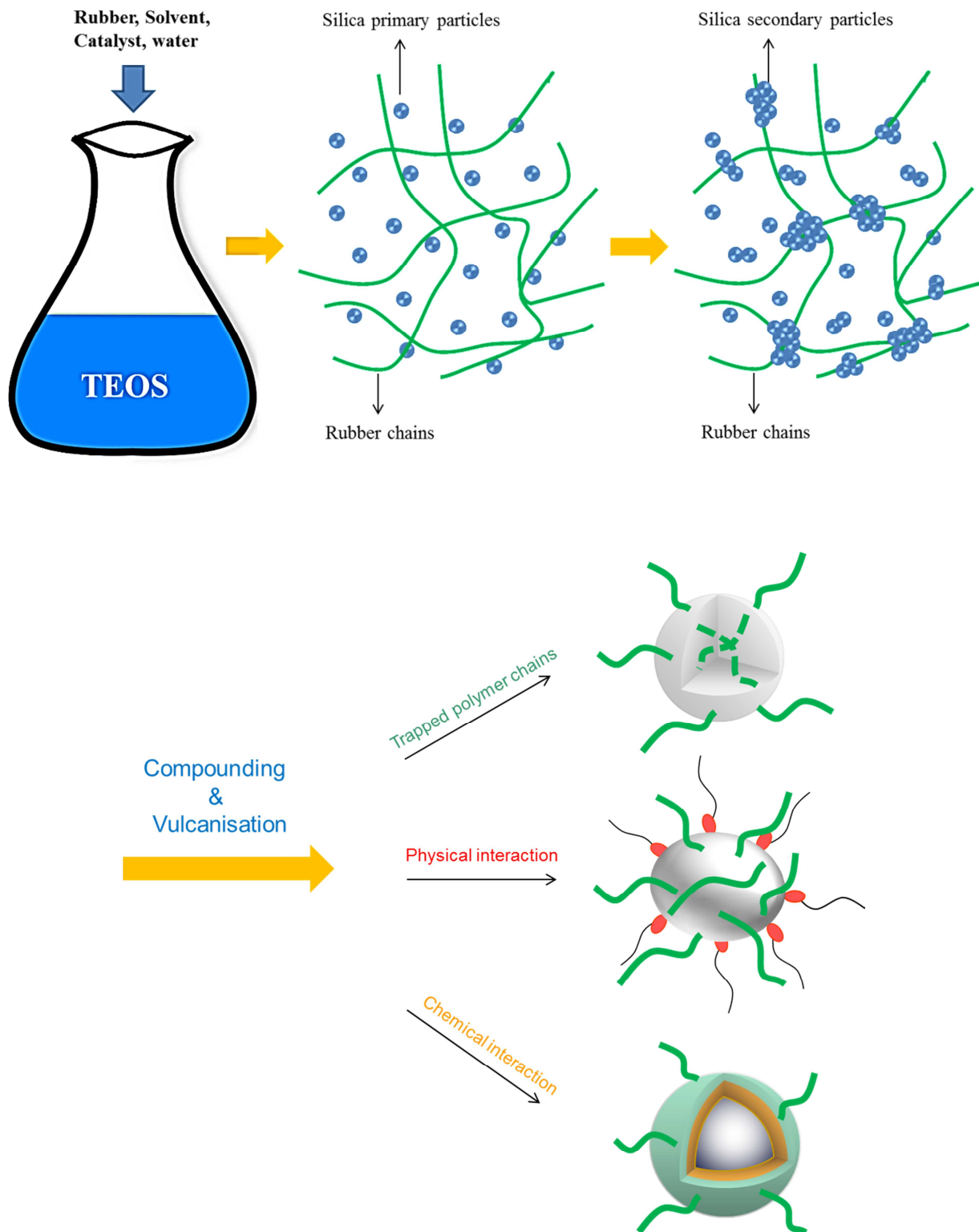
experimental results from dynamic mechanical analyser, abrasion and heat build-up are mainly utilized to construct the pentagon. The in-situ silica composites perform well in terms of lower heat build-up, lower rolling resistance, improved wet grip and ice skid resistance. Commercial precipitated silica composites are better in terms of abrasion properties. This implies that to achieve a (low) rolling resistance compound it is necessary to compromise on the abrasion properties. Developing silica particles in the rubber in solution following in-situ sol-gel route could be a solution to developed high performance tire tread compounds in terms of rolling resistance and wet skid properties. However, further and extensive in-depth studies are necessary to realize the work in practical tire application.

A detailed study focused on the understanding of the reinforcement of two different silica fillers in a SSBR rubber matrix. The main challenge was to study the effects of silica generation and incorporation, along with the influence of surface chemistry and rubber-filler interactions on reinforcement. Low field solid state ^1H NMR investigations highlighted the influence of surface chemistry, chemical nature of silica (alkaline or acidic) inherently influenced on the crosslink density of rubber. DQ-NMR versus equilibrium swelling correlations evidenced that the gradual incorporation of precipitated silica in rubber reduced the amount of chemical crosslinks, due to the adsorption of activators on silica surface and acidic characteristics. Generation of silica in rubber in presence of alkaline conditions and increase the amount of in-situ in rubber did not affected crosslink density of rubber. However, the mentioned effect (reduction of crosslink density in rubber); due to the incorporation of precipitated silica was rectified by the addition of TESPT silane coupling agent⁴. Finally, it was found that the generation of silica inside the rubber can reinforce the matrix significantly better than the direct incorporation silica into the rubber. The type of filler-rubber interaction (physical or chemical) was scientifically distinguished from DQ-NMR versus swelling correlation plots. The interaction mechanism of in-situ silica with the rubber was unique, which reinforced the rubber without any silane coupling agent. Entrapment of rubber chains inside the silica particles as well as strong mechanical tethering of rubber chains onto the surface of the in-situ silica particles were the plausible reasons for the enhanced rubber/in-situ silica filler interactions. The solid state ^{29}Si magic angle spinning NMR investigations described different chemical structures for commercial precipitated silica and in-situ silica powders and a higher hydroxyl density was observed for in-situ silica powder. The solid state ^{29}Si - ^1H cross polarization experiments highlighted that around 2% of silanol groups were modified by the addition TESPT coupling agent in in-situ silica composites and which is 0.2% in case of precipitated silica composites. The EDX investigations affirmed both the silica

surfaces being modified by TESPT silane, however, the extent silane modification was higher for in-situ silica. Finally, it could be concluded that silanization efficiency not only depends on the processing temperature and time, rather also on the reactive hydroxyl density of silica fillers³.

The necessity of silane coupling and type of silica-rubber interaction on the performance of silica composites were investigated in detail. The chemical interaction or modification of silica by NXT, MPTES, TESP and TESPT silanes offered excellent mechanical, dynamic mechanical, rebound resilience, lower heat build-up and abrasion properties compared to physical modification by DMS, APTES and ODTES silanes. The molecular interpretation of the Payne effect by Maier-Göriz model studies showed that the number of unstable chains adsorbed on the silica surface contributes to the reduction of modulus with increase in temperature. The crosslink density of rubber is mainly altered by the type of silane coupling agent and nature of interaction between rubber and silica. Eventually the type of interaction (physical or chemical) with rubber and silica fundamentally decided the reinforcement and performance of silica-rubber composites. However, the amount of silica used in rubber (30 phr) was considered as below as the reinforcement percolation of rubber and the higher amount of silica should be recommended to use in future studies.

The proposed plausible reinforcement mechanism of SSBR rubber by in-situ silica and its silane modification is given scheme 8.1. The synthesis of in-situ silica particles in presence of the polymer allows trapping of some of polymer molecules inside the filler aggregates as well as strong mechanical tethering of polymer chains on the silica surface is acting as additional crosslinking points, therefore, offers exceptional mechanical reinforcement of the rubber without silane⁵. The incorporation of silane coupling agents further improved the physical properties through enhanced silica-rubber interactions. In comparison to existing literature, current approach promises (a) an improved state of silica dispersion (b) higher amounts of silica loading into the rubber without sacrificing its processability (c) a better way to control and customize the particle size and distribution (d) more industrial feasibility and (e) a possible way to save mixing energy due to easy incorporation.



Scheme 8.1 Schematic representation of in-situ silica formation inside the rubber solution, formation of primary & secondary particles and their reinforcement mechanism

References

- 1 Raman, V. S.; Das, A.; Stockelhuber, K. W.; Eshwaran, S. B.; Chanda, J.; Malanin, M.; Reuter, U.; Leuteritz, A.; Boldt, R.; Wie; Heinrich, G., Improvement of mechanical performance of solution styrene butadiene rubber by controlling the concentration and the size of in situ derived sol-gel silica particles. *RSC Advances* 2016, 6 (40), 33643-33655.
- 2 Vaikuntam, S. R.; Bhagavatheswaran, E. S.; Stöckelhuber, K. W.; Wießner, S.; Heinrich, G.; Das, A., DEVELOPMENT OF HIGH PERFORMANCE RUBBER COMPOSITES FROM ALKOXIDE-BASED SILICA AND SOLUTION STYRENE–BUTADIENE RUBBER. *Rubber Chemistry and Technology* 2016, vol-90, No.3, 467-486.
- 3 Vaikuntam, S. R.; Stöckelhuber, K. W.; Bhagavatheswaran, E. S.; Wiessner, S.; Scheler, U.; Saalwächter, K.; Formanek, P.; Heinrich, G.; Das, A., Entrapped styrene butadiene polymer chains by sol-gel derived silica nanoparticles with hierarchical raspberry structures. *The journal of physical chemistry B*, 2018, 122, 2010-2022.
- 4 Valentín, J. L.; Mora-Barrantes, I.; Carretero-González, J.; López-Manchado, M. A.; Sotta, P.; Long, D. R.; Saalwächter, K., Novel Experimental Approach To Evaluate Filler–Elastomer Interactions. *Macromolecules* 2010, 43 (1), 334-346.
- 5 Miloskovska, E.; Hansen, M. R.; Friedrich, C.; Hristova-Bogaerds, D.; van Duin, M.; de With, G., In Situ Silica Nanoparticle Formation in a Rubber Matrix Monitored via Real-Time SAXS and Solid-State NMR Spectroscopy. *Macromolecules* 2014, 47 (15), 5174-5185.